Forest Planning under Climate Uncertainty

Martin B. Bagaram

A dissertation
submitted in partial fulfillment of the
requirements for the degree of

Doctor of Philosophy

University of Washington

2020

Reading Committee:

Sándor F. Tóth, Chair

Monika L. Moskal

Zelda Zabinsky

Program Authorized to Offer Degree:
School of Environmental and Forest Sciences

University of Washington

Abstract

Forest Planning under Climate Uncertainty

Martin B. Bagaram

Chair of the Supervisory Committee:
Associate Professor Sándor F. Tóth
School of Environmental and Forest Sciences

Forest management planning aims at selecting the set of stands that should receive treatments such as harvest (harvest scheduling) in different time periods to provide economic, environmental, social, etc., services. However, since forest planning spans several decades, it is subject to many uncertainties including forest growth uncertainty due to climate change. Climate change is of paramount interest because it is arguably one of the most important challenges that contemporary forest managers need to address. It is reported to heavily affect forest growth. Failure to incorporate growth uncertainty in forest management planning can be detrimental to natural resources sustainability since forest managers might implement policies that are not optimal to different climate scenarios. In this dissertation, I argue that climate change uncertainty needs to be explicitly addressed while developing strategic harvest plans.

I propose to model forest harvest scheduling in the face of forest growth uncertainty due to climate change as a stochastic optimization problem. This modeling framework allows to make robust decisions without knowing the actual forest growth and yield. However, the resulting optimization models belong to the family of mathematical models deemed hard to solve especially when a high number of scenarios (future growth possibilities) is considered. Moreover, one may argue that the added value of stochastic harvest scheduling models may not be warranted given how their development and implementation is more involved compared

to a deterministic model which ignores uncertainties.

This research proposes to study how the uncertainty in forest growth due to climate change can be incorporated in forest harvest scheduling. Specifically, in this research 1) I showed that overlooking climate change in harvest scheduling models affects the net present value and the conservation of natural resources; 2) I demonstrated that out of the four climate paths that may affect forest growth in the Pacific northwest, only two climate paths significantly affect the strategic forest harvest scheduling; and 3) I developed a heuristic that allows to handle large size stochastic optimization problems such as the ones in the case of harvest scheduling with climate uncertainty.

Table of Contents

Page

List of Figures

List of Tables

Table Number | Page

Acknowledgments

First, I would like to express my sincere appreciation to my supervisory committee Dr Sándor F. Tóth, Dr Monika Moskal, Dr Greg Ettl, Dr Zelda Zabinky, and Dr Andrés Weintraub for their time, patience, and valuable advice for the completion of this dissertation. The contribution of the chair of the committee Dr Sándor F. Tóth in securing funding and career guidance cannot be stressed enough.

I would like to thank the Precision Forestry Cooperative, the School of Environmental and Forest Sciences, and Department of Natural Resources (DNR) of Washington State that partially funded my PhD work. During my work, I had the opportunity to interact with Weikko Jaross who was my contact person at the DNR. I would like to express my gratitude to his guidance and advice on practical forest matters.

I extend my appreciations to my friends and lab mates Yosuke Ando, Liz van Wagtendonk, Celine Pastore, Melina Garcia and Daniel Quoc Dung Cao. My appreciation extends to the Graduate Advisors, David Campbell and Michelle Trudeau, who helped and supported me during my program.

My deepest appreciation goes to my girlfriend Bella Tsachidou, without whose support, I would have had considerable difficulty completing my dissertation; and above all to my family that supported me their own way although they couldn't understand what I was doing and why I was doing it.

Chapter 1. Introduction

1.1 Background

Forest management, defined as the science of growing, protecting and harvesting trees and related vegetation to sustain economic, physical, and social values (Alig, 2013), is affected by several disturbances such as fire, storm, windthrow, climate change, etc. (Mäkinen and Borges, 2013). Climate change is arguably one of the most significant challenges that contemporary foresters need to address in timely manner as it directly affects forest by fostering or hindering its growth, and indirectly by changing the frequency and the magnitude of extreme events such as storms, fire, etc. (Ma et al., 2019; Davis et al., 2017; Bell and Gray, 2016). These extreme events in return affect forest development. Although it is believed that forest responses to climate change will involve different strategies including change of forest location, shift of forest species and age classes on the landscape, and change of growth rate and timber yield (Alig, 2013), in this work, I mainly focus on growth rate and timber yield change since it is a factor that can be addressed with immediate results.

Mathematical programming is frequently used to model forest management because of its ability to capture stakeholders' objectives while at the same time satisfying a variety of restrictions like environmental policy and regulatory framework (Moriguchi et al., 2020; Schroder et al., 2016). Typically, forest management modelling uses the expected value of the yield of merchantable timber to produce harvest scheduling models. These models also known as the deterministic models, assume that the future forest growth will represent the average growth. However, because of climate change, there is a substantial uncertainty in forest growth and yield (Bell and Gray, 2016; Laflower et al., 2016; Alig, 2013).

Climate change results largely from changes in temperature, precipitation, and water availability due to atmospheric CO_2 levels (Alig, 2013). However, in this work we focus on forest growth change due to forecast climate change paths (climate paths). Climate experts define four potential climate paths known as representative concentration pathways (van Vuuren et al., 2011). These climate paths are forecast as possible futures with no information on their likelihood and thus it is not clear how this information can be incorporated in forest management planning. It is possible to translate the four climate paths into a number of forest growth scenarios much greater than four (Laflower et al., 2016). In the context of the Pacific Northwest, Latta et al. (2010) showed that the proposed four climate paths will affect forest growth differently.

1.2 Overview

Although each chapter of my dissertation stands alone, all of them are bound by the common theme of forest management under forest growth uncertainty.

In Chapter 2, I address uncertainty in forest management planning by modelling the forest harvest problem and finding the optimal set of actions that the decision maker needs to implement immediately without having information on the climate change. We refer to those decision as 'here and now' decisions. Although this method allows to have optimal decisions here and now, the method does not provide actionable decisions for the future. In addition, the set of uncertainty this method considers is quite large. I address these shortcomings in Chapter 3.

In Chapter 3, I develop a harvest scheduling model for a real forest, and study how different climate paths can be incorporated in forest management planning. Since climate change is forecast as climate paths, in this chapter, I show that all climate paths need to be explicitly considered when building harvest scheduling models. The planner can rely on just one climate path to make sound decisions.

Since solving stochastic optimization problems is computationally challenging, in Chapter 4, I propose a heuristic that allows to efficiently solve stochastic harvest scheduling models.

In addition to forest growth uncertainty, this heuristic is well suited for problems with uncertainty in the objective function such as uncertainty of the price of forest products.

References

Alig, R. (2013). Forest Management and Climate Change. In *Encyclopedia of Energy, Natural Resource, and Environmental Economics*, volume 2-3, pages 97–108. Elsevier, 1 edition.

Bell, D. M. and Gray, A. N. (2016). Assessing intra- and inter-regional climate effects on Douglas-fir biomass dynamics in Oregon and Washington, USA. *Forest Ecology and Management*, 379:281–287.

Davis, R., Yang, Z., Yost, A., Belongie, C., and Cohen, W. (2017). The normal fire environmentModeling environmental suitability for large forest wildfires using past, present, and future climate normals. *Forest Ecology and Management*, 390:173–186.

Laflower, D. M., Hurteau, M. D., Koch, G. W., North, M. P., and Hungate, B. A. (2016). Climate-driven changes in forest succession and the influence of management on forest carbon dynamics in the Puget Lowlands of Washington State, USA. *Forest Ecology and Management*, 362(2016):194–204.

Latta, G., Temesgen, H., Adams, D., and Barrett, T. (2010). Analysis of potential impacts of climate change on forests of the United States Pacific Northwest. *Forest Ecology and Management*, 259(4):720–729.

Ma, W., Zhou, X., Liang, J., and Zhou, M. (2019). Coastal Alaska forests under climate change: What to expect? *Forest Ecology and Management*, 448(February):432–444.

Mäkinen, A. and Borges, J. G. (2013). Review . Assessing uncertainty and risk in forest planning and decision support systems : review of classical methods. *Forest Systems*, 22(2):282–303.

Moriguchi, K., Ueki, T., and Saito, M. (2020). Establishing optimal forest harvesting regulation with continuous approximation. *Operations Research Perspectives*, 7(April):100158.

Schroder, S. A., Tóth, S. F., Deal, R. L., and Ettl, G. J. (2016). Multi-objective optimization to evaluate tradeoffs among forest ecosystem services following fire hazard reduction in the Deschutes National Forest, USA. *Ecosystem Services*, 22:328–347.

van Vuuren, D. P., Edmonds, J., Kainuma, M., Riahi, K., Thomson, A., Hibbard, K., Hurtt, G. C., Kram, T., Krey, V., Lamarque, J. F., Masui, T., Meinshausen, M., Nakicenovic, N., Smith, S. J., and Rose, S. K. (2011). The representative concentration pathways: An overview. *Climatic Change*, 109(1):5–31.

Chapter 2. Multistage Sample Average Approximation for Harvest Scheduling under Climate Uncertainty

Summary

Forest planners have traditionally used expected growth and yield coefficients to predict future merchantable timber volumes. However, because climate change affects forest growth, the typical forest planning methods using expected value of forest growth can lead to sub-optimal harvest decisions. In this paper, we propose to formulate the harvest planning with growth uncertainty due to climate change problem as a multistage stochastic optimization problem and use sample average approximation (SAA) as a tool for finding the best set of forest units that should be harvested in the first period even though we have a limited knowledge of what future climate will be. The objective of the harvest planning model is to maximize the expected value of the net present value (NPV) considering the uncertainty in forest growth and thus in revenues from timber harvest. The proposed model was tested on a small forest with 89 stands and the numerical results showed that the approach allows to have superior solutions in terms of net present value and robustness in face of different growth scenarios compared to the approach using the expected growth and yield. The SAA method requires to generate samples from the distribution of the random parameter. Our results suggested that a sampling scheme that focuses on generating high number of samples in distant future stages is favorable compared to having large sample sizes for the near future stages. Finally, we demonstrated that, depending on the level of forest growth change, ignoring this uncertainty can negatively affect forest resources sustainability.

2.1 Introduction

Climate change is arguably one of the most challenging issues that contemporary forest planners need to address. In general, forest practitioners need to provide a long term forest harvest scheduling plan that takes into account the preference of the stakeholders while complying with environmental, regional and ecological restrictions. Usually, forest planning aims at scheduling which forest units should receive a specific treatment such as harvesting, thinning, etc., in each period in order to achieve the management objectives. This planning also known as harvest scheduling, expands several decades, and is subject to many sources of uncertainty due to factors that include natural hazards (fire, windthrow, insects, etc), and technological limitation such as forest inventory errors, growth prediction errors, and poor foresight of the price of forest products on the market (Mäkinen and Borges, 2013; Ross and Tóth, 2016). It is important to incorporate all or some of these uncertainties in forest planning.

The need to incorporate uncertainty in forest harvest scheduling has been acknowledged several decades ago (Dixon and Howitt, 1980). Subsequently, Kooten et al. (1992) urged for consideration of forest growth uncertainty in the planning. The authors asserted that the cost of ignoring such uncertainty at a forest scale can be detrimental. When the uncertainty is ignored, we make decisions assuming the growth in the future will be the expected value of growth (average growth). However, it is rare that the actual growth will be the average one and therefore, many harvest decisions made in early periods of the planning horizon were not optimal. This leads to a failure to meet the planning objectives and satisfying many of the aforementioned restrictions. Owing to the computational challenges that the introduction of uncertainty in harvest modeling involves, Pukkala (1998) recommended that each forest harvest scheduling plan should be accompanied by an estimation of its uncertainty or its reliability. Notwithstanding all the exhortation to incorporate uncertainty in forest planning, harvest scheduling models, for a long time, have ignored uncertainty or were limited at reporting the sensitivity of the harvesting plans in case of change of one or many input parameters of the modeling. It is only recently that there has been a prolific number of papers addressing the integration of uncertainty in harvest planning. The most common uncertainties that have been addressed is the wood price and the wood demand (Alonso-Ayuso et al., 2011; Veliz et al., 2014; Piazza and Pagnoncelli, 2014; Pagnoncelli and Piazza, 2017; Alonso-Ayuso et al., 2018). Recently, there is an interest to incorporate climate uncertainty in forest planning. The first study that we are aware of that explicitly addresses the issue was conducted by Garcia-Gonzalo et al. (2016). The authors assessed how climate change affected the management decisions of a Eucalyptus forest in Portugal with a planning horizon of 15 years. A similar study was conducted by Álvarez-Miranda et al. (2018); Garcia-Gonzalo et al. (2020) using the same dataset.

In this paper, we model harvest planning as a stochastic optimization problem and use sample average approximation (SAA) as a tool for identifying the best set of actions one can take to meet the management objectives. In other words, we use SAA for solving harvest planning models. Stochastic optimization is a modeling framework for mathematical models dealing with uncertainty. In multistage stochastic programming, decisions are made sequentially at stages and the uncertainty unfolds during periods. Thus, the decision maker needs to implement a decision at the beginning of the planning horizon (first stage decisions) without knowing what the value of the uncertain parameter will be. After a period, in which the uncertainty is revealed, the decision maker can take recourse actions at subsequent stages. Therefore, it is important to make optimal decisions in the early stages of the planning without knowing the magnitude of the uncertainty that will unfold. Specifically, in strategic harvest scheduling, the decision maker needs to prioritize the set of forest units (stands) that should be harvested here and now or during the ongoing decade or period. After that period, the decision maker will have the opportunity to revisit the management in the following periods. In this case, the goal of the harvest scheduling is to decide the set of actions that managers should apply immediately "here and now" (first stage decisions).

SAA is a Monte Carlo simulation based approach for solving stochastic optimization problems. It consists of drawing repetitively samples from the distribution of the random parameter and solving the resultant average sample deterministic optimization problem. Each sample might lead to a different solution. However, if the sample size is large enough, the sample objective function value will approximate the true optimal value. Mak et al. (1999) showed that for minimization problems, the expectation of samples' objective value corresponds to the lower bound on the true optimal value of the stochastic optimization problem and that the bound monotonically increases as the sample size increases. SAA has been successfully applied in several fields such as portfolio selection (Wang and Ahmed, 2008), supply chain network design (Schütz et al., 2009; Chunlin and Liu, 2012), facility location problem (Emelogu et al., 2016) and personnel assignment (Pour et al., 2017). Notwithstanding all these applications, and the fact that SAA is well suited for problems where the objective function is difficult to evaluate such as harvest planning under climate uncertainties (Wang and Ahmed, 2008), to the extent of our knowledge, SAA has never been applied in forestry domain. In addition, unlike stochastic programming which requires to know the probability distribution of the samples, SAA known as a data-driven optimization method, considers the samples to be equiprobable. The idea is that if the sample size is large enough, then the sample statistics will represent those of the actual population the sample is taken from. Hence, there is no need to know the actual distribution of the uncertainty. This is particularly important for harvest scheduling under climate uncertainty because climate change is forecast as possible futures without any probabilities. Moreover, although the method performs well for two-stage stochastic problems (Mohammadi Bidhandi and Patrick, 2017), it is unclear how the method will perform on a multistage harvest scheduling problem.

The objective of this paper is to fill the gap in the literature on SAA and multistage stochastic harvest scheduling models. For multistage stochastic optimization problems, each sample of the uncertainty is known as a scenario. It is known that the number of scenarios to consider grows exponentially with the number of stages in multistage stochastic programs. Forest harvesting scheduling models are typically characterized by long planning horizons with many stages. The contributions in this paper are as follows:

1. Introduce a method to handle climate change uncertainty in forest harvest scheduling that allows to make sound decisions in early stages of planning. Poor decisions in early stages are significantly more detrimental to many businesses compared to decisions in later stages. Hence, later stage decisions can be considered as secondary.

2. Propose a method to generate the set of scenarios to reduce the sample size and keep the optimization model tractable. If we generate possible scenarios of forest growth in i.i.d (independent identical distributed) fashion, then we might have a very large sample size before SAA solution converges to optimality. This large sample size can make the problem computationally intractable. We propose a sampling scheme that focuses at having higher number of replications for distant stages.

We will show that stochastic harvest scheduling has an advantage over the expected value approach (deterministic model presented in Appendix 2.A) because it allows to implement policies that are optimal for all foreseen forest growth changes by providing management decisions that would be implemented if we consider the uncertainty and if we do not. The rest of this document is structured as follows. In Section 2.2, we present the materials and methods used in this research. We describe in that section the SAA method and the scenario generation scheme. We dedicate Section 2.3 to presenting our findings. Finally, in Section 2.4, we discuss the results and outline future research.

2.2 Material and methods

2.2.1 Problem description and formulation

We present in this section the multistage stochastic harvest scheduling problem with forest growth uncertainty due to climate change. Let $t \in \mathcal{T} = \{1, \ldots, T\}$ be the set of stages in which forest units are eligible for harvest in the future. We reserve $t = 0$ to the time "now" (first stage decision), where there is no uncertainty on the forest growth. We define $\xi := \{\xi_1, \ldots, \xi_T\}$ to be the random vector characterizing forest growth change due climate change. Hence, ξ_t is the random parameter of ξ at time t. Each ξ_t has a support Ξ_t which is the range of values that the random parameter ξ_t can take. The meaning of parameters, variables and sets is given in Table 2.1.

The objective of the decision maker is to maximize the expected net present value (NPV) from timber harvest. This can be formulated in a generic form as (2.1) and (2.2):

$$\max \sum_{s \in \mathcal{S}} r_s x_s + \mathbb{E}\left[R(x, \xi)\right] \tag{2.1}$$

$$\text{subject to} \quad x \in \{0, 1\}^{|\mathcal{S}|}, \tag{2.2}$$

where we take the expectation with respect to ξ and, $R(x, \xi^i)$ is the optimal value of the harvest scheduling given the harvest in the first stage (x) and the occurrence of one forest growth scenario ξ^i. In this formulation, the decision variables are only the first stage variables which means that the decision maker mainly cares about how to select the stands that can be harvested in the first period so that the expected NPV is maximized. The value of $R(x, \xi^i)$ is obtained by solving the following optimization problem:

$$\max \sum_{s\in\mathcal{S}} \left[\sum_{t\in\mathcal{T}} r_{st}^{\xi^i} y_{st}^{\xi^i} + r_{s0}^{\xi^i} w_s^{\xi^i} \right] \tag{2.3}$$

subject to

$$x_s + w_s^{\xi^i} + \sum_{t=1}^{T} y_{st}^{\xi^i} = 1 \qquad s = 1, \ldots, |\mathcal{S}| \tag{2.4}$$

$$\sum_s v_s x_s = H_0 \tag{2.5}$$

$$\sum_s v_{st}^{\xi^i} y_{st}^{\xi^i} = H_t^i \qquad t = 1, \ldots, T \tag{2.6}$$

$$H_t^i \leq \alpha H_{t-1}^i \qquad t = 1, \ldots, T \tag{2.7}$$

$$H_t^i \geq \beta H_{t-1}^i \qquad t = 1, \ldots, T \tag{2.8}$$

$$H_t^i \leq \gamma H_{t-2}^i \qquad t = 2, \ldots, T \tag{2.9}$$

$$H_t^i \geq \lambda H_{t-2}^i \qquad t = 2, \ldots, T \tag{2.10}$$

$$\sum_{s\in\mathcal{S}} a_s \left[\sum_{t=1}^{\mathcal{T}} age_{st}(x_s + y_{st}^{\xi^i}) + age_{s0} w_s^{\xi^i} \right] \geq \sum_s a_s age_s. \tag{2.11}$$

$$w^{\xi^i} \in \{0,1\}^{|\mathcal{S}|}, \;\; y^{\xi^i} \in \{0,1\}^{|\mathcal{S}| \times T}, \;\; H_t^i \geq 0 \qquad \forall t \in \{0, 1, \ldots, T\}. \tag{2.12}$$

The objective function (2.3) maximizes the net present value from subsequent stages after the current harvest (x). This objective function includes the cost of harvest and replantation for each forest unit. In addition, this objective function accounts for the value of the stands that are not harvested during the planning horizon because those stands have a monetary value. Constraint set (2.4) imposes that if a stand is harvested now, then it cannot be harvested in the subsequent years. In other words, a forest unit can only be harvested once during the whole planning horizon. The use of w_s variables is to account the stands that are not scheduled for harvest in the whole planning horizon. Constraint set (2.5) and (2.6) compute the volume of wood harvested now and in the future periods during the planning horizon, respectively. The volume computed in each period depends on the scenario ξ^i. Constraint sets (2.7) and (2.8) impose that the volume fluctuation between two

Table 2.1: *Variable, set and parameters used in problem formulation*

Sets	
$\mathcal{S}$	set of stands or forest management units ($s \in \mathcal{S}$)
$\mathcal{T}$	set of time period in which the decision are implemented or stage at which the decisions are taken ($t \in \mathcal{T}$)
Ω	set of scenarios ($\xi^i \in \Omega$)
Variables	
x_s	binary variable: 1 if management unit s is scheduled to be harvested in the first period (now); and 0 otherwise
$w_s^{\xi^i}$	binary variable: 1 if management unit s should not be harvested during the whole planning horizon given the scenario ξ^i; and 0 otherwise
$y_{st}^{\xi^i}$	binary variable: 1 if the stand s should be harvested in t given the scenario ξ^i; 0 otherwise
H_t^i	volume harvested in year t under scenario ξ^i (m^3). We omit the superscript i for $t = 0$
Parameters	
r_s	discounted net harvest revenue from stand s if the stand is harvested now ($)
$r_{st}^{\xi^i}$	net harvest revenue from stand s if the stand is harvested in year t according to scenario ξ^i ($)
$r_{s0}^{\xi^i}$	discounted value of the stand at the end of the planning horizon if it is not harvested during the whole planning horizon under scenario ξ^i ($)
v_s	merchantable yield of stand s in the first period (m^3/ha)
$v_{st}^{\xi^i}$	projected merchantable yield of stand s if harvested in year t according to scenario ξ^i (m^3/ha)
a_s	area of stand s (ha)
age_{st}	age of stand s at the end of the planning horizon if harvested in year t (yr)
$age_{s.}$	current age of the stand s (yr)
age_{s0}	age of stand s at the end of the planning if not harvested during the planning horizon (yr)
α	acceptable lower bound on the fluctuation of volume of wood from one period to the next
β	acceptable upper bound on the fluctuation of volume of wood from one period to the next
γ	acceptable lower bound fluctuation of volume of wood between two non consecutive periods
λ	acceptable upper bound fluctuation of volume of wood between two non consecutive periods

consecutive stages should be within a given lower and upper bounds, respectively. These sets of constraints are also known as even flow constraints since they ensure that the volume of timber harvested is almost evenly distributed in time. Even with constraint sets (2.7) and (2.8), there is a possibility that the volume harvested declines with time. Hence volume at $t = 4$ might be much lower than volume at $t = 1$, for instance. To attenuate this effect, we impose supplementary wood flow constraints which are constraint sets (2.9) and (2.10). These two sets of constraints impose flow restriction between two non-consecutive stages. Constraint set (2.11) states that the age of the forest at the end of the planning horizon should be greater or equal to the current age of the forest. This constraint is a proxy for sustainability; it ensures that forest resources are not depleted during the planning horizon. Finally, the definition of the variables is given in (2.12).

2.2.2 Climate change data

In this paper the uncertainty in forest growth stems from climate change. In this section, we present how climate change was translated into forest growth suitable to the harvest planning model. Climate change in this project refers to the change in forest growth. Hence, the change can be positive or negative. The change is small in near future, stage 1, compared to the distant future (stage 4). There is a ten year difference between two consecutive stages. In this project, we consider the case of Pacific Northwest where most models forecast that climate change will lead to the increase of forest growth. We report in Table 2.2 the growth change used for the analysis. This growth change data is based on (Latta et al., 2010, Table 3). Forest growth is age dependent and this is reflected in growth change. In addition, this growth change modeling reflects a Geometric Brownian Motion process where the absolute increments of growth are not independent from one period to another although the percentages of change are. The `Lower` and `Upper` in the table correspond to the lowest and highest possible growth change, respectively, at each stage. Formally speaking, [`Lower`, `Upper`] at stage t, represents Ξ_t of the random parameter ξ_t.

To assess the performance of the proposed modeling framework, we change the lower bound on the growth change by multiplying it by a factor ϵ. This allows to assess the performance of the proposed method for climate change scenarios that forecast decrease in forest growth. We assessed values of ϵ equal 1, 20 and 40. Only $\epsilon = 40$ corresponds to forest decline whereas, ϵ of 20 corresponds to a decrease in forest growth.

Table 2.2: *Forest growth change (%) due to climate change*

Stage	Lower	Upper
1	-1.2	11.1
2	-2.4	22.2
3	-3.6	33.3
4	-4.8	44.4

2.2.3 Multistage sampling

We have presented both the optimization model we intend to solve in this paper and the uncertain parameter. In this section, we describe how to sample from the distribution of the uncertain parameter. To achieve that objective, let $\mathcal{N} = \{N_1, \ldots, N_T\}$ be a sequence of positive integers. At the first stage (stage 1), we generate N_1 replications drawn from Ξ_1, the support of the random parameter ξ_1. To minimize the number of replications necessary, we generate the N_1 by diving Ξ_1 into N_1 intervals. From each interval, we sample uniformly one realization of ξ_1. We repeat this procedure for stage 2 and so forth for the following stages. At the end, we connect the realization at $t = 0$ to all realizations at $t = 1$. We connect all realizations at $t = 1$ to all others at $t = 2$ and we continue until the last stage. The result of this procedure is a scenario tree with a total number of scenarios or sample size $n = \prod_{t=1}^{T} N_t$. Each path from this scenario tree can be viewed as a scenario with probability $1/n$. Varying the values of N_t allows to have different sample sizes which can be solved using SAA as described in the following section. It is not clear, however, whether having $N_1 \geq N_2 \geq \cdots \geq N_T$ is preferable to a sampling scheme with $N_1 \leq N_2 \leq \cdots \leq N_T$. To answer this question, we tested the solution by considering a sampling scheme with $N_1 = N_2 = \cdots = N_T$ in Section 2.3.1 and evaluate in Section 2.3.2, the solution behavior when we use the two other sampling schemes.

2.2.4 Solution method

We used SAA as the method for solving the stochastic harvest scheduling model since the main challenge of the decision maker is to find the set of stands that are suitable for harvest in the first period. SAA method is a Monte Carlo simulation based approach for solving stochastic optimization problems. A random sample is generated with uniform probability distribution, and then the expected value function of the stochastic problem is approximated by the corresponding sample average function. The sample average approximation problem which is specified by the generated sample is then solved by a deterministic optimization technique which is mixed integer programming in this study. This procedure is repeated by increasing the size of the samples to obtain solutions that are close enough to the true optimal solution.

To formally introduce the SAA method we used to solve the harvest scheduling problem, we reformulate the harvest scheduling problem in (2.1) and (2.2) in a compact form, just for practicability. We can rewrite the problem as

$$\max_{x \in X} f(x, \xi) := \max_{x \in X} \mathbb{E}\left[\sum_{s \in \mathcal{S}} \left[r_s x_s\right] + R(x, \xi)\right], \tag{2.13}$$

where X is the feasible set (constraints (2.2), (2.4) to (2.12)). We can write (2.13) because the term $r_s x_s$ has no uncertainty.

Let $\xi^1, \ldots, \xi^n$ be a sample of size n drawn from the distribution of ξ. The sample is generated using the method described in Section 2.2.3. We can write the sample average objective function as:

$$f_n(x) := \frac{1}{n} \sum_{i=1}^{n} f(x, \xi^i). \tag{2.14}$$

where

$$f(x, \xi^i) = \sum_{s \in \mathcal{S}} r_s x_s + \sum_{s \in \mathcal{S}} \Big(\sum_{t \in \mathcal{T}} r_{st}^{\xi^i} y_{st}^{\xi^i} + r_{s0}^{\xi^i} w_s^{\xi^i} \Big). \tag{2.15}$$

The idea of SAA is to solve (2.16) instead of (2.13)

$$z_n = \max_{x \in X} f_n(x) \tag{2.16}$$

We now describe the steps for solving a stochastic optimization problem using SAA as outlined in Figure 2.1.

Step a & b: Generate a large sample of size (N) and solve it using (2.16) to obtain a first stage candidate solution $\hat{x}$. The choice of N depends on the model that can be solved in a reasonable time. The fact that this problem is only solved once, partially motivates on choosing the largest possible sample size.

Step c: Generate M samples of size n. The idea is to start with lower values of n and increase the sample size progressively. Kleywegt et al. (2001) describes a procedure for choosing the value of M. In a nutshell, M should be chosen in a way that allows to compute different statistics such as the mean, variance and confidence interval.

Step d: Solve SAA problem of each sample m to get z_n^m defined as $z_n^m = \max_{x \in X} \frac{1}{n} \sum_{i=1}^n f_n\left(x, \xi^i\right)$ and the upper bound $\overline{z}_n^M = \frac{1}{M} \sum_{m=1}^M z_n^m$. $\overline{z}_n^M$ is an upper bound because it is the average of upper bounds z_n^m obtained by using only a set of scenarios, and therefore the solution is more optimistic.

Step e: For each sample m, fix the first stage variables to $\hat{x}$ obtained from step a & b to get a lower bound on the optimal solution $\hat{z}_n^m(\hat{x}) = \max \frac{1}{n} \sum_{i=1}^n f_n\left(\hat{x}, \xi^i\right)$

Step f: Compute the average optimality gap as $\overline{G}(\hat{x}) = \overline{z}_n^M - \frac{1}{M} \sum_{m=1}^M \hat{z}_n^m(\hat{x})$. We can also compute for each sample m the optimality gap as

$$G_n^m(\hat{x}) = \max_{x \in X} \frac{1}{n} \sum_{i=1}^n f_n\left(x, \xi^i\right) - \frac{1}{n} \sum_{i=1}^n f_n\left(\hat{x}, \xi^i\right) \tag{2.17}$$

where $f_n\left(\hat{x}, \xi^i\right)$ is obtained by fixing the first stage variable in f_n to $\hat{x}$ from Step a. Notice that $G_n^m(\hat{x}) \geq 0$. We can then compute the average optimality gap $\overline{G}(\hat{x}) = \frac{1}{M} \sum_{m=1}^M G_n^m(\hat{x})$

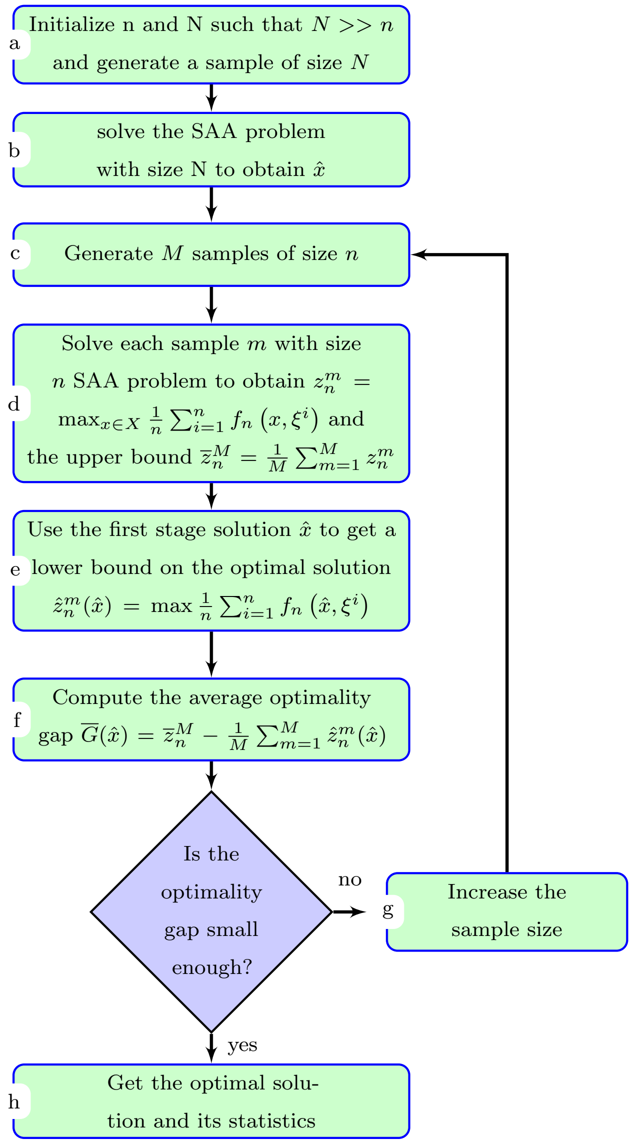

Figure 2.1: *Flow chart of SAA*

and its variance $s_{\overline{G}}^2 = \frac{1}{M(M-1)} \sum_{m=1}^{M} \left(G_n^m(\hat{x}) - \overline{G}(\hat{x}) \right)^2$. Mak et al. (1999) proved that the optimality gap depends on the sample size n . In fact, they proved that as $n \to \infty$, the optimality gap converges to zero and the SAA objective function value converges to the true optimal objective value with probability one. In other words, the sample size is large enough if we have a small optimality gap.

Step g: If the optimality gap computed in step f is not sufficiently small, then increase the sample size n and go back to step c. The decision of whether the optimality gap is sufficiently small and its variance is sufficiently low is domain specific.

Step h: If the optimality gap is small enough, then we have obtained the optimal solution and we can compute the confidence interval on the optimality gap as: $\mu_{\hat{x}} \in \left[0, \overline{G}(\hat{x}) + t_{M-1,\alpha} S_{\overline{G}}\right]$ with a confidence of $100(1-\alpha)$ with α being Type I error.

2.2.5 Importance of SAA

To assess the advantage of solving the stochastic optimization problem with SAA instead of the deterministic model that only considers the average scenario (the model that ignores climate change uncertainty), we compute the so-called value of stochastic solution (VSS) (Birge, 1982). Let $\bar{x}$ be the first stage solution we would get if we implemented the average growth solution, respectively. Similarly, let x^* be the optimal solution of the stochastic model obtained from SAA. We denote by z^i and $\bar{z}^i$ the net NPVs of the scenario ξ^i when the first stage variables are fixed to x^* and $\bar{x}$, respectively. Finally, let $z(\bar{x}) = \frac{1}{|\Omega|} \sum_{\xi^i \in \Omega} \bar{z}^i$ whereas, $z(x^*) = \frac{1}{|\Omega|} \sum_{\xi^i \in \Omega} z^i$. We compute VSS as follows: $VSS = z(x^*) - z(\bar{x})$. In term of relative value, we present VSS in basis points (bps)[1]as:

$$VSS(bps) = \frac{VSS}{z(\bar{x})} * 10,000 \tag{2.18}$$

In case where some scenarios are not feasible after fixing the first stage to $\bar{x}$, we report the number of infeasible scenarios.

2.2.6 Experiment

We present in this section, the values of several parameters introduced in the methods in order to conduct a numerical experiment. The numerical experiment was run on a Windows desktop with an AMD 8 Core processor of 4 GHz and 8 GB of RAM. We have used CPLEX

[1]1 Basis points (BPS) is equivalent to 0.01%. It is commonly used in economics and finance

12.8 to solve the stochastic model using python 3 as the modeling language. We solved each model to 0.5% mixed integer programming (MIP) optimality gap. For each model, we generated 30 independent replications ($M = 30$). We used bootstrapping to compute the 95% confidence level for different metrics. N was set to 625 scenarios and we varied the sample size n from 16 to 625. We tested the modeling on Phyllis Leeper forest with 89 stands (http://ifmlab.for.unb.ca/fmos/datasets/PhyllisLeeper/). Model parameters α and γ were set to 0.85, whereas β and λ were set to 1.15. The planning horizon was 50 years divided into 5 planning periods of 10 years each.

2.3 Results

2.3.1 Effect of sample size on the optimality gap

The results of the experiments are summarized in Figure 2.2. The sample size is the number of scenarios. These results were obtained by setting $N_1 = N_2 = N_3 = N_4$. The solutions show that as the sample size increases, the NPV decreases converging toward the optimal objective function value. In addition, we have tighter confidence intervals as the sample size increases. A similar behavior is observed for the optimality gap. However, larger sample sizes lead to a significant increase in solution time. We can conclude that solving problems with up to 256 scenarios is sufficient to capture the variability and obtain solutions that are close enough to the true optimal solution since increasing the sample size to 625 did not significantly reduce the optimality gap and its variance. Furthermore, although we need larger sample size to reduce the optimality gap and its variance, we need to compromise on solution time. The solution time increases exponentially with the sample size.

2.3.2 Effect of sampling scheme on the optimality gap

In this section, we test the effect of scenario generation scheme on the optimality gap. The scheme used to generate scenarios for the four stages is presented in Figure 2.3. In the figure, the sampling scheme represents four digits corresponding to N_1, N_2, N_3 and N_4. For instance, `1155` means that $N_1 = 1,\ N_2 = 1,\ N_3 = 5$ and $N_4 = 5$ leading to 1*1*5*5=25 scenarios. This means that the schemes `1555` and `5551` lead to the same number of scenarios (125 scenarios). As we can see from Figure 2.3, the optimality gap and its variability when $N_1 = 1$ is larger than when $N_1 > 1$. The lowest optimality gap is obtained with $N_1 = 3$. In general having higher values of N_t for higher t seems to be favorable.

2.3.3 Advantage of SAA in stochastic harvest scheduling over the deterministic approach

The stochastic optimization solution allows to have superior solution in terms of NPV. In addition, it allows to have solutions that are robust (feasible) for a set of climate change scenarios that are not feasible if we implement here and now the deterministic solution (Table 2.3). As the uncertainty on forest growth change magnitude increases, the value of stochastic solution increases as well. When we considered $\epsilon = 20$, out of 200 scenarios, 3 scenarios were infeasible.

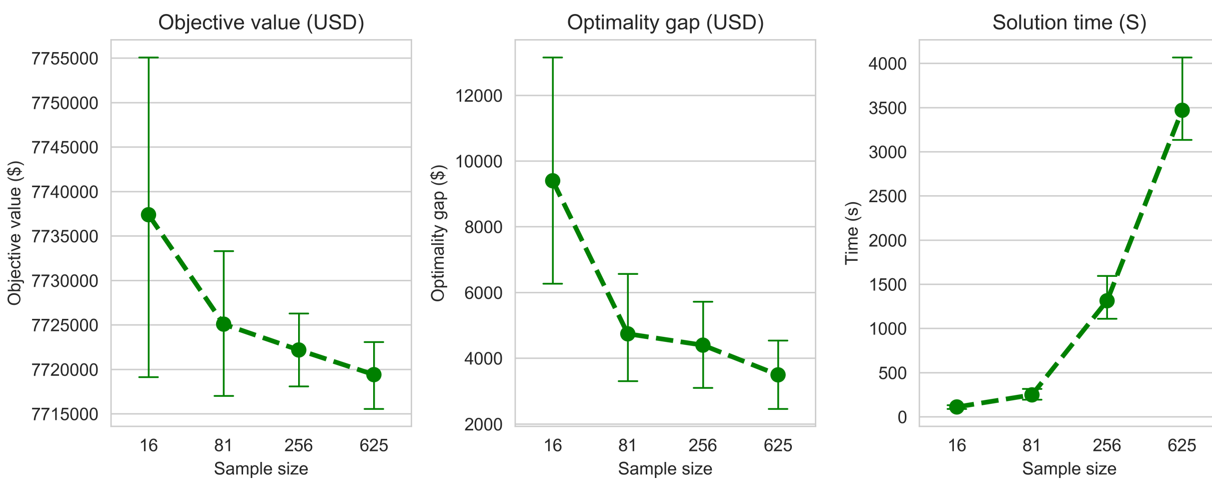

Figure 2.2: *Performance measurement of SAA for harvest scheduling. Error bars indicate 95% confidence interval*

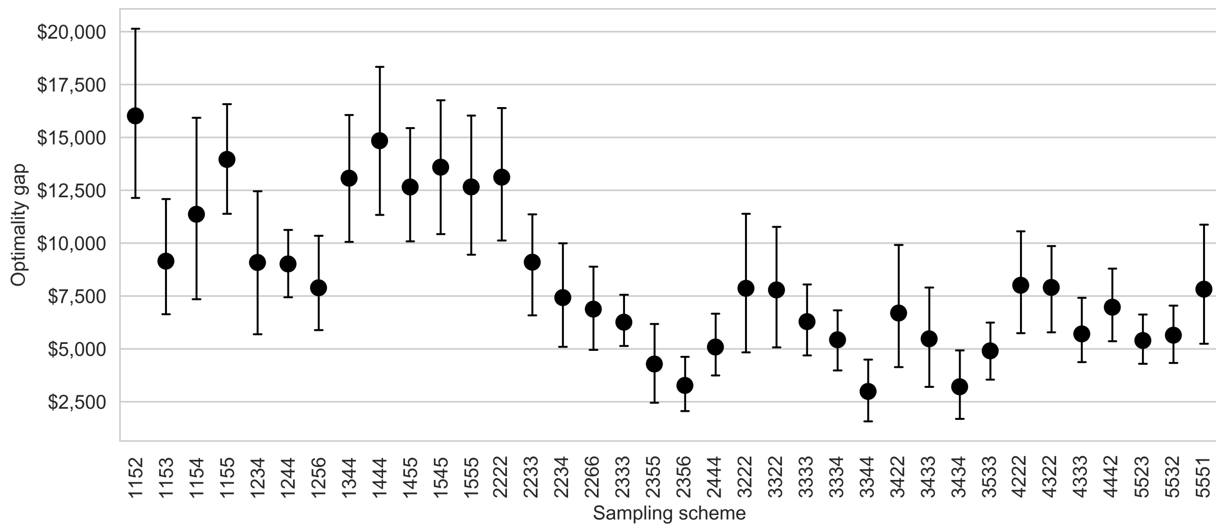

Figure 2.3: *Change of optimality gap values due to the sample size and the configuration of the sampling scheme using severe climate change data*

Table 2.3: *Value of the stochastic solution*

$\|\Omega\|$	ϵ	$z(\bar{x})$	$z(x^*)$	infeasible scen.	VSS	VSS(bp)
256	1	7,775,108	7,782,679	0	7,571	9.96
200	20	7,160,950	7,256,069	3	95,119	132.83
200	40	4,940,204	6,737,368	60	1,797,163	3,637.83

2.4 Discussion and conclusions

Climate change is a serious issue in forest management planning. In a study conducted in Norway, the majority of forest managers showed the importance of addressing climate change in forest planning (Heltorp et al., 2018). Several researchers conducted similar studies in different ecosystems and reached analogous results (Scheller and Parajuli, 2018; Liu et al., 2020). To ensure the sustainability of forest resources, forest managers need to incorporate forest growth uncertainty in harvest scheduling models. In this work, we formulated a stochastic harvest scheduling model with forest growth uncertainty due to climate change and solved the model using sample average approximation (SAA). We tested the modeling and solution using climate change data transformed to forest growth change. We compared the robustness of the stochastic solution to the deterministic one by randomly generating a set of scenario and comparing the expected NPV if we implement the stochastic solution and the NPV if we use the deterministic solution. The numerical results showed that SAA allows to have stochastic solutions that are close enough to the true optimal solution when the sample size is large enough. However, large sample size leads to an exponential increase of solution time. This pattern of the computational complexity growing exponentially with the sample size was previously suggested by Kleywegt et al. (2001).

One of the main limitations of the proposed method is the computation required in step d of the algorithm presented in Figure 2.1. As we discussed in the previous paragraph, the increase of the sample size leads to an exponential increase in solution time. It is therefore important to have a strategy that allows to reduce the sample size while producing solutions that allow the convergence of SAA solutions to the true optimal solutions. Our tests suggest that with the appropriate sampling scheme, it is possible to reach convergence with smaller sample sizes. For instance, the sampling schemes `2356` and `3344` yielding sample sizes of 180 and 144, respectively, have smaller optimality gaps and variances compared to a sample size of 625 which stemmed from a sampling scheme of `5555`. In conclusion, when we adopt the adequate sampling strategy that allows to sufficiently explore the first stage and generate large samples for future stages, we can limit the number of scenarios necessary for the SAA solution to converge to the true optimal solution.

The proposed model not only allows the managers to make intelligent decision now, but also allows the preservation of forest resources that take time to replenish once depleted. Indeed, the stochastic solution is robust to different growth scenario whereas, the deterministic one is infeasible to many of the tested growth scenarios. These results are in line with the ones obtained by Álvarez-Miranda et al. (2018); Garcia-Gonzalo et al. (2020). The infeasibility of the deterministic solution stems mainly from the fact that the wood flow constraints are violated due to an intensive harvest in early periods.

In addition, the solution method proposed in this paper is easy to develop and implement by many forest managers. Unlike the methods used in Garcia-Gonzalo et al. (2016, 2020) that require to know the probability distribution of the random parameter, SAA does not require such information. The method relies on the fact that if the sample size is large enough, then the sample statistics will approximate those of the actual population. The method is also suitable for many applications where the objective function cannot be computed in a closed form such as the so-called black-box optimization problems (Kim and Ryu, 2011) and the stochastic knapsack problem (Kleywegt et al., 2001). In forestry, this method is well suited for harvest scheduling problems with wood price and demand uncertainties because we can extract samples from historical demand and price without the need to model the price like done in Rios et al. (2016); Alonso-Ayuso et al. (2018). Compared to stochastic programming which requires the so-called non-anticipativity constraints (Bagaram et al., 2020; Garcia-Gonzalo et al., 2020), the SAA model is relatively smaller in terms of number of constraints (and possibly in terms of number of variables, depending on the formulation) since it does not require such constraints.

Regarding climate change data, we used the information of climate change forecast with statistical models developed in Latta et al. (2009). Unlike the data from Garcia-Gonzalo et al. (2016); Álvarez-Miranda et al. (2018); Garcia-Gonzalo et al. (2020), which originated from a process-based modeling, statistical models of forest growth under climate change are much more common (e.g. Elli et al. (2020)). Hence, the method developed in this study can easily be extended to other forest systems. Moreover, it is straight forward to translate forecast of precipitation, air moisture and temperature into forest growth compared to processed-based models which require the expertise in plant biology.

Finally, this research can be extended by considering other sources of uncertainty such as the price of wood, or the demand of forest products. In this study we assumed that climate change does not lead to species transition. In some cases, one might need to consider the species shift because of climate change. It would be interesting to include this information in the decision-making process and provide to forest practitioners a range of options when implementing harvest scheduling plans and the choice of species for regeneration.

Appendix

2.A Deterministic harvest scheduling model

The objective function (2.A.1) is to maximize the net present value from forest harvest. This objective function includes the cost of harvest and re-plantation for each forest unit. In addition, this objective function accounts for the value of the stands that are not harvested during the planning horizon because those stands have a monetary value. Constraint set (2.A.2) imposes that if a stand is harvested now, then it cannot be harvested in subsequent years. In other words a forest unit can only be harvested once during the whole planning horizon. The use of n_s variables is to account the stands that are not scheduled for harvest in the whole planning horizon. Constraint set (2.A.3) compute the volume of wood harvested now and in the future periods during the planning horizon, respectively. Constraint sets (2.A.4) and (2.A.5) impose that the volume fluctuation between two consecutive stages should be within a fixed lower and upper bounds, respectively. These sets of constraints are also known as even flow constraint since they ensure that the exploitation of forest resources is evenly distributed in time. Even with constraint sets (2.A.4) and (2.A.5), there is a possibility that the volume harvested declines with time. Hence volume at $t = 4$ is much lower than volume at $t = 0$, for instance. To attenuate this effect, we impose supplementary wood flow constraints which are constraint sets (2.A.6) and (2.A.7). These two set of constraints impose flow restriction between two non consecutive stages. Constraint set (2.A.8) states that the age of the forest at the end of the planning horizon should be greater or equal to the current age of the forest. This constraint is a proxy for sustainability; it ensures that forest resources are not depleted during the planning horizon. Finally, the definition of the variables are given in (2.A.9).

$$\max \sum_{s=1}^{|\mathcal{S}|} \left[\sum_{t=0}^{T} r_{st} x_{st} + r_{s0} w_s \right] \tag{2.A.1}$$

subject to

$$n_s + \sum_{t=0}^{T} x_{st} = 1 \qquad s = 1, \ldots, |\mathcal{S}| \tag{2.A.2}$$

$$\sum_{s} v_{st} x_{st} = H_t \qquad t = 0, \ldots, T \tag{2.A.3}$$

$$H_t^i \leq \alpha H_{t-1} \qquad t = 1, \ldots, T \tag{2.A.4}$$

$$H_t^i \geq \beta H_{t-1} \qquad t = 1, \ldots, T \tag{2.A.5}$$

$$H_t \leq \gamma H_{t-2} \qquad t = 2, \ldots, T \tag{2.A.6}$$

$$H_t^i \geq \lambda H_{t-2} \qquad t = 2, \ldots, T \tag{2.A.7}$$

$$\sum_{s \in \mathcal{S}} a_s \left[\sum_{t=0}^{\mathcal{T}} age_{st} x_{st} + age_{s0} w_s \right] \geq \sum_{s} a_s age_{s.} \tag{2.A.8}$$

$$w_s \in \{0,1\}, \ \forall s, \ x \in \{0,1\}^{|\mathcal{S}| \times T+1}, \ \ H_t \geq 0 \quad \forall t \tag{2.A.9}$$

References

Alonso-Ayuso, A., Escudero, L. F., Guignard, M., Quinteros, M., and Weintraub, A. (2011). Forestry management under uncertainty. *Annals of Operations Research*, 190(1):17–39.

Alonso-Ayuso, A., Escudero, L. F., Guignard, M., and Weintraub, A. (2018). Risk management for forestry planning under uncertainty in demand and prices. *European Journal of Operational Research*, 267(3):1051–1074.

Álvarez-Miranda, E., Garcia-Gonzalo, J., Ulloa-Fierro, F., Weintraub, A., and Barreiro, S. (2018). A multicriteria optimization model for sustainable forest management under climate change uncertainty: An application in Portugal. *European Journal of Operational Research*, 269(1):79–98.

Bagaram, M. B., Jaross, W., and Weintraub, A. (2020). A Parallelized Variable Fixing Process for Solving multistage Stochastic Programs with Progressive Hedging An Application to Harvest Scheduling in the Face of Climate Change A Parallelized Variable Fixing Process for Solving multistage Stochastic Programs. *preprint*, (June).

Birge, J. R. (1982). The value of the stochastic solution in stochastic linear programs with fixed recourse. *Mathematical Programming*, 24(1):314–325.

Chunlin, D. and Liu, Y. (2012). Sample Average Approximation Method for Chance Constrained Stochastic Programming in Transportation Model of Emergency Management. *Systems Engineering Procedia*, 5:137–143.

Dixon, B. L. and Howitt, R. E. (1980). Resource Production Under Uncertainty: A Stochastic Control Approach to Timber Harvest Scheduling. *American Journal of Agricultural Economics*, 62(3):499–507.

Elli, E. F., Sentelhas, P. C., and Bender, F. D. (2020). Impacts and uncertainties of climate change projections on Eucalyptus plantations productivity across Brazil. *Forest Ecology and Management*, 474(March):118365.

Emelogu, A., Chowdhury, S., Marufuzzaman, M., Bian, L., and Eksioglu, B. (2016). An enhanced sample average approximation method for stochastic optimization. *International Journal of Production Economics*, 182:230–252.

Garcia-Gonzalo, J., Pais, C., Bachmatiuk, J., Barreiro, S., and Weintraub, A. (2020). A Progressive Hedging Approach to Solve Harvest Scheduling Problem under Climate Change. *Forests*, 11(2):224.

Garcia-Gonzalo, J., Pais, C., Bachmatiuk, J., and Weintraub, A. (2016). Accounting for climate change in a forest planning stochastic optimization model. *Canadian Journal of Forest Research*, 46(9):1111–1121.

Heltorp, K. M. A., Kangas, A., and Hoen, H. F. (2018). Do forest decision-makers in Southeastern Norway adapt forest management to climate change? *Scandinavian Journal of Forest Research*, 33(3):278–290.

Kim, S. and Ryu, J.-h. (2011). The sample average approximation method for multi-objective stochastic optimization. In *Proceedings of the 2011 Winter Simulation Conference (WSC)*, pages 4021–4032. IEEE.

Kleywegt, A. J., Shapiro, A., and Homem-De-Mello, T. (2001). The sample average approximation method for stochastic discrete optimization. *SIAM Journal on Optimization*, 12(2):479–502.

Kooten, G. C. V., Kooten, R. E., and Brown, L. G. (1992). Modeling the effect of uncertainty on timber harvest: A suggested approach and empirical example. *Journal of Agricultural and Resource Economics*, 17(1).

Latta, G., Temesgen, H., Adams, D., and Barrett, T. (2010). Analysis of potential impacts of climate change on forests of the United States Pacific Northwest. *Forest Ecology and Management*, 259(4):720–729.

Latta, G., Temesgen, H., and Barrett, T. M. (2009). Mapping and imputing potential productivity of Pacific Northwest forests using climate variables. *Canadian Journal of Forest Research*, 39(6):1197–1207.

Liu, K., He, H., Xu, W., Du, H., Zong, S., Huang, C., Wu, M., Tan, X., and Cong, Y. (2020). Responses of korean pine to proactive managements under climate change. *Forests*, 11(3):1–19.

Mak, W. K., Morton, D. P., and Wood, R. K. (1999). Monte Carlo bounding techniques for determining solution quality in stochastic programs. *Operations Research Letters*, 24(1):47–56.

Mäkinen, A. and Borges, J. G. (2013). Review . Assessing uncertainty and risk in forest planning and decision support systems : review of classical methods. *Forest Systems*, 22(2):282–303.

Mohammadi Bidhandi, H. and Patrick, J. (2017). Accelerated sample average approximation method for two-stage stochastic programming with binary first-stage variables. *Applied Mathematical Modelling*, 41:582–595.

Pagnoncelli, B. K. and Piazza, A. (2017). The optimal harvesting problem under price uncertainty: the risk averse case. *Annals of Operations Research*, 258(2):479–502.

Piazza, A. and Pagnoncelli, B. K. (2014). The optimal harvesting problem under price uncertainty. *Annals of Operations Research*, 217(1):425–445.

Pour, A. G., Naji-Azimi, Z., and Salari, M. (2017). Sample average approximation method for a new stochastic personnel assignment problem. *Computers and Industrial Engineering*, 113:135–143.

Pukkala, T. (1998). Multiple risks in multi-objective forest planning : integration and importance. *Forest Ecology and Management*, 111:265–284.

Rios, I., Weintraub, A., and Wets, R. J. (2016). Building a stochastic programming model from scratch: a harvesting management example. *Quantitative Finance*, 16(2):189–199.

Ross, K. L. and Tóth, S. F. (2016). A model for managing edge effects in harvest scheduling using spatial optimization. *Scandinavian Journal of Forest Research*, 31(7):646–654.

Scheller, R. M. and Parajuli, R. (2018). Forest management for climate change in New England and the Klamath Ecoregions: Motivations, practices, and barriers. *Forests*, 9(10).

Schütz, P., Tomasgard, A., and Ahmed, S. (2009). Supply chain design under uncertainty using sample average approximation and dual decomposition. *European Journal of Operational Research*, 199(2):409–419.

Veliz, F. B., Watson, J.-P., Weintraub, A., Wets, R. J.-B., and Woodruff, D. L. (2014). Stochastic optimization models in forest planning: a progressive hedging solution approach. *Annals of Operations Research*, pages 259–274.

Wang, W. and Ahmed, S. (2008). Sample average approximation of expected value constrained stochastic programs. *Operations Research Letters*, 36(5):515–519.

Chapter 3. Integrating Forest Growth Uncertainty due to Climate Change in Harvest Scheduling

Summary

Climate change affects forest growth and yield and therefore, requires making sound decision without knowing what the future climate will be. To address this uncertainty, we propose a multistage stochastic programming framework. Although scenario tree generation is the most crucial step in multistage stochastic programming, its definition for stochastic harvest scheduling with forest growth under climate uncertainty is not a trivial task. Typically, scenario trees are generated using historical data, expert opinions, or the combination of both. However, because climate change is forecast as climate paths, these typical techniques require some adaptations to reduce the range of uncertainty set to consider in the stochastic programming. Although it has been shown that the four climate paths forecast by climate experts will disparately affect forest growth in the Pacific Northwest, the likelihood of these climate paths is unknown. The challenge in incorporating climate change in harvest planning models is exacerbated by the fact that there is uncertainty in how these climate paths translate into forest growth. In this paper, we devise an approach for generating scenario trees for stochastic harvest scheduling with climate uncertainty. To reduce the uncertainty under consideration, we propose to first consider the four climate paths separately and to generate scenario trees assuming the climate path of interest will occur. Second, we compare the net present value of making correct or wrong assumption of future climate path. The analysis showed that having an optimistic attitude, which is to manage forest expecting increase of

forest growth due to climate change, is preferable.

3.1 Introduction

The continuous provision of forest products and services is at the core of forest planning. Although there exist different land tenure with diverging primary objectives such as conservation of wildlife habitat (St John et al., 2018), preservation of rare species (Ross and Tóth, 2016; Tóth et al., 2009), and provision of ecosystem services (Schroder et al., 2016), one of the main concerns of forest companies, is the maximization of their net present value while having sustainable production of forest products. For these companies, forests in addition of being resources, are also the product they market. Therefore, sustainability of forest products and resources is not only a slogan but a state-of-the-art business practice. To achieve this objective, these companies need to forecast their forests future growth and yield. The typical approach used in achieving this endeavor is the use of historical growth and yield data. However, since climate change affects forest growth and yield, these parameters estimated from historical data do not reflect the future state of the forest (Elli et al., 2020).

Growth and yield parameters are used to build harvest scheduling or harvest planning which aims at prescribing forest units or stands that ought to receive a specific treatment, e.g. harvest in each time period. When these parameters are known with certainty, such as in the case of using their expected values, the harvest scheduling is qualified of deterministic harvest models. There are several methods describing approaches for solving such models (St. John and Tóth, 2015; Ross and Tóth, 2016; Moriguchi et al., 2020). However, this expected value approach is not suitable when the forest growth is subject to considerable change due to climate change. It is therefore advised to have a stochastic optimization model that allows planners to make robust decisions with limited information of what the actual forest growth will be. The stochastic model considers the range of possible values of growth and yield instead of a single value like in the case of the deterministic model. These possible values also known as scenarios are the discretization of the random parameter. The set of scenarios forms a scenario tree with a probability associated with each scenario. This discretization process is crucial for stochastic programming because poor discretization lead to suboptimal decisions (Rios et al., 2016). Although this study is not the first one addressing uncertainty in forest management planning, see (Álvarez-Miranda et al., 2018; Garcia-Gonzalo et al., 2020), to the best of our knowledge, this is the first study that considers the peculiar nature of climate change. Indeed, climate change is forecast as possible but not probable futures, and it is not clear how this information should be incorporated in building harvest scheduling models.

The challenge of building stochastic harvest scheduling models under climate uncertainty occurs at three levels. First, climate change is forecast as climate paths or pathways with each one representing some assumptions on the future (advancement in technology, human population growth, CO_2 emission, etc.). The challenge is that there is no information on the likelihood of each one of those climate paths. In the Pacific Northwest, there was a study conducted on how forest growth will change in face of four different climate paths (Latta et al., 2010). The results showed that forest behavior under each one of those climate paths will be different depending on the location and the altitude of the forest. Similar results were obtained in a different study in Brazil (Elli et al., 2020). If we decide to build a stochastic model, considering all the climate paths, then our model would consider a too large set of uncertainties which may lead to suboptimal decisions.

Second, there is uncertainty on how forest will grow under each one of those climate paths. Even if we knew which climate path will materialize, there is substantial uncertainty as to what magnitude the actual growth will change. Thus, there is uncertainty of the harvest scheduling considering a single climate path.

Ultimately, because of climate change mitigation efforts and the advancement in technology, there is no guarantee that if the climate of the next decade represents one of the climate paths, then the same climate will remain in the following decades. Indeed, because of mitigation efforts, it is possible to transition from one climate path to a different one in the same decade. It is important to highlight that the objective of generating the scenario tree is not to have a perfect scenario tree but a tree that captures the underlying stochastic process that is suitable for strategic planning. It is logical therefore, to wonder what represents a good tree and how do we know we possess a tree faithfully describing the underlying stochastic process.

The objective of this paper is to devise a method for incorporating forest growth uncertainty stemming from climate change into harvest scheduling models for forest companies. Our contributions are as follows:

1. We investigate strategies to adopt for sampling scenarios necessary for incorporating climate change into forest management planning. Beforehand, we propose considering the climate paths separately. Under each climate path, since the growth change distribution due to modeling limitation of forest growth under climate change is barely known, we assess the solution behavior when considering scenarios following normal and uniform theoretical distributions. The normal distribution assigns high weights to scenarios that are close to the expected growth whereas, the uniform distribution assigns the same weight to all the scenarios. Second, we propose computing the solution from each climate path and its bounds. This solution is an indicator of a true solution that is achievable considering that climate path. If using the solution from one climate path in the solution provided by a different climate path leads to objective function values that are within the bounds, then we can conclude that the two climate paths do not yield significantly different solutions and therefore considering one of the two climate paths is sufficient.

2. We develop a very comprehensive harvest scheduling model that is suitable for both tactical and strategical harvest planning which integrates all the constraints in the forest industry in particular the spatial constraints. To our knowledge, most papers limit themselves to simplified harvest models. We show as well that if the decision maker is more interested in maximizing their net present value, then the optimal attitude they should have is to expect an optimistic climate change which predicts an increase of forest growth.

The rest of this paper is organized as follows. We cover the literature on scenario generation for stochastic programming in Section 3.2. In Section 3.3, we present the procedure used for generating scenario trees, we stress as well the properties that a suitable scenario tree ought to have. In Section 3.4, we apply the methodology to a case study; and finally in Section 3.5, we discuss the results and provide some conclusions and recommendation for future work.

3.2 Literature review

To begin, it is worth emphasizing that though this paper deals with stochastic programming, the uncertainty in mathematical models can be addressed through several modeling paradigms such as robust optimization, stochastic programming, and chance constrained optimization (Apap and Grossmann, 2017; Crespi et al., 2018; Marla et al., 2020). The aim of robust optimization is to guarantee feasibility over the specified uncertainty set (Séguin et al., 2017). It is known that when the full set of uncertainty is considered, robust optimization results in the worst-case solution. Since robust optimization aims at producing feasible solutions, it is a method that produces conservative solutions. According to Apap and Grossmann (2017), robust optimization is only suitable for short term planning where feasibility is the main concern. In general, harvest scheduling is a long-term planning problem that might not be suitable for robust optimization.

In the case of stochastic programming, the decision maker needs to implement a decision at the beginning of the planning horizon without knowing what the value of the uncertainty parameter(s) will be. After a period, in which the uncertainty might reveal itself, the decision maker can take a recourse action. If the sequence of implementing decisions and taking recourse actions occurs only once, then the stochastic programming is referred to as a two-stage stochastic program, otherwise the stochastic programming is known as multistage stochastic programming. Because multistage stochastic programming does not fix all actions that should be taken in advance, it is a method suitable for long term planning such as harvest scheduling (Apap and Grossmann, 2017). However, unlike robust optimization, stochastic programming relies on the discretization of the continuous uncertain parameters and the probability associated with each realization of the uncertainty. Each realization of the uncertain parameters is known as a scenario and the set of scenarios form the scenario tree. The scenario tree generation constitutes the first step for building multistage stochastic programming models.

There are many methods for building scenario trees. These methods include moment matching, sampling average approximation, clustering and conditional sampling. Moment matching is a method aiming at matching statistical moments between the scenario tree and the distribution of the random parameter. The technique was developed by Fleishman (1978) for univariates, however Høyland et al. (2003) extended its use to multivariate cases. The principle of this method is to generate a scenario tree with its properties (with moments such as average, standard deviation, skewness and kurtosis) matching the ones of the theoretical distribution of the random parameter. A description of the steps to undertake for implementing moment matching is described in Høyland et al. (2003). A shortcoming of the method is that the scenario generation step itself requires solving an optimization problem that is not linear. Furthermore, as shown by Hochreiter and Pflug (2007) and highlighted by Löhndorf (2016) there could be many theoretical distributions having the same first moments such as the one listed. The method has been mainly successfully applied for scenario generation in portfolio management (Høyland and Wallace, 2001; Høyland et al., 2003; Ponomareva et al., 2015). Nevertheless, Rios et al. (2016) tested the performance of the method for forest harvest scheduling with price uncertainty with limited success.

The sampling average approximation (SAA) technique is relatively simple to implement. It consists of drawing repetitively many samples from the distribution of the random parameter and solving the optimization problem. It is shown that, if the sample size is large enough, the average solution will approximate the true solution. With that regard, Mak et al. (1999) showed that the expectation of individual solutions corresponds to the lower bound on the true solution of the stochastic model and that the bound monotonically increases as the sample size increases (for minimization problems). For a formal description, the reader is referred to Löhndorf (2016). Sample average approximation (SAA) has been applied in several fields such as portfolio selection (Wang and Ahmed, 2008), supply chain design and supply chain network, transportation (Schütz et al., 2009; Chunlin and Liu, 2012), and personnel assignment (Pour et al., 2017). One limitation of the method is that it may require solving hundreds or thousands of optimization problems in order to achieve stability. Although the method performs well for two-stage stochastic problems, it does not yield the level of flexibility a decision maker may need in the case of multistage stochastic programming.

The idea of scenario clustering is to generate a set of data paths known as a 'fan' (Beraldi and Bruni, 2013) that represents possible futures and then to proceed into grouping these paths into a scenario tree. This technique is sometimes referred to as distribution free scenario generation since it relies on generating paths that correspond to past scenarios (Dupacová et al., 2000) or experts view of the future (Hochreiter and Pflug, 2007; Heitsch and Römisch, 2009). The main purpose of the scenario clustering is to reduce the computational burden of a scenario tree that is too fine (Séguin et al., 2017). Nevertheless, the technique inherits the drawbacks of the methods used for generating the initial scenario tree (Xu et al., 2015). The technique has been extensively employed in the field where the future behavior of the stochastic process is deemed to be akin to previous observations. Particular domains of applications of the method include portfolio management (Gülpinar et al., 2004; Hochreiter and Pflug, 2007; Beraldi and Bruni, 2013), interest rate management in investments (Pranevicius and Sutiene, 2007), hydroelectric power management (Dembo et al., 1990; Gröwe-Kuska et al., 2003; Xu et al., 2015), and reservoir management (Li et al., 2018).

None of the aforementioned methods is out of the box suitable for harvest scheduling with climate uncertainty. For instance, in the case of Álvarez-Miranda et al. (2018); Garcia-Gonzalo et al. (2020), forest growth scenarios resulting from climate change were provided by an independent research. Therefore, the scenario tree might not be tailored to address the level of uncertainty in forest growth. In addition, because the scenario tree was given in these studies, they did not explicitly consider the two levels of uncertainty that are considered in this research. In the following section, we describe our methodological approach in overcoming the challenges that harvest scheduling under climate uncertainty poses especially when we consider forest growth prediction from statistical models.

3.3 Methodology

To formally introduce the scenario generation procedure, we present the general form of the stochastic problem we intend to solve. Let us consider that the stochastic problem of interest is presented as (3.1) where ξ is the continuous random vector which does not depend on x; the expectation is taken with respect to ξ. X is the set of constraints that the decision variable vector x needs to satisfy, and z^* is the true objective function value of the stochastic program.

$$z^* = \min_{x \in X} \mathbb{E}\, f(x, \xi) \tag{3.1}$$

However, we cannot solve directly problem (3.1) because of the presence of the continuous random vector ξ, we can use the approximation of (3.1) by

$$\tilde{z} = \min_{x \in X} \mathbb{E}\, f(x, \tilde{\xi}), \tag{3.2}$$

where $\tilde{\xi}$ is the discretization of the random continuous vector into a scenario tree (see Section 3.3.1 for formal definition of the scenario tree). Since $\tilde{\xi}$ is discrete realizations of the random vector ξ, we could rewrite (3.2) using the summation. However, we leave this definition for later once we have defined the structure of $\tilde{\xi}$.

3.3.1 Scenario trees generation

Scenario tree structure

Before diving into how to build scenario trees, first let's briefly describe the scenario tree structure. The random process in multistage stochastic programming can be represented as a "scenario tree" which has the following structure. Let $\mathcal{T}$ denote the set of periods in the planning horizon with $T = |\mathcal{T}|$ being the number of stages at which decisions can be made. A node of the scenario tree represents the realization of the uncertain parameters and variables at a given time period. It is a possible state of the forest at a given time $t \in \mathcal{T}$. Let n and $\mathcal{N}$ describe the node and the lexicographically numbered set of nodes $\{1, ..., |\mathcal{N}|\}$ in the tree, respectively. From each node n, for $t \in \mathcal{T} \setminus \{T\}$ there is at least one branch leading to another node m with probability P_m. Let Ω represent the finite set of representative scenarios in the tree. A scenario $\omega \in \Omega$ is a particular realization of the uncertain parameter represented as a path from the root-node to a leaf-node (terminal nodes). Each scenario ω has a probability or weight denoted by w^ω. Note that $\sum_{\omega \in \Omega} w^\omega = 1$. We can now rewrite (3.2) as:

$$\tilde{z} = \min_{x \in X} \sum_{\omega=1}^{|\Omega|} w^\omega f(x, \omega), \tag{3.3}$$

where $f(\cdot, \omega)$ is the optimization function evaluated for the scenario ω.

Decisions are made at each stage and implemented in the subsequent period. For instance, in Figure 3.1, $t = 1$ represents the first stage (stage 1). At the first stage, the decision maker needs to decide which forest units will be harvested in the first period without knowing which scenario will occur. The period is the time between two consecutive stages. Hence, $t = 1$ marks the beginning of the first period and $t = 2$ marks its end. In the example of Figure 3.1, we have three stages and two periods. The value of the random parameter is only revealed in periods while the decision needs to be taken at the stage before the uncertainty is revealed. The natural question becomes: What is the procedure to generate the scenarios necessary for solving (3.3)? and what is the appropriate number of scenarios $|\Omega|$? We address the two questions in the next sections.

Scenario generation procedure

Scenario generation is more than a science, it is an art (Casey and Sen, 2005) that gives the modeler the flexibility to decide on the structure of the scenario tree through discretization of the random vector. Fine discretization of the continuous random vector leads to a computationally intractable stochastic program, while a coarse discretization leads to a tree that may completely alter the structure of the underlying stochastic process the scenario tree ought to represent. Although many researchers focused on scenarios' generation for stochastic programming, the scenario tree is not an end but a wherewithal to solve stochastic programs.

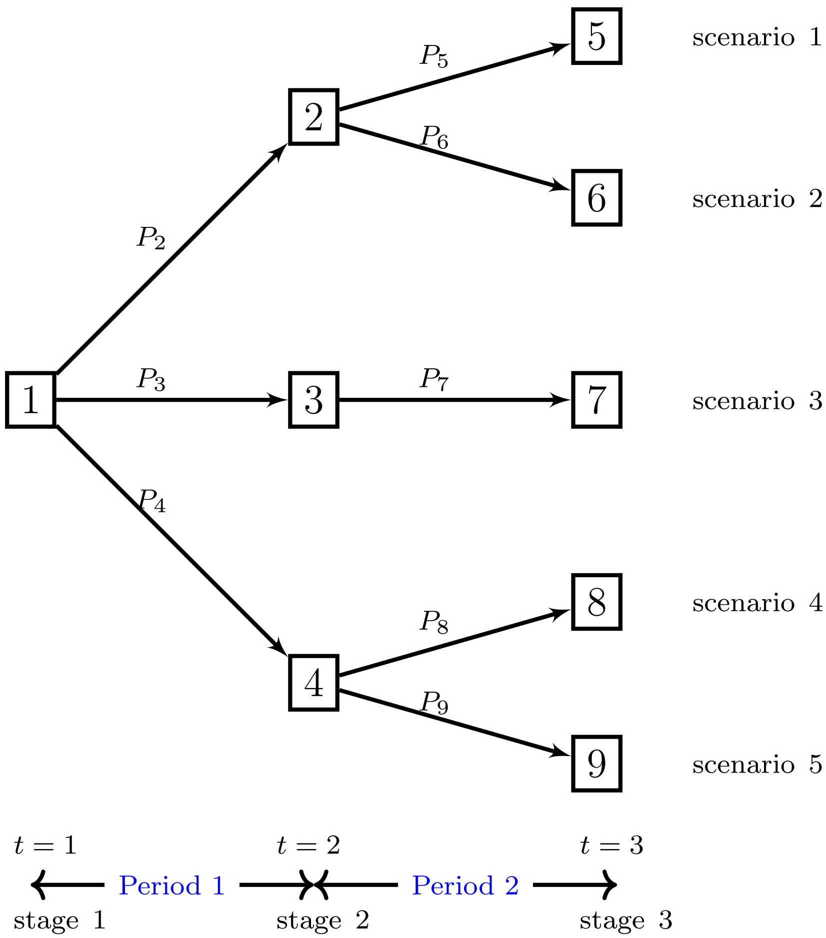

Figure 3.1: *Scenario tree representation of stochastic programming. The scenario tree shows five scenarios with three stages*

The scenario tree, therefore, ought to have some properties like stability, unbiasedness and minimal stochastic optimality gap[1]. These properties will be discussed in Section 3.3.2.

The framework used for building scenario trees in this research is based on conditional sampling. The method consists of fitting at each node of the scenario tree a conditional probability density function and sampling from it the values that successor nodes will have. Hence, except the root-node which has no predecessor node, the value of each node depends

[1]This is different from MIP optimality gap

on its predecessor's value. This method has the advantage of controlling the range of values that each node may take depending on the process that led to it. In addition, the modeler could specify edge cases that should be represented by the scenario tree.

The procedure implemented for scenario generation is inspired from Alonso-Ayuso et al. (2018), however, with many differences. It consists of dividing the sampling space of forest growth change into an equal number of parts corresponding to number of branches the scenario tree should have at the given stage. To illustrate the method, let's suppose the random parameter is normally distributed as illustrated in Figure 3.2. In the figure, $t = \{1, 2, 3\}$ represents stages at which decisions are taken. Let L and U be the lower and the upper bounds, respectively, of the support of the random parameter ξ. The node a is the root-node and there is no growth change associated with it. However, the values of nodes b, c and d are drawn from a normal distribution with mean μ_a, standard deviation σ_a and support Ξ_a. We denote by Φ_a the associated cumulative density function. For all nodes j in the scenario tree, we require that $\Xi_j \subseteq [L, U]$. Notice that for normally distributed random variables with mean μ_a and variance σ_a^2, 99.73% of the cumulative density is within the interval $\Xi'_a = [\mu_a - 3\sigma_a, \mu_a + 3\sigma_a]$. Let β designate the number of branches that should originate from node a (β is the number of successor nodes). Let's divide Ξ'_a into equal intervals of width $w = 6\sigma_a/\beta$. The probability associated with each one of the successor nodes is given using the cumulative density for the interval in which the successor node is uniformly drawn from. For instance, the value of $b \in [L, \mu_a - 3\sigma_a + w]$ with a probability of P_b which is the cumulative density of that interval. For example, from Figure 3.2, $\beta = 3$, $w = 2\sigma_a$. Hence, nodes b and c, for instance, are uniformly drawn from interval $[L, \mu_a - \sigma_a]$ with a probability of 0.16 and $[\mu_a - \sigma_a, \mu_a + \sigma_a]$ with a probability of 0.68, respectively, In other words, $P_b = \Phi_a(\mu_a - \sigma_a) = 0.16$ and $P_c = \Phi_a(\mu_a + \sigma_a) - \Phi_a(\mu_a - \sigma_a) = 0.68$. To build the scenario tree, we repeat the process for each node until the leaf nodes corresponding to the terminal stage. As shown, in Figure 3.2, we arbitrarily chose the number of branches $\beta = 3$. One may wonder whether such a value of β, dictating the number of scenarios in the scenario tree, is justified. The question is what represents the appropriate number of branches suitable? To answer to this question, we need to assess the properties of the generated scenario tree.

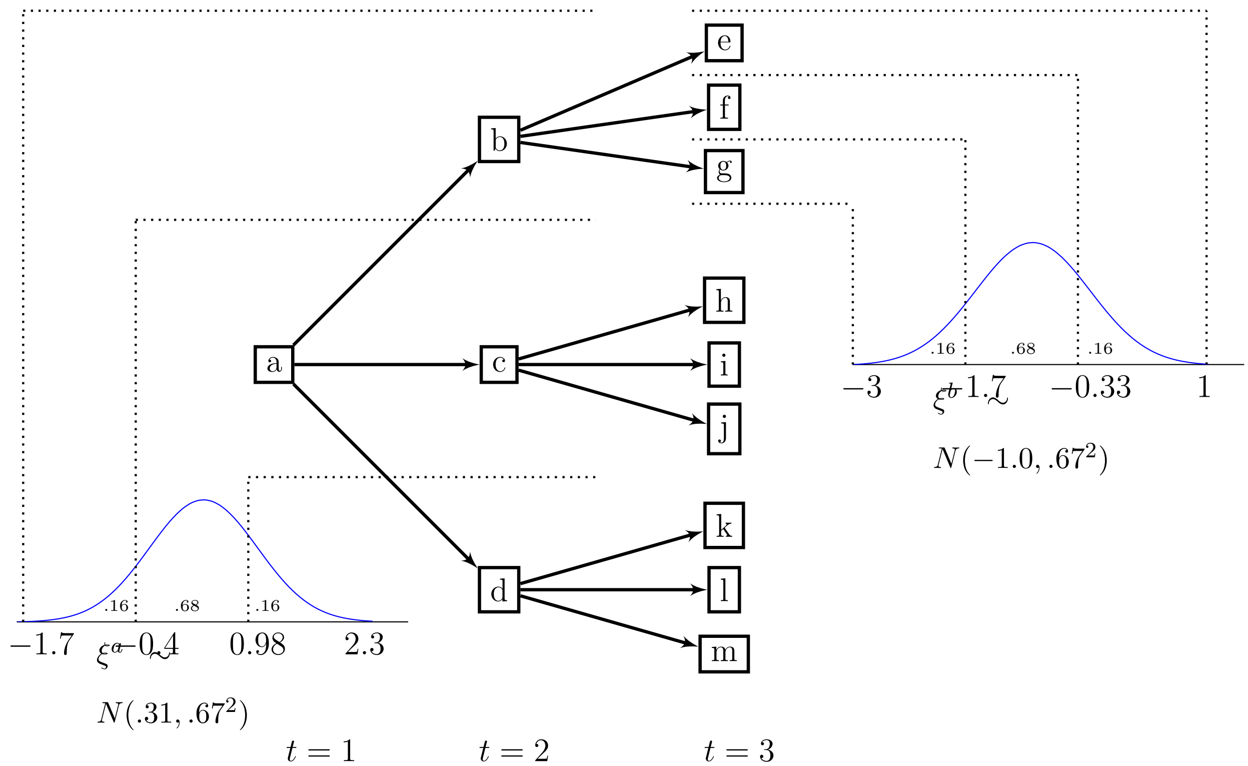

Figure 3.2: *Growth change scenario generation process*

3.3.2 Properties of a good scenario tree

Since the process of generating scenario trees described in Section 3.3.1 is stochastic, two runs of the scenario generation procedure might lead to two different scenario trees. However, this difference should not be significant as to affect the optimal solution of the stochastic programming. If the difference is substantial, then the scenario tree is not stable. This stability in scenario generation is measured through in-sample stability and out-of-sample stability (Kaut and Wallace, 2007).

In-sample stability

In-sample stability measures whether the difference in the solution using two different scenario trees generated from the same process is just due to the randomness in the process and not to the structure of the scenario tree. Let's suppose we generate two scenario trees $\tilde{\xi}_1$ and $\tilde{\xi}_2$ with the same structure (same number of scenarios and same number of branches at each stage). By in-sample stability, the objective function values of the two scenario trees are approximately equal as:

$$\min_{x \in X} \mathbb{E}\, f(x, \tilde{\xi}_1) \approx \min_{x \in X} \mathbb{E}\, f(x, \tilde{\xi}_2). \tag{3.4}$$

A different way of expressing in-sample stability is to consider $\tilde{\xi}_1, \tilde{\xi}_2, \dots, \tilde{\xi}_k$ scenario trees with increasing size, such that $|\tilde{\xi}_1| < |\tilde{\xi}_2| < \cdots < |\tilde{\xi}_{k-1}| < |\tilde{\xi}_k|$ where $|\cdot|$ is the number of scenarios. If there is in-sample stability then

$$\min_{x \in X} \mathbb{E}\, f(x, \tilde{\xi}_{k-1}) \approx \min_{x \in X} \mathbb{E}\, f(x, \tilde{\xi}_k). \tag{3.5}$$

In other words, increasing the size of the scenario tree does not alter the solution and therefore, the scenario tree reached in-sample stability.

Out-of-sample stability

Out-of-sample stability is guaranteed if for two scenario trees $\tilde{\xi}_1$ and $\tilde{\xi}_2$ with the same structure, we can write:

$$\mathbb{E}\left[f\left(\arg\min_{x \in X} \mathbb{E}\left[f(x, \tilde{\xi}_1) \right], \xi \right) \right] \approx \mathbb{E}\left[f\left(\arg\min_{x \in X} \mathbb{E}\left[f(x, \tilde{\xi}_2) \right], \xi \right) \right]. \tag{3.6}$$

In practice, (3.6) is impossible to evaluate because we cannot evaluate the value of the approximated solution on each value of the continuous random vector. After all, we would not need the scenario tree if we could solve directly the continuous random process expressed by ξ.

Since (3.6) is impossible to verify, we can check out-of-sample stability by implementing a Monte-Carlo like approach (Mak et al., 1999; Rios et al., 2016) and assuming out-of-sample stability if we can state that

$$\frac{1}{n}\sum_{i=1}^{n} f(\tilde{x}^1, \tilde{\xi}_i) \approx \frac{1}{n}\sum_{i=1}^{n} f(\tilde{x}^2, \tilde{\xi}_i), \tag{3.7}$$

where $\tilde{\xi}_1, ..., \tilde{\xi}_n$ are i.i.d scenario tree samples of the same structure like $\tilde{\xi}$ and $\tilde{x}^k = \arg\min_{x \in X} \mathbb{E}\left[f(x, \tilde{\xi}_k)\right], \quad k = 1, 2.$

Alternative stability measurement

A different way we measured the scenario tree stability since we are confident the scenario generation procedure possesses sufficient randomness, was through relative stability measurement (Guo et al., 2019). We generated a given number of scenarios of the same structure and computed the objective function for each one of them. We can find the largest (z^+) and the smallest (z^-) objective function values and compute the relative variability as $(z^+ - z^-)/z^+$. Then, we picked the scenario structure with a minimum number of scenarios that leads to a relative variability lower than a threshold fixed, say 1% or 0.5% (low variability means high stability).

Unbiasedness

Even when in-sample and out-of-sample stability are guaranteed, the discretization could still lead to a biased solution. The scenario tree leads to unbiased solutions if the expected solution and the true solution are approximately equal such as:

$$\mathbb{E}\left[f\left(\arg\min_{x \in X}\big[\mathbb{E}\, f(x, \tilde{\xi})\big], \xi\right)\right] \approx \min_{x \in X} \mathbb{E}\, f(x, \xi). \tag{3.8}$$

Although (3.8) is important for assuring that the scenario generation leads to a solution diverging little from the true solution, it cannot be evaluated since the original problem cannot be solved because of the presence of the continuous random vector ξ. Kaut and Wallace (2007) recommend to approximate the continuous variable through a 'reference tree'. Such a tree is the biggest possible tree that can be solved and it must be generated from a process known to be unbiased. We can assume an unbiassed scenario tree if on one hand, the process that generates the tree is random and on the other hand, the scenario tree fulfills the aforementioned properties.

3.3.3 Confidence interval on stochastic optimality gap

We have stated that it is impossible to solve the original problem with the continuous random vector ξ, as consequence, its approximation with $\tilde{\xi}$ was required. Even if the approximation leads to a scenario tree with the aforementioned properties (in-sample and out-of-sample stability, unbiasedness), we still need to know to what extent the objective function value of the approximation diverges from the true optimal value. The stochastic optimality gap $e(\tilde{\xi}, \xi)$ evaluates the error (negative bias in the case of minimization problems) of approximating ξ by $\tilde{\xi}$. Hence, $e(\tilde{\xi}, \xi)$ is computed as:

$$e(\tilde{\xi}, \xi) = \mathbb{E}\, f(\tilde{x}, \xi) - \min_{x \in X} \mathbb{E}\, f(x, \xi) \tag{3.9}$$

$$= \mathbb{E}\, f(\tilde{x}, \xi) - z^* \tag{3.10}$$

$$= \mu_{\tilde{x}}\ ; \tag{3.11}$$

where $\mu_{\tilde{x}}$ is the stochastic optimality gap of the solution $\tilde{x}$ obtained from the scenario tree $\tilde{\xi}$. Since we cannot evaluate the stochastic optimality gap directly, we can assess its bounds. The computation of those bounds are provided in Bayraksan and Morton (2006). We can estimate the stochastic optimality gap by computing its upper bound. We readily know that its lower bound is zero, corresponding to the solution from the scenario tree approximation which is as good as the true solution. The stochastic optimality gap of a candidate solution $\hat{x}$ is given by:

$$G_n(\hat{x}) = \frac{1}{n} \sum_{i=1}^{n} f(\hat{x}, \tilde{\xi}_i) - \min_{x \in X} \frac{1}{n} \sum_{i=1}^{n} f(x, \tilde{\xi}_i)\ ; \tag{3.12}$$

where $\tilde{\xi}_i$ is a scenario tree from the discretization of the random parameter ξ. Note that the term $G_n(\hat{x})$ is always positive. In-sample stability increases with the number of scenarios (the number of branches at each stage) for the four climate paths (Figure 3.1). The relative stability presented in Table 3.4 shows that except for the climate path B1, when the random parameter is uniformly distributed, which has a relative stability less than 1% when considering three branches at Consequently, it is necessary to define its upper bound. There are many methods used to that end. Those methods include multiple replications procedure (MRP), two replications procedure (TRP) and single replication procedure (SRP) (Mak et al., 1999; Bayraksan and Morton, 2006). However, in this research, we focus on MRP presented in Algorithm 1 because it allows to compute more robust bounds.

Algorithm 1 MRP

Input: Candidate solution $\hat{x}$, the number of samples n, the number of replications n_G and $\alpha \in [0, 1]$

1: **for** $i = 1, 2, ..., n_G$ **do**
2: Sample i.i.d observations $\tilde{\xi}_{i1}, \tilde{\xi}_{i2}, ..., \tilde{\xi}_{in}$ from the distribution of ξ
3: Calculate $G_n^i(\hat{x})$ using the (3.12)
4: **end for**
5: Calculate gap estimate $\overline{G}_{n_G}$ and variance $s_G^2(n_G)$

$$\overline{G}_{n_G} = \frac{1}{n_G} \sum_{i=1}^{n_G} G_n^i(\hat{x}) \qquad s_G^2(n_G) = \frac{1}{n_G - 1} \sum_{i=1}^{n_G} \left(G_n^i(\hat{x}) - \overline{G}_{n_G} \right)^2$$

6: Output the one-sided confidence interval on $\mu_{\hat{x}}$

$$\mu_{\hat{x}} = \left[0, \overline{G}_{n_G} + \frac{t_{n_G - 1, \alpha} s_G(n_G)}{\sqrt{n_G}} \right]$$

As highlighted by Bayraksan and Morton (2006), although the stochastic optimality gap is not normally distributed, from the central limit theorem, since $\overline{G}_{n_G}$ is the mean of i.i.d random variables it can be approximated to a normal distribution.

3.3.4 Convergence of two climate paths

We have so far covered how to generate good scenario trees for the purpose of stochastic programming; we have computed the bounds on the stochastic optimality gap that arise from approximating the continuous random vector by a scenario tree. However, we still have an issue of how to deal with the different climate scenarios (climate paths) that are forecast by climate scientists. We present here a method for reducing the number of climate paths that are worthy of consideration. Let's suppose two climate paths i and j $(i \neq j)$. We can solve (3.2) for the two climate paths to obtain the tuple of solutions and objective function values $(\hat{x}_i, \hat{z}_i)$ and $(\hat{x}_j, \hat{z}_j)$ corresponding to climate paths i and j, respectively. We claim that the two climate paths are not different if they have the same solution. However, because it is possible to have multiple optimal solutions or to have two different solutions that lead to the same objective function value, we use the objective function to evaluate the similarity between the two climate paths.

Hence, we conclude convergence if using the solution $\hat{x}_i$ from climate path i in the function of climate path j leads to the same objective function as $\hat{z}_i$. Put differently, we claim convergence of two climate paths i and j if

$$\hat{z}_i \approx \mathbb{E}\left[f_i\Big(\underset{x \in X}{\arg\min}\, \mathbb{E}[f_j(x, \tilde{\xi})], \tilde{\xi} \Big) \right] ; \tag{3.13}$$

where f_i and f_j are the objective functions of the optimization problem for climate paths i and j, respectively. If there is convergence, then one of the climate paths is sufficient to capture the underlying random process and there is no need to consider both climate paths. In practice, we can conclude that the two scenario paths lead to the same solution if the right hand side term of (3.13) belongs to the confidence interval of z_i^*. From the previous sections, we have all the material to compute the confidence interval on the true objective function value z_i^* of the climate path i using a candidate solution $\hat{x}_i$ as follows:

$$z_i^* \in \left[\hat{z}_i,\ \hat{z}_i + \left(\overline{G}_{n_G}(\hat{x}_i) + \frac{t_{n-1,\alpha} s_G(n_G)}{\sqrt{n_G}} \right) \right]. \tag{3.14}$$

The confidence interval in (3.14) is one sided. It is computed taking into account the stochastic optimality gap from Algorithm 1. For minimization problems, $\hat{z}$ is negatively biased; which means that $\mathbb{E}\,\hat{z} \leq z^*$ (Mak et al., 1999, Theorem 1). This stems from the fact that the solution from the discretization is more optimistic because it only considers a finite number of scenarios we optimize against.

3.3.5 Practical considerations

In practice, it is difficult to compute the stochastic optimality gap ($G_n(\hat{x})$ arising from the discretization of the random parameter), as defined in (3.12) . The difficulty stems from the impossibility to solve certain mixed integer programs to the full optimality in a reasonable clock time. Here, we need to highlight that the optimality gap discussed is related to the mixed integer program (MIP) and the solver used to solve the MIP. That gap (g) is computed by comparing the objective value of the incumbent solution (x) to the best lower bound $\mathcal{L}$ (for minimization problems) as follows:

$$g = \frac{f(x) - \mathcal{L}}{f(x) + \varepsilon}\ , \tag{3.15}$$

where ε is a small quantity that prevents from dividing by zero. $g = 0$ means that the incumbent solution x is the optimal solution of the MIP. However, for harvest scheduling MIPs, it is difficult to achieve such a solution in a reasonable time. The common practice is to set an acceptable stopping optimality gap, $g > 0$. Unfortunately, this simplification affects (3.12). We cannot guarantee anymore that each $G_n(\hat{x})$ is positive because the solution to $\min\limits_{x\in X} \sum_i^n f(x, \tilde{\xi}_i)$ might not be the true optimal solution. We solve this issue by computing the lower bound on the stochastic optimality gap as computed in (3.12) by only using positive $G_i(\hat{x})$. We compute both the lower bound ($G_n^l(\hat{x})$) and upper bound ($G_n^u(\hat{x})$) on the stochastic optimality gap using (3.16)

$$G_n(\hat{x}) = \begin{cases} G_n^l(\hat{x}) = \frac{1}{n}\sum_{i=1}^{n} f(\hat{x},\tilde{\xi}_i) - \min_{x\in X}\frac{1}{n}\sum_{i=1}^{n} f(x,\tilde{\xi}_i) & \text{if (3.12) is positive} \\ \\ G_n^u(\hat{x}) = \frac{1}{n}\sum_{i=1}^{n} f(\hat{x},\tilde{\xi}_i) - \frac{1}{n}\sum_{i=1}^{n}\mathcal{L}_i, & \text{Otherwise} \end{cases} \tag{3.16}$$

where $\hat{x}$ is a candidate solution of the stochastic program, $\tilde{\xi}_i$ is a scenario tree from the discretization of the uncertain parameter, and $\mathcal{L}_i$ is the lower bound obtained while solving the stochastic mixed integer program with an optimality gap g. As a consequence, from the Algorithm 1, we have to compute the mean stochastic optimality gap by computing its lower and upper values as $\overline{G}^l_{n_G}$ and $\overline{G}^u_{n_G}$, respectively.

3.4 Case study

3.4.1 Climate change data

Although climate experts define several potential climate paths known as representative concentration pathways (van Vuuren et al., 2011), in this research, we are more interested in how climate change influences forest growth rather than the actual climate change parameters such as precipitation, temperature, etc. There exist two paradigms to translate climate data into forest growth. The two paradigms are known as process-based modeling and statistical or empirical modeling. Process-based models are known for offering the flexibility to integrate different interactions that explain forest growth. However, these models are mostly suitable for short rotation forests such as eucalyptus plantations (Miehle et al., 2009; Álvarez-Miranda et al., 2018; Garcia-Gonzalo et al., 2020) which are not the kind of forests in the Pacific Northwest. It goes without saying that the empirical modeling is more suitable for this study. Hence, using empirical modeling, Latta et al. (2010) showed that in the Pacific Northwest, the four climate paths forecast by climate experts will affect forest growth disparately. The authors predicted also what the change of potential forest growth will be in 100 years. As results, they provided the potential mean annual increment (pMAI) of forests for the year

2100.

In Table 3.1, *pMAI* refers to the potential mean annual increment change, which is the average forest growth change in one year. The value in the table represents the potential mean annual increment change that will be observed in 100 years. It is assumed that the change will be linear from now (year 2020) up to that year. The four climate paths, A1B, A2, B1, and Commit (hereafter referred to as C) correspond to different climate forecast in response to human activities, technological advancement, population growth, etc. The values in Table 3.1, represents the expected pMAI, however, the values were calculated from a spatial auto-regressive model developed in Latta et al. (2009). The model used as input environmental parameters such as the slope, air moisture, temperature, precipitation, and predicted forest growth. As results, there is a large uncertainty on the predicted pMAI and the prediction interval is quite large (Latta et al., 2009). To account for this uncertainty, we use the prediction interval instead of the expected pMAI in harvest scheduling models.

Table 3.1: *Potential mean annual increment change*

	A1B	A2	B1	Commit
pMAI ($m^3/ha/year$)	2.5	3.1	1.3	0.2

3.4.2 Scenario trees

To generate scenario trees, we use the conditional sampling method described in Section 3.3.1. Forest growth change used is the one presented in Table 3.1. The statistical model predicting the forest growth change had a root mean squared error δ. We use the error term δ to build the 99% prediction interval of the growth change associated with each climate path. For practicality, we used the predicted growth change $\pm 3\delta$ ($pMAI \pm 3\delta$) to build the lower and upper bounds of the predicted growth change. We generated scenario trees for each climate path by sampling within the lower and upper bounds of the prediction interval (see Section

3.3.1 for more details).

To generate the scenarios for each climate path, we propose supposing forest growth change ξ, within each prediction interval follows either a normal or uniform distribution. The normal distribution assigns high probabilities to scenarios that are closer to the expected predicted forest growth change, whereas uniform distribution assigns the same probabilities to all scenarios within the prediction interval. The objective of having the two distributions is to test the sensitivity of the solutions to different probability schemes.

The planning horizon adopted in this experiment is 50 years divided into five periods (with five decision stages as well). For each distribution, we generated scenario trees by using $\beta = \{2, 3, 4, 5\}$ corresponding to two, three, four, and five branches at each stage and leading to 16, 81, 256, and 625 scenarios, respectively. For each branching scheme, we proceeded into generating ten replications of the scenario tree with the same structure. These replications served into computing in-sample, out-of-sample stability and the convergence of two climate paths.

There are a few assumptions this research relies on. First, we assume the forest of interest is small enough in size that our management decisions do not significantly affect climate change. Consequently, the stochastic programming is the one with exogenous uncertainty (Hooshmand and MirHassani, 2016; Apap and Grossmann, 2017). If we were interested in managing forests at a global level, then we would have had to consider a case where our decisions may affect back climate change. In this latter case, the stochastic programming is known as stochastic programming with endogenous uncertainty (Hooshmand Khaligh and MirHassani, 2016; Hooshmand and MirHassani, 2018). Second, the growth change is linear from one period to another. Third, although forest growth changes, the forest site will still be suitable for the species of interest and therefore there is no need to worry about species shifting from one site to another. This assumption is warranted by the first assumption that the study area is relatively small.

3.4.3 Optimization model

In this section, we present the optimization model that served as harvest scheduling model. The main objective of harvest scheduling in commercial forests is the maximization of the net present value from the harvest actions during the planning horizon. The list of parameters, variables and sets is reported in Table 3.2.

Objective function

The objective function which aims at maximizing the expected net present value considering all the scenarios can be written in the form of:

$$\max \sum_{\omega \in \Omega} w^{\omega} \left[\sum_{t \in \mathcal{T}} \left(p_t H_t^{\omega} - \sum_{s \in \mathcal{S}} c_{st} x_{st}^{\omega} \right) + \sum_{s \in \mathcal{S}} p_0 n_s^{\omega} \right]. \tag{3.1}$$

We make sure to subtract from the revenue we get from the harvest of each forest unit, the cost of replanting the same unit. Hence, we balance between the revenue from harvesting a unit and the cost of replanting it. The objective function (3.1) maximizes the net present value while meeting various sustainability and logical restrictions.

Constraints

(a) A stand can be harvested only once during the planning horizon

$$n_s^{\omega} + \sum_{t \in \mathcal{T}} x_{st}^{\omega} = 1 \quad \forall s \in \mathcal{S} \quad \forall \omega \in \Omega \tag{3.2}$$

(b) Volume of wood harvested each period

$$\sum_{s \in \mathcal{S}} a_s v_{st}^{\omega} x_{st}^{\omega} = H_t^{\omega} \quad \forall t \in \mathcal{T} \quad \forall \omega \in \Omega \tag{3.3}$$

(c) Wood flow constraints

$$H_t^{\omega} - (1 - f_{min}) H_{t+1}^{\omega} \geq 0 \quad \forall t \leq |\mathcal{T}| - 1, \quad \forall \omega \in \Omega \tag{3.4}$$

$$H_t^{\omega} - (1 + f_{max}) H_{t+1}^{\omega} \leq 0 \quad \forall t \leq |\mathcal{T}| - 1, \quad \forall \omega \in \Omega \tag{3.5}$$

Table 3.2: *Nomenclature*

Indices	
s	Stand
t	Time of harvest or the year
ω, ω'	Scenario
Variables	
H_t^ω	Volume harvested in year t under scenario ω (m^3)
n_s^ω	Binary variable: 1 if stand s should not be harvested during the whole planning horizon under scenario ω; and 0 otherwise
x_{st}^ω	Binary variable: 1 if stand s is scheduled to be harvested in year t under scenario ω; and 0 otherwise
z_{st}	Binary: 1 if stand s has been harvested before the current management such that the stand is not green-up yet at time t; and 0 otherwise. It is not an actual variable since it is defined while building the model
Parameters	
A_{max}	Maximum contiguous area that should not be exceeded during harvest for green-up (120 acres in Washington state)
a_s	Area of stand s (ha)
age_{st}	Age of stand s at the end of the planning horizon if harvested in year t (yr)
$age_{s.}$	Current age of the stand s (yr)
age_{s0}	Age of stand s at the end of the planning if not harvested during the planning horizon (yr)
b	Minimum age that a stand can have before it is considered green-up or old enough to not be considered as an opening
c_{st}	Discounted cost of regenerating stand s in year t (\$)
f_{max}	Allowable upper bound of percentage of fluctuation of volume of wood
f_{min}	Allowable lower bound of percentage of fluctuation of volume of wood
p_0	Discounted value of the forest at the end of the planning horizon if it is not harvested (\$)
p_t	Discounted price of wood in year t under scenario ω (\$)
v_{st}^ω	Productivity of stand s if harvested in year t according to scenario ω (m^3/ha)
w^ω	Weight or probability of scenario ω
Sets	
$\mathcal{B}$	Set of stands that are big such that their area exceeds A_{max}
$\mathcal{C}$	Set of stands forming a minimum infeasible cluster. (They don't include large units which size exceeds A_{max})
$\mathcal{K}_s$	Set of stands neighbor to the stand s
Λ	Set of minimally infeasible clusters. (They don't include large units which area exceed the maximum opening size)
$\mathcal{S}$	Set of stands
$\mathcal{T}$	Set of years for the planning horizon
Ω	Set of scenarios in the scenario tree

(d) Spatial configuration restrictions (Adjacency rules)

$$\sum_{s\in\mathcal{C}}\left(z_{st}+\sum_{\substack{q=t-b\\q>0}}^{t}x_{sq}^{\omega}\right)\leq|\mathcal{C}|-1\quad\forall t\in\mathcal{T},\quad\forall\mathcal{C}\in\Lambda,\quad\forall\omega\in\Omega \tag{3.6}$$

$$x_{st}^{\omega}+z_{it}+\sum_{\substack{q=t-b\\q>0}}^{t}x_{iq}^{\omega}\leq 1\quad\forall t\in\mathcal{T},\quad\forall s\in\mathcal{B},\quad\forall i\in\mathcal{K}_s,\quad\forall\omega\in\Omega \tag{3.7}$$

$$\sum_{i\in\mathcal{K}_s}\sum_{\substack{q=t-b\\q>0}}^{t}x_{iq}^{\omega}\leq M(1-x_{st}^{\omega}-z_{st})\quad\forall t\in\mathcal{T},\quad\forall s\in\mathcal{B},\quad\forall\omega\in\Omega \tag{3.8}$$

$$z_{st}=1\qquad\text{if } s \text{ harvested in } t' \text{ and } t<b+t' \text{ with } t'\in[-b,0] \tag{3.9}$$

(e) Ending inventory (ending age)

$$\sum_{s\in\mathcal{S}}a_s\left[\sum_{t\in\mathcal{T}}age_{st}x_{st}^{\omega}+age_{s0}n_s^{\omega}\right]\geq\sum_{s}a_s age_{s.}\quad\forall\omega\in\Omega \tag{3.10}$$

(f) Non anticipativity

$$x_{st}^{\omega}=x_{st}^{\omega'}\quad\omega\neq\omega'\quad\forall s,t \tag{3.11}$$

If two scenarios ω and ω' are indistinguishable at time t, then the decision in the two scenarios should be the same at that time t.

(g) Nature of variables

$$H_t^{\omega}\in\mathbb{R}^+,\ x_{st}^{\omega}\in\{0,1\},\ n_{st}^{\omega}\in\{0,1\}\quad\forall t\in\mathcal{T},\quad\forall s\in\mathcal{S},\quad\forall\omega\in\Omega \tag{3.12}$$

Meaning of the constraints

Constraint set (3.2) states that each forest unit can only be harvested once for each scenario. We use the variable n_s^ω as a counter of the stands that are not scheduled for harvest during the whole planning horizon. The set of constraints (3.3) computes the volume of wood harvested in each period for each scenario. As we can see, the parameter v_{st}^ω depends on the scenario ω. Constraint sets (3.4) and (3.5) are volume flow restrictions and they ensure that the volume of wood harvested in period t is within f_{min} and f_{max} percentage of the one harvested in the period $t-1$. The set of constraints (3.10) states that the age of the forest at the end of the planning horizon should be greater or equal to the current age of the forest. This set of constraints is a proxy for sustainability; it ensures that resources are not depleted during the planning horizon. Constraint set (3.11) imposes non-anticipativity for scenario ω and ω'. It states that if there are two scenarios ω and ω' that are indistinguishable in time t, then the decision should be the same for the two scenarios up to that time t.

Constraints (3.6), (3.7), (3.8) and (3.9) refer to the green-up constraints. Green-up constraints or green-up rules are a set of regulations that aim at limiting the size of the openings and the length of time before adjacent forest units can be harvested. A_{max} is the maximum opening area that contiguous forest units harvested can create. A forest unit is considered as an opening if the forest in that unit is not older than b. In practice we do not need the variable z_{st} since its values will be defined while building the model. However, for easiness of the model and its readability, that variable was necessary. Constraints (3.6) say only a feasible cluster is allowed. It includes the fact that there might be stands that have not yet reached the green-up requirement at the start of the planning because those stands were harvested in the previous planning. Constraints (3.7) impose that a large unit cannot be scheduled for harvest if it is adjacent to any other unit that is not green-up yet. The units that are adjacent and not green-up yet could be of two sources. They could originate from the previous harvest planning in which case the stands on that unit are less than b years old prior to this planning. The second case is that the stand is harvested either in an anterior or the current year. Constraint set (3.8) says that if there is a large stand harvested then no neighbor to that stand can be eligible for harvest. Notice that for any t, $x^{\omega}_{st} + z_{st} \leq 1, \forall \omega, s$. This equation is deactivated if the large stand is unscheduled for harvest (M is a big number). Constraint set (3.9) just informs that the values of z are defined while building the model. $z_{st} = 1$ if the stand has been harvested in the prior management such that it is still considered not green-up yet in time t.

During implementation, Constraint set (3.6) is written slightly differently as follows:

$$\sum_{s \in \mathcal{C}} \sum_{\substack{q=t-b \\ q>0}}^{t} x^{\omega}_{sq} \leq \max\left(0, |\mathcal{C}| - 1 - \sum_{s \in \mathcal{C}} z_{st}\right) \quad t \in \mathcal{T}, \quad \forall \mathcal{C} \in \Lambda, \quad \forall \omega \in \Omega \tag{3.13}$$

This reformulation is important because the value of $\sum_{s \in \mathcal{C}} z_{st}$ can be greater than $|\mathcal{C}| - 1$. Let's for example have a cluster of two stands ($|\mathcal{C}| = 2$) that were harvested in the previous planning such that the two stands are not green-up yet at t^*, thus $\sum_{s \in \mathcal{C}} z_{st^*} = 2$. With the new formulation, the right-hand side will be zero; as a result, the cluster cannot be harvested until the stands have reached the harvestable age. This situation arises because we do not have control over previous managements and how minimally infeasible clusters were defined. Equations (3.12) define the domain of the variables.

Recourse constraints

Although the above model is sufficient to define the harvest scheduling, we still need to define the structure of the recourse variables in case the decision maker assumes a climate path, say A2, will occur and actually climate path C, for instance, materializes. Notice that except the wood flow constraints (Constraint sets (3.4) and (3.5)), all other constraints will remain satisfied. Hence, to satisfy the wood flow constraints, we suppose that in case of shortage of wood in any time period, because we were expecting one climate path and a different one occurred, we have to purchase wood on the market from a competitor to fulfill the demand. It goes without saying that the price at which we buy the wood exceeds the price at which we would sell ours. The rational behind this reasoning is that the competitor has no incentive to sell to us their wood. In sum, we incur a high cost for not having enough inventory to fulfill the implicit demand. Similarly, in case of excess of wood, we incur a cost of holding excessive inventory. Wood flow constraints are one of the most important policy in forest management planning. It ensures employment and the stability of the involved local communities (Liu, 2002). To implement these policies, we need to define a set of variables and parameters.

First, let π_t^+ be the cost of holding inventory $e_t^{+\omega}$ in case the wood we produce in period t exceeds the maximum allowable harvest in period t ($\overline{H}_t^{\omega}$) from the wood flow constraints of the scenario ω. Second, let π_t^- be the price at which we buy wood on the market in case we have a shortage of production if the wood we produce in period t is bellow the minimum volume, $\underline{\mathrm{H}}_t^{\omega}$, required by the wood flow constraints by a value of $e_t^{-\omega}$. We can compute the shortage volume and the excess of inventory by using (3.14) and (3.15), respectively.

$$e_t^{-\omega} = \max(\underline{\mathrm{H}}_t^{\omega} - H_t^{\omega}, 0) \tag{3.14}$$

$$e_t^{+\omega} = \max(H_t^{\omega} - \overline{H}_t^{\omega}, 0) \tag{3.15}$$

Note that $e_t^{+\omega} * e_t^{-\omega} = 0,\ \forall t, \omega$ because we cannot have at the same time shortage and excess. The new objective function becomes

$$\max \sum_{\omega \in \Omega} w^{\omega} \left[\sum_{t \in \mathcal{T}} \left(p_t H_t^{\omega} - \pi_t^+ e_t^{+\omega} - \pi_t^- e_t^{-\omega} - \sum_{s \in \mathcal{S}} c_{st} x_{st}^{\omega} \right) \right]. \tag{3.16}$$

This objective is necessary in computing the net present value if the decision maker plans for one climate path and actually a different climate path occurs. Since the decision variables are fixed, this is just computing the new objective function value of wrongly assuming the future climate path.

Values of the model's parameters

The methodology was tested on Phyllis Perry forest with 89 stands at different maturity age. The planning horizon was 50 years divided into five planning periods of ten years each.

Table 3.3: *Optimization model parameters*

Parameter	Value
b	5 years
f_{min}	15%
f_{max}	15%
π_t^+	$0.8p_t$
π_t^-	$2p_t$
Discount rate	3.5%
Planning horizon	50 years
Length of a period	10 years

We solved the models for all data sets using IBM ILOG CPLEX 64-bit 12.9.0 on a Dell Power Edge 510 Server with an Intel Xeon(R) CPU, E5-2680 v3 @2.50 GHz (two processors) with 256 GB RAM and the Windows Server 2012R2 64-bit operating system. The optimization model was implemented on Python. We ran CPLEX using the default settings except limiting the run time to 24h (wall clock time) and setting the optimality gap (g) to 2% for each model. We excluded from the analysis all models that terminated because of time limit. Table 3.3 summarises the values of several parameters used in the optimization model. To check for stability, we generated ten replications of each scenario tree structure.

3.4.4 Experimental results

In-sample stability

In-sample stability increases with the number of scenarios (the number of branches at each stage) for the four climate paths (Figure 3.1). The relative stability presented in Table 3.4 shows that except for the climate path B1, when the random parameter is uniformly distributed, which has a relative stability less than 1% when considering three branches at each stage ($\beta = 3$), all other climate paths reach that stability level when four branching is considered ($\beta = 4$). The four branching at each stage corresponds to 256 growth scenarios.

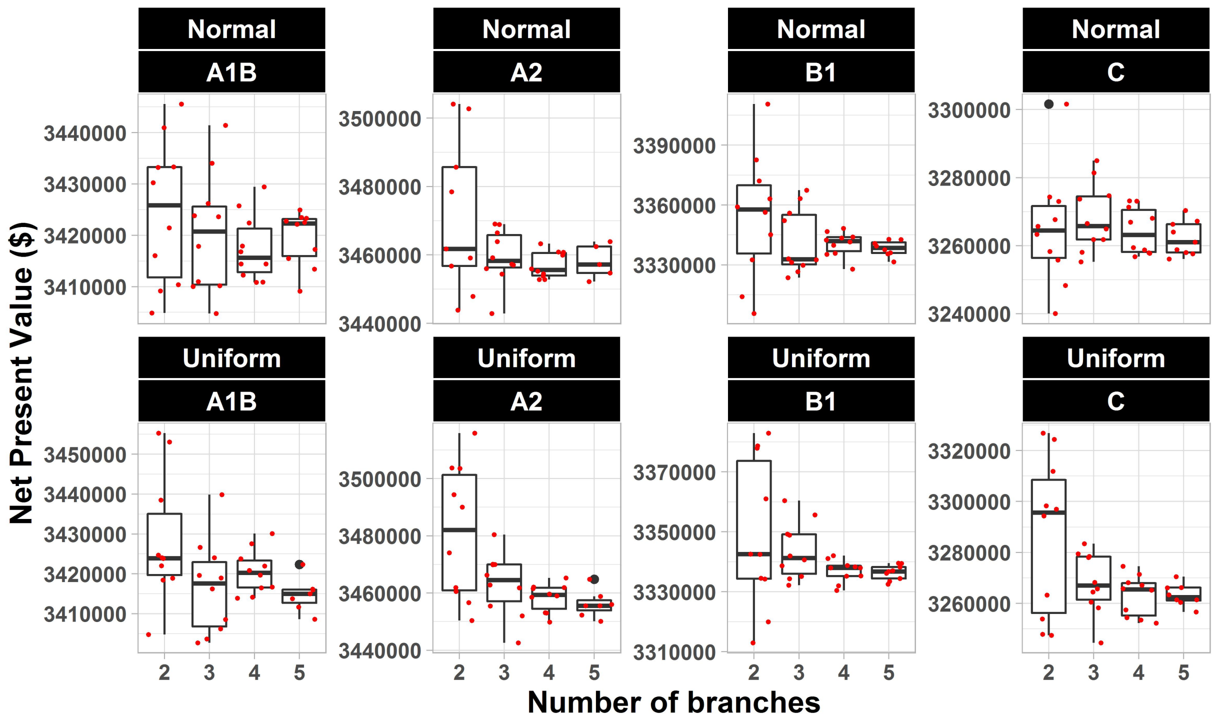

Figure 3.1: *In-sample stability analysis*

Out-of-sample stability

We get high out-of-sample stability when considering four branching (or 256 scenarios) compared to five branching ($\beta = 5$ or 625 scenarios). However, these stabilities do not appear to be statistically different. The trade-off between the time required to solve the problem with 625 scenarios and the increase of out-of-sample stability does not motivate the adoption of the scheme with five branching. Hence, the best sampling schema is four branching at each stage leading to 256 scenarios (Figure 3.2).

Table 3.4: *Percentage of stability using maximum and minimum values for both normal and uniform distributions (relative stability)*

	Normal				Uniform			
Branch (# scenarios)	A1B	A2	B1	C	A1B	A2	B1	C
2 (16)	1.21	2.15	3.06	1.65	1.63	1.88	2.49	2.34
3 (81)	1.20	1.37	1.34	1.11	1.05	1.09	0.86	1.46
4 (256)	0.69	0.44	0.66	0.73	0.43	0.40	0.31	0.59
5 (625)	0.45	0.34	0.35	0.50	0.39	0.38	0.37	0.43

Stochastic optimality gap

The results of the upper and lower bounds on stochastic optimality gap for the four climate paths are reported in Table 3.5. The lower bound of the stochastic optimality gap ranges from 0.09% to 0.18% corresponding to the climate path A1B and C, respectively, when the growth is normally distributed. However, the upper bound on the stochastic optimality is less than 2%.

Convergence of climate paths

Table 3.6 displays the expected net present value that we get if we commit to each of the climate paths. The expected NPV is high when we manage the forest expecting climate path A2 regardless of if that climate path actually materializes or not. Managing the forest expecting climate path C leads to the lowest NPV. The results of two-way ANOVA shows that the expected NPV we get depends on the climate path we commit to (Table 3.7). However, the distribution of the random parameter for each climate path has no significant effect. In other words, the probabilities of the scenarios did not have any significance on the value of

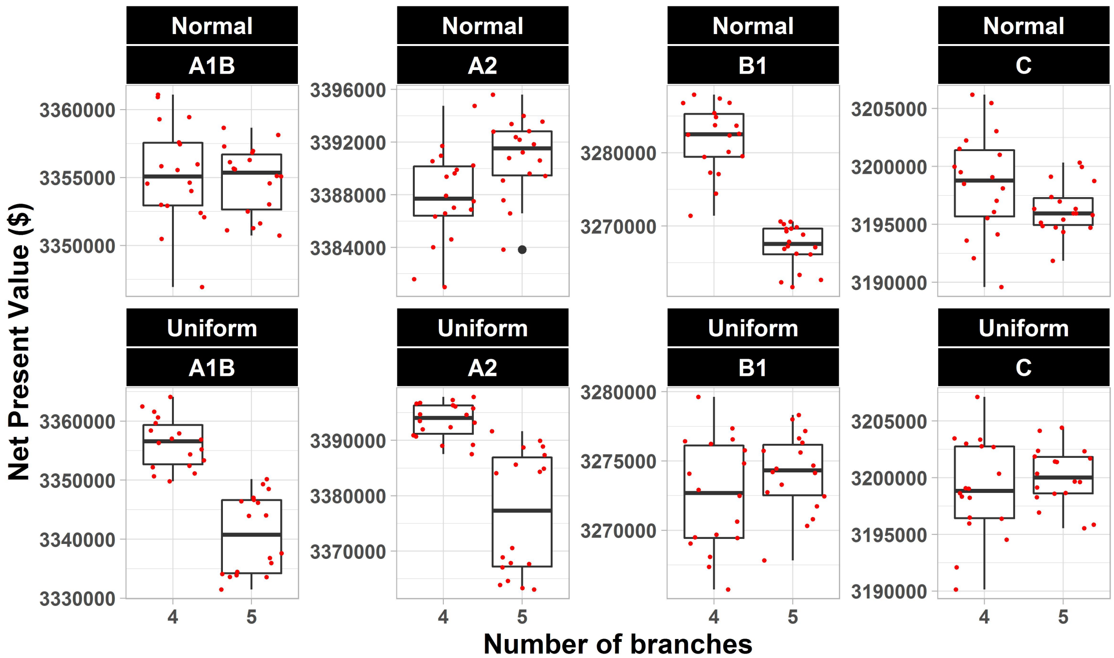

Figure 3.2: *Out-of-sample stability analysis*

the NPV.

Figure 3.3 presents the summary of the net present value (NPV) of managing the forest expecting one climate path while the materialized climate path may be the same or a different one. For instance, if we manage the forest expecting climate path A1B and climate path A2 occurs, the NPV is expected to increase, although it remains in the uncertainty margin. However, if climate path B1 or C occurs, then the obtained NPV will be much lower than the one we would get if actually the climate A1B had occurred. Similarly, if we expect climate A2, for instance, and climate path C occurs, the NPV obtained is much higher than the NPV we would get if we managed the forest expecting climate path C and it actually materialized. This second analysis may be counter intuitive. It seems like if we knew which climate path would occur, we would make the best decision here and now, and therefore the NPV should be higher for such a good foresee. The second thing one may wonder is whether we are not over-harvesting if we plan foreseeing an optimistic forest growth climate path, say climate

Table 3.5: *Stochastic optimality gap on each climate path. The percentage of the bound is relative to the mean NPV*

Distribution	Climate path	Mean NPV($)	$\overline{G}^l_{30}$($)	$\overline{G}^l_{30}$(%)	$\overline{G}^u_{30}$($)	$\overline{G}^u_{30}$(%)
Normal	A1B	3,354,555	2,980	0.09	62,593	1.87
	A2	3,387,797	6,063	0.18	65,974	1.95
	B1	3,278,346	3,914	0.12	60,970	1.86
	C	3,208,195	5,743	0.18	58,427	1.82
Uniform	A1B	3,355,126	4,677	0.14	63,121	1.88
	A2	3,391,432	4,401	0.13	65,150	1.92
	B1	3,272,744	5,609	0.17	63,356	1.94
	C	3,200,770	4,444	0.14	60,942	1.90

path A2, and actually climate path C materializes. The following paragraphs address these two points.

First, when we plan for an optimistic climate path, the best decision is to increase the volume of forest harvested here and now (harvested in the first period) because the future forest growth will increase and compensate the volume we may have over-harvested here and now. Second, the discounting affects revenues and costs that we incur in the future, hence the future actions are less significant. It is clear, therefore, that if we only care about the ending age inventory requirement (constraint set (3.10)) and the wood flow, the best decision is to plan for optimistic future forest growth and if we lack forest material in the future, we can still purchase wood even at a higher cost as long as the ending age constraint is satisfied.

Second, we can see as illustrated on Figure 3.4, that the volume of wood harvested is the same by the end of the planning horizon, regardless of if the management anticipated correctly the climate path to occur or not. Indeed, if we expect an optimistic climate path,

Table 3.6: *Expected NPV when the forest is managed expecting a specific climate path regardless of which climate path actually materializes for both the normal and the uniform distributions. SD = standard deviation*

Distribution	Climate	NPV($)	SD(NPV)
Normal	A1B	3,335,126	30,825.77
	A2	3,352,117	33,563.86
	B1	3,288,788	27,300.93
	C	3,244,643	26,940.26
Uniform	A1B	3,333,478	33,689.93
	A2	3,350,849	38,496.11
	B1	3,285,235	29,311.52
	C	3,238,941	28,359.64

say A2, we tend to increase the volume of wood harvested in the first period. However, if a less optimistic climate path, say C, occurs, we will harvest less volume in the future compared to the volume we would have harvested if we knew from the beginning that the climate path C would occur.

3.5 Conclusions and discussion

In this study, we have developed a framework for incorporating forest growth and yield uncertainty due to climate change in harvest scheduling models. We considered forest growth change with different climate paths separately. We generate growth scenarios within the prediction interval of each climate path. Increasing the number of scenarios allows to capture the variability of the forest growth that affects optimal management decisions. However, there is no real benefit at increasing that number beyond a given point since it increases the

Table 3.7: *Two-way ANOVA of the NPV distribution and the climate path (climate) as factors*

	df	Sum Sq	Mean Sq	F Value	Pr(>F)
Distribution	1	3.70E+08	3.70E+08	0.3784	0.5394
Climate	3	2.93E+11	9.77E+10	99.888	<2e-16
Distribution × Climate	3	1.24E+08	4.14E+07	0.0423	0.9884
Residuals	152	4.87E+10	9.79E+08		

problem computational complexity without significantly increasing the quality of the scenario tree. The analysis showed that out of the four climate paths considered, one may just focus on the two extreme climate paths, namely climate path A2 and C since the decisions one makes considering the two others (climate path A1B and B2) are included in the decision if these two climate paths.

Subsequently, at the high level, it does not really matter which climate path will materialize; the optimal decision is to plan forest harvests expecting an optimistic climate, which in this study is climate path A2. Whether the uncertainty of the forest response is normally or uniformly distributed around its expected value, the results have shown that there is no significant impact considering one or the other.

Although, we advocate that the decision maker ought to have an optimistic attitude expecting a future increase of the forest growth in the context of Pacific northwest, this recommendation can be viewed with skepticism especially for a large forestry company. The idea of purchasing forest products in case of shortage makes sense for a small company but may not be appealing to a large company that is the leading in the industry. Similarly, we would like to stress that this recommendation has to be taken with caution since it is not a sustainable practice if the whole forest industry adopt it. One way this caution can be integrated in the model is to reinforce the wood flow constraints to be feasible for all climate

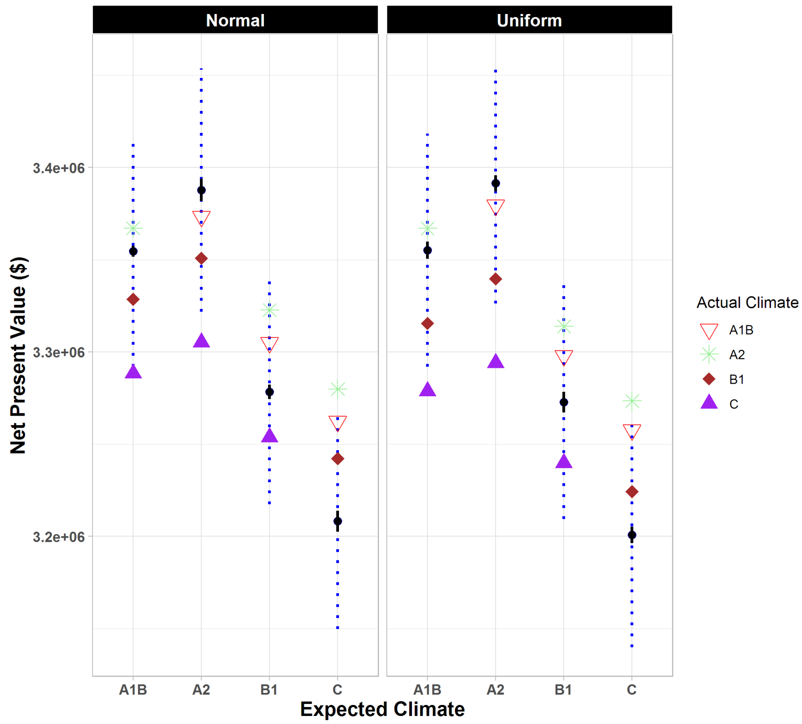

Figure 3.3: *Net present value from a management expecting one climate path versus the materialization of a different climate path. Dashed blue lines correspond to the confidence of the NPV from a correct prediction of the climate path.*

paths.

One of the limitations of this research is that we supposed that climate change will affect forest growth without any feedback from our management decisions. Although this assumption was valid for our case, it is a limitation of this research. Similarly, we supposed that if there is a shortage of wood supply because of our management decisions, then we could procure some wood from competitors. This might not be true if all decision makers adopt this attitude. Moreover, supposing just two distributions of the random variable may be limiting. In the continuation of this research, we intend to use distributionally robust optimization to integrate more distributions in the harvest scheduling and at the same time consider all the climate paths at once. Finally, we supposed in this research that the price

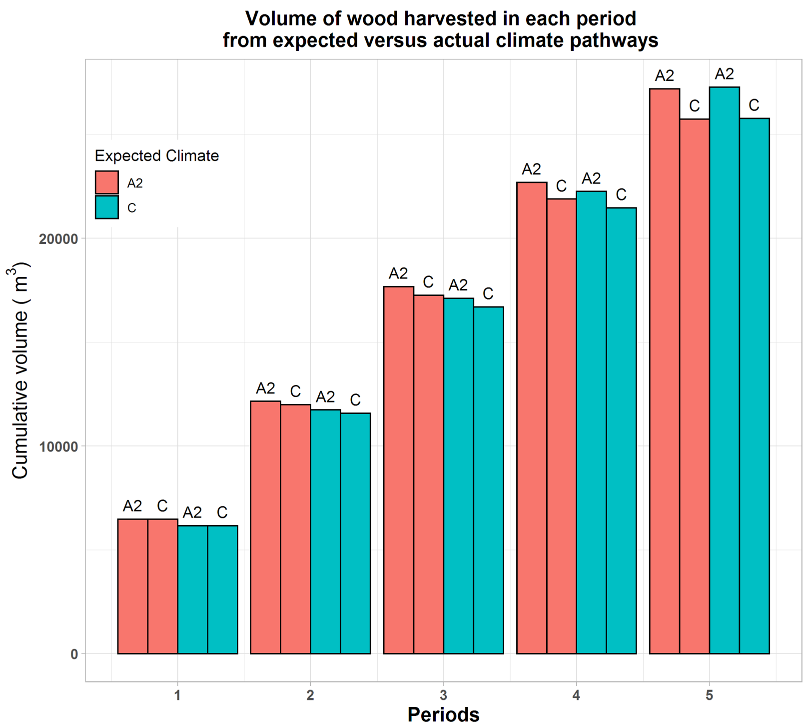

Figure 3.4: *Cumulative volume of wood harvested in each period when planning for either climate paths A2 and C and actually any of the two materializes for normally distributed growth change. The letters on the bars designate the actual climate path that occurred*

of wood is independent from climate change. Although we do not have enough evidence to refute this assumption, we do think it might not be the case. Wood can become a prime commodity if climate change leads to a substantial reduction in forest growth. However, this change can be attenuated by the technological advancement that can reduce the need of wood for construction.

References

Alonso-Ayuso, A., Escudero, L. F., Guignard, M., and Weintraub, A. (2018). Risk management for forestry planning under uncertainty in demand and prices. *European Journal of Operational Research*, 267(3):1051–1074.

Álvarez-Miranda, E., Garcia-Gonzalo, J., Ulloa-Fierro, F., Weintraub, A., and Barreiro, S. (2018). A multicriteria optimization model for sustainable forest management under climate change uncertainty: An application in Portugal. *European Journal of Operational Research*, 269(1):79–98.

Apap, R. M. and Grossmann, I. E. (2017). Models and computational strategies for multistage stochastic programming under endogenous and exogenous uncertainties. *Computers and Chemical Engineering*, 103:233–274.

Bayraksan, G. and Morton, D. P. (2006). Assessing solution quality in stochastic programs. *Mathematical Programming*, 108(2-3):495–514.

Beraldi, P. and Bruni, M. E. (2013). A clustering approach for scenario tree reduction: An application to a stochastic programming portfolio optimization problem. *Top*, 22(3):1–16.

Casey, M. S. and Sen, S. (2005). The Scenario Generation Algorithm for Multistage Stochastic Linear Programming. *Mathematics of Operations Research*, 30(3):615–631.

Chunlin, D. and Liu, Y. (2012). Sample Average Approximation Method for Chance Constrained Stochastic Programming in Transportation Model of Emergency Management. *Systems Engineering Procedia*, 5:137–143.

Crespi, G. P., Kuroiwa, D., and Rocca, M. (2018). Robust optimization: Sensitivity to uncertainty in scalar and vector cases, with applications. *Operations Research Perspectives*, 5:113–119.

Dembo, R. S., Chiarri, A., Martin, J. G., and Paradinas, L. (1990). Managing Hidroeléctrica Española's Hydroelectric Power System. *Interfaces*, 20(1):115–135.

Dupacová, J., Consigli, G., and Wallace, S. W. (2000). Scenarios for Multistage Stochastic Programs. *Annals of Operations Research*, 100:25–53.

Elli, E. F., Sentelhas, P. C., and Bender, F. D. (2020). Impacts and uncertainties of climate change projections on Eucalyptus plantations productivity across Brazil. *Forest Ecology and Management*, 474(March):118365.

Fleishman, A. I. (1978). A method for simulating non-normal distributions. *Psychometrika*, 43(4):521–532.

Garcia-Gonzalo, J., Pais, C., Bachmatiuk, J., Barreiro, S., and Weintraub, A. (2020). A Progressive Hedging Approach to Solve Harvest Scheduling Problem under Climate Change. *Forests*, 11(2):224.

Gröwe-Kuska, N., Heitsch, H., and Römisch, W. (2003). Scenario reduction and scenario tree construction for power management problems. *2003 IEEE Bologna PowerTech - Conference Proceedings*, 3:152–158.

Gülpinar, N., Rustem, B., and Settergren, R. (2004). Simulation and optimization approaches to scenario tree generation. *Journal of Economic Dynamics and Control*, 28(7):1291–1315.

Guo, Z., Wallace, S. W., and Kaut, M. (2019). Vehicle Routing with Space- and Time-Correlated Stochastic Travel Times: Evaluating the Objective Function. *INFORMS Journal on Computing*, Articles i(September):1–17.

Heitsch, H. and Römisch, W. (2009). Scenario tree modeling for multistage stochastic programs. *Mathematical Programming*, 118(2):371–406.

Hochreiter, R. and Pflug, G. C. (2007). Financial scenario generation for stochastic multi-stage decision processes as facility location problems. *Annals of Operations Research*, 152(1):257–272.

Hooshmand, F. and MirHassani, S. (2016). Efficient constraint reduction in multistage stochastic programming problems with endogenous uncertainty. *Optimization Methods and Software*, 31(2):359–376.

Hooshmand, F. and MirHassani, S. A. (2018). Reduction of nonanticipativity constraints in multistage stochastic programming problems with endogenous and exogenous uncertainty. *Mathematical Methods of Operations Research*, 87(1).

Hooshmand Khaligh, F. and MirHassani, S. (2016). A mathematical model for vehicle routing problem under endogenous uncertainty. *International Journal of Production Research*, 54(2):579–590.

Høyland, K., Kaut, M., and Wallace, S. W. (2003). A Heuristic for Moment-Matching. *Computational Optimization and Applications*, 24:169–185.

Høyland, K. and Wallace, S. W. (2001). Generating Scenario Trees for Multistage Decision Problems. *Management Science*, 47(2):295–307.

Kaut, M. and Wallace, S. W. (2007). Evaluation of scenario-generation methods for stochastic programming. *Pacific Journal of Optimization*, 3(2):257–271.

Latta, G., Temesgen, H., Adams, D., and Barrett, T. (2010). Analysis of potential impacts of climate change on forests of the United States Pacific Northwest. *Forest Ecology and Management*, 259(4):720–729.

Latta, G., Temesgen, H., and Barrett, T. M. (2009). Mapping and imputing potential productivity of Pacific Northwest forests using climate variables. *Canadian Journal of Forest Research*, 39(6):1197–1207.

Li, Q. Q., Li, Y. P., Huang, G. H., and Wang, C. X. (2018). Risk aversion based interval stochastic programming approach for agricultural water management under uncertainty. *Stochastic Environmental Research and Risk Assessment*, 32(3):715–732.

Liu, C. M. (2002). A Primal-dual Steepest-edge Method for Even-flow Harvest Scheduling Problems. *International Transactions in Operational Research*, 9(1):33–50.

Löhndorf, N. (2016). An empirical analysis of scenario generation methods for stochastic optimization. *European Journal of Operational Research*, 255(1):121–132.

Mak, W. K., Morton, D. P., and Wood, R. K. (1999). Monte Carlo bounding techniques for determining solution quality in stochastic programs. *Operations Research Letters*, 24(1):47–56.

Marla, L., Rikun, A., Stauffer, G., and Pratsini, E. (2020). Often, the RO Approach and the CCPRobust Modeling and Planning: Insights from Three Industrial Applications. *Operations Research Perspectives*, page 100150.

Miehle, P., Battaglia, M., Sands, P. J., Forrester, D. I., Feikema, P. M., Livesley, S. J., Morris, J. D., and Arndt, S. K. (2009). A comparison of four process-based models and a statistical regression model to predict growth of Eucalyptus globulus plantations. *Ecological Modelling*, 220(5):734–746.

Moriguchi, K., Ueki, T., and Saito, M. (2020). Establishing optimal forest harvesting regulation with continuous approximation. *Operations Research Perspectives*, 7(April):100158.

Ponomareva, K., Roman, D., and Date, P. (2015). An algorithm for moment-matching scenario generation with application to financial portfolio optimisation. *European Journal of Operational Research*, 240(3):678–687.

Pour, A. G., Naji-Azimi, Z., and Salari, M. (2017). Sample average approximation method for a new stochastic personnel assignment problem. *Computers and Industrial Engineering*, 113:135–143.

Pranevicius, H. and Sutiene, K. (2007). Scenario tree generation by clustering the simulated data paths. *Proceedings of 21st European Conference on Modeling and Simulation*, page 203208.

Rios, I., Weintraub, A., and Wets, R. J. (2016). Building a stochastic programming model from scratch: a harvesting management example. *Quantitative Finance*, 16(2):189–199.

Ross, K. L. and Tóth, S. F. (2016). A model for managing edge effects in harvest scheduling using spatial optimization. *Scandinavian Journal of Forest Research*, 31(7):646–654.

Schroder, S. A., Tóth, S. F., Deal, R. L., and Ettl, G. J. (2016). Multi-objective optimization to evaluate tradeoffs among forest ecosystem services following fire hazard reduction in the Deschutes National Forest, USA. *Ecosystem Services*, 22:328–347.

Schütz, P., Tomasgard, A., and Ahmed, S. (2009). Supply chain design under uncertainty using sample average approximation and dual decomposition. *European Journal of Operational Research*, 199(2):409–419.

Séguin, S., Fleten, S. E., Côté, P., Pichler, A., and Audet, C. (2017). Stochastic short-term hydropower planning with inflow scenario trees. *European Journal of Operational Research*, 259(3):1156–1168.

St. John, R. and Tóth, S. F. (2015). Spatially explicit forest harvest scheduling with difference equations. *Annals of Operations Research*, 232:235257.

St John, R., Tóth, S. F., and Zabinsky, Z. B. (2018). Optimizing the geometry of wildlife corridors in conservation reserve design. *Operations Research*, 66(6):1471–1485.

Tóth, S. F., Haight, R. G., Snyder, S. A., George, S., Miller, J. R., Gregory, M. S., and Skibbe, A. M. (2009). Reserve selection with minimum contiguous area restrictions: An application to open space protection planning in suburban Chicago. *Biological Conservation*, 142(8):1617–1627.

van Vuuren, D. P., Edmonds, J., Kainuma, M., Riahi, K., Thomson, A., Hibbard, K., Hurtt, G. C., Kram, T., Krey, V., Lamarque, J. F., Masui, T., Meinshausen, M., Nakicenovic, N., Smith, S. J., and Rose, S. K. (2011). The representative concentration pathways: An overview. *Climatic Change*, 109(1):5–31.

Wang, W. and Ahmed, S. (2008). Sample average approximation of expected value constrained stochastic programs. *Operations Research Letters*, 36(5):515–519.

Xu, B., Zhong, P.-A., Zambon, R. C., Zhao, Y., and Yeh, W. W.-G. (2015). Scenario tree reduction in stochastic programming with recourse for hydropower operations. *Water Resources Research*, 51(8):6359–6380.

Chapter 4. A Variable Fixing Heuristic for Solving multistage Stochastic Programs with Progressive Hedging

Summary

Long time horizons, typical of forest management, make planning more difficult due to added exposure to climate uncertainty. Current methods for stochastic programming limit the incorporation of climate uncertainty in forest management planning. To account for climate uncertainty in forest harvest scheduling, we discretize the potential distribution of forest growth under different climate scenarios and solve the resulting stochastic mixed integer program. Increasing the number of scenarios allows for a better approximation of the entire probability space of future forest growth but at a computational expense. To address this shortcoming, we propose a new heuristic algorithm designed to work well with multistage stochastic harvest scheduling problems. Starting from the root-node of the scenario tree that represents the discretized probability space, our progressive hedging algorithm sequentially fixes the values of decision variables associated with scenarios that share the same path up to a given node. Once all variables from a node are fixed, the problem can be decomposed into sub-problems that can be solved independently. We tested the algorithm performance on six forests considering different number of scenarios. The results showed that our algorithm performed well when the number of scenarios was large.

4.1 Introduction

Uncertainty is common in all disciplines that involve decision making. In forestry, planners need to prescribe, several decades in advance, actions that should be taken in a forest in order to achieve a given management objective. Those actions include the segments of roads that should be built in a given period to allow hauling, the forest units or stands that should be treated to reduce the risk of fire, the stands that should be logged in each time period to produce timber and secure employment to the local community, etc. The most common objective is the maximization of the net present value subject to environmental, budgetary, and logistics restrictions (St. John and Tóth, 2015). The prescriptive models allowing to assign forest units to different actions in different time periods are known as harvest scheduling models. To build harvest scheduling models, forest planners have traditionally used expected growth and yield coefficients to predict future merchantable timber volumes. However, uncertainties in long-term temperature and precipitation coupled with increasing wildfire, windstorms or landslides due to climate change may affect forest development. The traditional approach fails to account for uncertainty in forest growth and leaves forest planners unprepared in case of occurrence of any of these uncertainties. The uncertainty in forest planning can be addressed by a particular class of mathematical programming known as stochastic programming. One can distinguish between two-stage stochastic programming and multistage stochastic programming. In two-stage stochastic programming, a decision is made, then the uncertainty is revealed and a recourse action that depends on the revealed uncertainty is taken. However, in the case of multistage stochastic programming the sequence of decision and uncertainty revealing itself occurs more than once giving therefore more flexibility to the decision maker to take recourse actions as uncertainty unfolds progressively.

Multistage stochastic programs are mainly composed of scenarios and stages. Scenarios are the set of possible future outcomes of the uncertain parameter and stages represent the level at which decisions can be made and/or recourse actions can be taken. We call 'period', the time that separates two consecutive stages. The uncertainty unfolds progressively in each period. Since at the beginning of the planning we cannot anticipate which scenarios would unfold, we require that the decision made at the first stage must be the same for all scenarios. This requirement is known as non-anticipativity constraints. Non-anticipativity constraints (NAC) impose that if two scenarios cannot be distinguished up to any given stage, then the decision made in the two scenarios up to that stage must be the same. Multistage stochastic programming has been commonly used to model uncertainty in forest harvest scheduling because of the long planning horizon that characterizes forest harvest scheduling and the presence of interdependent relationships between periods such as the maximum contiguous area harvested from one period to another should not exceed a given limit. For instance, Veliz et al. (2014) solved a multistage stochastic harvest scheduling model with uncertainty in wood price, wood demand and productivity while Alonso-Ayuso et al. (2018) focused on the uncertainty in the price and risk aversion. Finally, Álvarez-Miranda et al. (2018) assessed how key ecosystems services change in forest management if there is growth uncertainty stemming from climate change.

Although climate change might be one of the biggest challenges of forest management, it has received little attention in forest harvest planning in part because stochastic programs, especially multistage stochastic programs, are considered one of the most challenging classes of optimization problems to solve (Thénié and Vial, 2008; Higle et al., 2010; Zou et al., 2019). For instance, the number of scenarios in Álvarez-Miranda et al. (2018) was limited to 32 although climate scientists forecast at least four climate pathways (Moss et al., 2010) which may translate into hundreds of possible forest growths.

Real-life applications of multistage stochastic problems lead to large models that are hard to solve directly (Sanei Bajgiran et al., 2017). The size of the models is directly related to the number of scenarios used to represent the uncertainty. Although uncertain parameters may be continuous, to make the problem suitable for stochastic programming, the discrete realization of the uncertainty is cast in a structure known as a scenario tree. In the scenario tree, each node represents a state decision and the branches of the tree represent the realization of the uncertainty. As more scenarios are included in the tree, the model will better approximate the entire probability space of the uncertain parameter (Kaut and Wallace, 2007). However, increasing the number of scenarios makes the resulting stochastic programming models hard to solve. It is therefore necessary to develop some decomposition algorithms. The two most common decomposition methods are Benders decomposition (Benders, 1962) also known as stage-wise decomposition or vertical decomposition and progressive hedging (Rockafellar and Wets, 1991) also called scenario-wise decomposition or horizontal decomposition. Sen (2005) provided an overview of the algorithms for stochastic programming decomposition. Additional summary of different solution methods for stochastic programming is available in Escudero et al. (2018).

Benders decomposition (BD) is a delayed constraints generation approach for solving mixed integer programs. It has been mainly applied to two-stage stochastic programming problems with some assumptions on the nature of the first stage and second stage variables. Küçükyavuz and Sen (2017) give a summary of conditions for application of BD to two-stage stochastic programs. According to Egging (2013), BD is well suitable when there is only a small set of constraints that prevent the decomposition of the problem into blocks. This is not the case in forest harvest scheduling characterized by long planning horizons and constraints such as even-flow of wood and ending inventory linking variables from one decision stage to another of multistage stochastic programs. For instance, Egging (2013) had limited success when extended their BD algorithm to multistage stochastic programs. We acknowledge however, that there are multistage applications where BD had been used (Yossiri et al., 2015; Fattahi et al., 2018; Zhou et al., 2019).

Progressive hedging (PH), on the other hand, was developed by Rockafellar and Wets (1991) for convex two-stage stochastic programs and is proven to produce a global optimal solution for continuous problems. For non-convex problems such as stochastic mixed integer programs (SMIP) the algorithm is not proven to converge. It relaxes non-anticipativity constraints and iteratively solves the stochastic program by independently solving its scenarios and penalizing the violation of non-anticipativity constraints. PH is appealing because it is a method based on scenario-wise decomposition and thus at each iteration the stochastic program solved is equivalent to a risk neutral problem that is the same as the deterministic problem which ignores uncertainty. Consequently, the algorithm can deal with a large number of scenarios.

Despite its benefits, PH performs poorly for non-convex multistage stochastic programs. Several researchers have proposed PH-heuristics for solving SMIP in different applications. The most promising PH-based heuristic explored is fixing variables that participate in defining non-anticipativity constraints as they meet consensus (See Section 4.2.2 for definition of non-anticipativity variables). For instance, Veliz et al. (2014) fixed non-anticipativity variables during PH iterations as these meet consensus. After a given percentage of variables, 80% for instance, consent on the value they should take, the reduced problem, which is the SMIP with some NAC variables fixed (named here and after reduced extensive form, REF) is then solved directly. The inconvenience of this approach is that the reduced extensive form may be infeasible because too many variables have been fixed (for proof see appendix 4.A). The infeasibility occurs when there is uncertainty in the yield of the forest such as in the case of climate change. In this case, the algorithm wasted considerable time iterating. On the other hand, solving the reduced extensive form problem can still be difficult if the number of variables fixed is too low. The third limitation stems from the fact that the reduced form problem is not separable and thus solving it cannot be parallelized. Similarly, for a two-stage problems in resources management, Watson and Woodruff (2011) proposed a scheme for fixing variables. Their algorithm applicability was limited to a special class of resources management where constraints are one sided. They proposed "slamming" technique which forces non-anticipativity variables to converge, although they have not met consensus yet. They showed that this technique accelerated PH convergence. Recently, Manerba and Perboli (2019) proposed fixing variables as well. In their case, they had both binary and continuous decision variables and proposed therefore to fix the binary NAC variables and the resulting linear stochastic program, since convex, can easily be solved using progressive hedging.

Aside from fixing variables, researchers have investigated other strategies for improving PH application to non-convex problems. Some of the strategies are only applicable to two-stage stochastic programs. For instance, Atakan and Sen (2018) proposed a branch-and-bound algorithm for stochastic mixed integer programs and tested the algorithm on stochastic server location problem. Similarly, Barnett et al. (2017) proposed a combination of branch-and-bound and PH using the former as a wrapper. In the same context, Gade et al. (2016) proposed an algorithm for computing the lower bound of PH for two-stage SMIP. Other researchers invested into reducing the duality gap that arises from relaxation of the non-anticipativity constraints (Gade et al., 2016; Boland et al., 2018). In the same spirit, Boland et al. (2016) looked into the minimum number of non-anticipativity constraints that need to be reinforced to ensure the quality of SMIP. Beraldi and Bruni (2013); Pranevicius and Sutiene (2007) looked at reducing the number of scenarios by clustering them into bundles that can be solved independently. All these algorithms, remain dependent on some assumptions of the nature of the first stage variables or the second stage variables, or both. In addition, their applicability is limited to two-stage SMIP and specific to certain disciplines. However, the main challenge that remains is that PH does not converge for non-convex problems which are common in forest planning. In forest planning there are some problems that possess only binary decision variables (there could be some accounting continuous variables which do not participate in decision making). Some of those problems are found in spatial explicit forest management planning where the decision variables are the forest units that should receive a specific treatment. This class of problems with pure binary decision variables is the focus of this research.

In this work, we aim at overcoming some limitations that are posed by using PH for multistage stochastic harvest scheduling problems with uncertainty in the yield. The objective is to have a heuristic that efficiently solves multistage stochastic harvest scheduling with little loss of optimality. i-) We propose decomposing SMIP into scenarios and solving them by a special heuristic form of progressive hedging that is completely parallelizable. We capitalize on the idea of fixing variables as they meet consensus and extend it so that the reduced extensive form problem is parallelizable. Our form of PH heuristic exploits the structure of the scenario tree by fixing variables starting from the root-node. ii-) We assess the impact of fixing variables on the value of the optimal solution. iii-) We investigate as well some acceleration strategies that allow to accelerate the algorithm by extending the slamming technique proposed for two-stage stochastic programs by Watson and Woodruff (2011) to multistage stochastic programming. iv-) We use climate change to show one source of uncertainty in the yield although there can be other sources of yield uncertainty like the errors in measurement of forest growth or uncertainty of future yield due to prediction models. The algorithm is suitable as well to price uncertainty. Our aim is not to model perfectly the uncertainty in forest growth due to climate change but to provide an algorithm that can be used for real life application in stochastic forest harvest scheduling.

The remainder of this paper is organized as follows. In Section 4.2, we provide a background on stochastic programming problem formulation and formally introduce the progressive hedging algorithm. In Section 4.3, the special form of PH for solving forest harvest planning is presented. We provide in Section 4.4 the computational experiment and the interpretation of the results. Finally, Section 4.5 concludes the paper and presents the limitations of the algorithm and future work.

4.2 Background

To illustrate variables fixation variant of the progressive hedging algorithm, it is necessary to represent the scenario tree that is the abstraction of the realization of uncertainty in growth and yield and formerly introduce progressive hedging (PH) algorithm.

4.2.1 Scenarios representation

The stochastic program representation can be visualized as a tree, the so called "scenario tree". It can be represented as follows. Let $\mathcal{T}$ denote the set of periods in the planning horizon with $T = |\mathcal{T}|$ being the number of periods. In the tree, a node represents the realization of the uncertain parameter and variable at a given time period. Let n and $\mathcal{N}$ describe the node and the lexicographically numbered set of nodes $\{1, ..., |\mathcal{N}|\}$ in the tree, respectively. From each node n, for $t \in \mathcal{T} \setminus \{T\}$ there is at least one branch leading to another node m with a conditional probability p_m with $m \in \mathcal{I}_n$ that is the set of nodes, immediate successors of the node n. $\sum_{m \in \mathcal{I}_n} p_m = 1$. We denote by $\mathcal{N}^t$ the subset of nodes belonging to period t such that $\mathcal{N} = \cup_{t \in \mathcal{T}} \mathcal{N}^t$ and $\mathcal{N}^t \cap \mathcal{N}^{t+1} = \emptyset$ for $t \in \mathcal{T} \setminus \{T\}$. Let Ω represent the finite set of representative scenarios in the tree. A scenario $\omega \in \Omega$ is a particular realization of the uncertain parameter represented as a path from the root-node to a leaf-node. Each scenario ω has an associated probability or weight denoted by w^ω. Note that $\sum_{\omega \in \Omega} w^\omega = 1$. Similarly, let $\mathcal{N}_\omega$ represent the set of nodes forming the scenario ω. In other words, $\mathcal{N}_\omega$ is the set of nodes in a path from the root-node to a leaf node. There is a number of scenarios that traverse each node. Let $\Omega(n)$ denote the set of scenarios that traverse the node n. We have $\Omega(1) = \Omega$, $\Omega(n) \cap \Omega(n') = \emptyset \; \forall n \neq n'$ and $n, n' \in \mathcal{N}^t$. Finally, let $\tilde{\mathcal{S}}^n$ denote the set of successor nodes to the node n, for $n \in \mathcal{N}$. We have $\mathcal{N}^1$ is a singleton and $\tilde{\mathcal{S}}^n = \emptyset$ for $n \in \mathcal{N}^T$ (leaf-nodes). Furthermore, let α^n denote the immediate ancestor node of node n for $n \in \mathcal{N} \setminus \{1\}$, since $n = 1$ is the root-node of scenario tree. To introduce non-anticipativity, we need to define η as the set of nodes having more than one leaf-node as successor ($|\tilde{\mathcal{S}}^n \cap \mathcal{N}^T| > 1 \implies n \in \eta$). For instance, in Figure 4.1, nodes 2 and 3 have as leaf-node successors the set of nodes $\{5, 6\}$ and $\{7\}$, respectively. Therefore, node $2 \in \eta$ but node 3 does not. Finally, Let X^ω represents the matrix of variables for all $t \in \mathcal{T}$ for the scenario $\omega \in \Omega$. As the result, the stochastic program can be stated as follows:

$$\max_X \sum_{\omega \in \Omega} w^\omega f_\omega(X) \tag{4.1}$$

$$s.t. \; X^\omega \in C^\omega \quad \forall \omega \in \Omega \tag{4.2}$$

$$X^\omega = X^{\omega'} \quad \forall \omega, \omega' \in \Omega(n), \; \omega \neq \omega', \; n \in \eta \tag{4.3}$$

(4.1) maximizes the expectation from all scenarios. (4.2) says that all the solutions should be feasible with respect to the constraints of the scenario. C^ω is the feasible set for scenario ω. Finally, (4.3) imposes the non-anticipativity constraints (NAC) which require that the solution up to a period t from two scenarios should be the same if the two scenarios are indistinguishable up to period t. We call this model the extensive form (EF).

Notice we could write constraint (4.3) in a different form. Let $X_n^\omega := \{x_{1n}^\omega, x_{2n}^\omega, \ldots, x_{sn}^\omega\}$

be the vector of variables at node $n \in \eta$ under scenario ω and x_{sn}^{ω} is the state variable of the forest unit or 'stand' s. Let $\mathbf{Z}_n$ represent a vector of binary variables at node n. Imposing constraint (4.4) is equivalent to reinforcing NAC. Progressive hedging exploits this formulation.

$$X_n^{\omega} - \mathbf{Z}_n = 0 \quad \forall \omega \in \Omega(n),\ n \in \eta \tag{4.4}$$

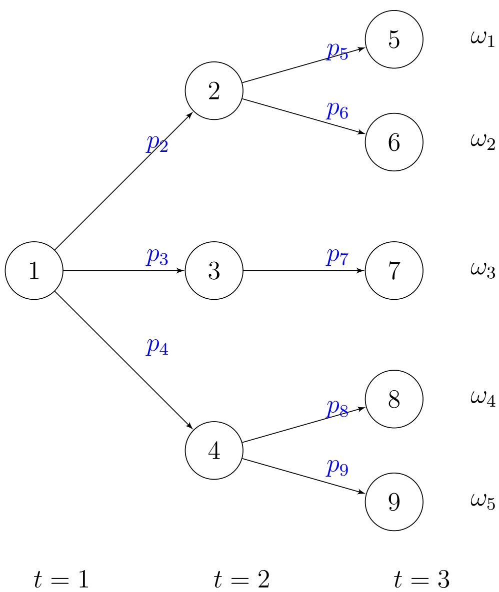

$$\mathcal{N}^1 = \{1\},\ \mathcal{N}^2 = \{2,3,4\},\ \mathcal{N}^3 = \{5,6,7,8,9\}$$
$$\mathcal{N}_1 = \{1,2,5\},\ \mathcal{N}_2 = \{1,2,6\}$$
$$\eta = \{1,2,4\}$$
$$\mathcal{I}_1 = \{2,3,4\},\ \mathcal{I}_2 = \{5,6\},\ \mathcal{I}_3 = \{7\}$$
$$\Omega(2) = \{\omega_1, \omega_2\}$$

Figure 4.1: *Scenario tree representation of stochastic programming*

4.2.2 Progressive hedging

Progressive hedging (PH) is a scenario based decomposition algorithm proposed by Rockafellar and Wets (1991) for stochastic programming models. The idea of progressive hedging is to relax the non-anticipativity constraints (NAC, Equations 4.4) in an augmented Lagrangean manner (Hestenes, 1969; Rockafellar, 1977; Rockafellar and Wets, 1991; Feizollahi et al., 2017) so that each scenario (sub-problem) can be solved independently. This assumes that solving sub-problems independently is much easier and faster. Non-anticipativity constraints require that values of variables that share the same ancestor nodes should be equal across scenarios up to that node. In other words, if two scenarios ω and ω' are indistinguishable up to period t, then the solutions of the two scenarios should be the same up to that period. For instance, in Figure 4.2, each variable at time $t = 1$ should be the same across all the five scenarios and values of variables in period $t = 2$ should be the same for scenarios 1 and 2. However, these constraints are not reinforced when scenarios are solved independently. Through progressive penalization of violations of NAC, the algorithm is proven to ultimately converge to the optimal solution for convex stochastic programs. In a nutshell, progressive hedging follows these steps:

1. Solve each scenario without penalization

2. Compute the average (z) for each variable

3. If solutions have sufficiently converged, then stop

4. Update penalization terms
   $\lambda = \rho(x - z) + \lambda$

5. Solve scenarios with penalization terms

6. Go to step 2

Algorithm 2 describes progressive hedging for multistage stochastic programming. The inputs of the algorithm are the penalty factor ρ, the maximum number of iterations $kmax$ and the termination criterion ϵ which indicates the level of consensus of non-anticipativity constraints that is acceptable. $\epsilon = 0$ means that the algorithm stops if all the non-anticipativity constraints are satisfied. In the algorithm, line 2 initializes a Lagrangian multiplier (λ) for each NAC constraint. A Lagrangian multiplier is associated with each Equation (4.4). To compute the average, of each variable we need to have the conditional probability associated to each branch of the scenario tree in the detached form (Figure 4.2). Equations (4.5) compute the conditional probability from node n to node m which is an immediate successor. That probability (q^{ω}_{nm}) is proportional to the number of leaf nodes associated with node m because the number of leaf-nodes informs on the number of scenarios passing by node m. For instance, from Figure 4.2, $q^1_{12} = q^2_{12} = \frac{p_2}{2}$, $q^1_{25} = p_5$ and $q^3_{13} = p_3$. Line 6 and 17 compute the average of each variable at node $n \in \eta$. Line 7 and 18 update the Lagrangian multiplier associated with each non-anticipativity constraint. Line 14 computes the NAC convergence euclidean distance. This distance is zero if all the NAC are satisfied.

$$q^{\omega}_{nm} = \frac{p_m}{|\Omega(m)|}, \quad \forall m \in \mathcal{I}_n \text{ and } m \in \mathcal{N}_{\omega} \tag{4.5}$$

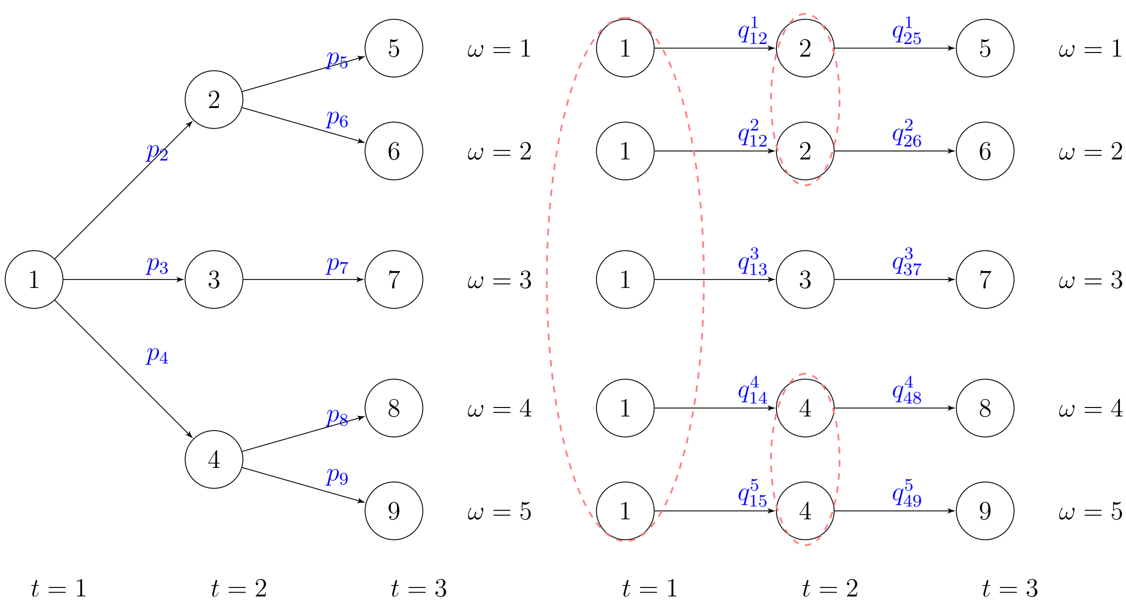

Figure 4.2: *Example of scenario representation in compact form (left) and in a detached form (right). The red-dotted ellipses show the non-anicipativity constraints that need to be imposed*

Algorithm 2 Progressive hedging multistage

function PH($\rho, kmax, \epsilon$)
  Initialize $\lambda_n^{0,\omega} = 0 \quad \forall n \in \eta, \quad \forall \omega \in \Omega(n)$
  for $\omega \in \Omega$ **do**
    $x^{0,\omega} = \arg\max_x \{f_\omega(x) : x \in C^\omega\}$
  end for
  $z_n^0 = \sum_{\omega \in \Omega(n)} q_{nm}^\omega x_n^{0,\omega} \quad \forall n \in \eta, \quad \forall m \in \mathcal{I}_n$
  $\lambda_n^{1,\omega} = \lambda_n^{0,\omega} + \rho(x_n^{0,\omega} - z_n^0) \quad \forall n \in \eta, \quad \forall \omega \in \Omega(n)$
  for $k = 1$ to $kmax$ **do**
    for $\omega = 1$ to $|\Omega|$ **do**
      $x^{k,\omega} = \arg\max_x \{g_\omega(x) = f_\omega(x) - \lambda^{k,\omega}(x - z^{k-1}) - \frac{\rho}{2}\|x - z^{k-1}\|_2^2 : x \in C^\omega\}$
      $\phi_\omega^k = \max_x g_\omega(x)$
    end for
    $\phi^k = \sum_{\omega \in \Omega} w^\omega \phi_\omega^k$
    if $\sqrt{\sum_{\omega \in \Omega} w^\omega \|x^{k,\omega} - z^{k-1}\|_2^2} < \epsilon$ **then**
      return $(x^k,\ \lambda^k,\ \phi^k)$
    end if
    $z_n^k = \sum_{\omega \in \Omega(n)} q_{nm}^\omega x_n^{k,\omega} \quad \forall n \in \eta, \quad \forall m \in \mathcal{I}_n$
    $\lambda_n^{k+1,\omega} = \lambda_n^{k,\omega} + \rho(x_n^{k,\omega} - z_n^k) \quad \forall n \in \eta, \quad \forall \omega \in \Omega(n)$
  end for
  return $(x^{kmax},\ \lambda^{kmax},\ \phi^{kmax})$
end function

4.3 Variables fixation

Progressive hedging variable fixing (PHVF) algorithm is identical to the classic progressive hedging algorithm (Algorithm 2). However, instead of letting variables converge progressively, PHVF fixes variables as they converge. Line 10 in progressive hedging algorithm (Algorithm 2) is replaced by Algorithm 3. The algorithm starts by fixing variables in the root-node as they converge. For instance, for a given node $n \in \eta$ if a variable has a value of 1 across all scenarios $\omega \in \Omega(n)$, that variable will be fixed to 1 across all those scenarios. This process is better described in Algorithm 3. However, unless a variable belongs to the root-node, it can only be fixed if all variables in the immediate ancestor α^n have been entirely fixed. The first thing to notice is that once the scenario tree is decomposed, there are more scenarios traversing the root-node (Figure 4.2). In addition, as we move away from the root-node toward the leaf-nodes, there is a fewer number of scenarios passing by any given node. Hence, if for instance, there are three branches originating from the root-node (as displayed in Figure 4.2), $|\mathcal{I}_1| = 3$, then after fixing the root-node, we get three distinct sub-extensive forms (SEF) ($\Omega(2)$, $\Omega(3)$, and $\Omega(4)$) that can be solved independently (Figure 4.1). Furthermore, the three SEF are much easier to solve compared to the original problem $\Omega(1)$. The algorithm description exploits that property of the scenario tree.

4.3.1 Algorithm description

During PHVF, at each iteration, and for each scenario, the problem on line 10 of Algorithm 2 needs to be solved. We refer to C^ω as the feasible set created by constraints (4.2) for each scenario. Note that if the uncertainty is only in the objective function (for instance, price uncertainty) then $C^\omega = C^{\omega'}$, $\forall \omega \neq \omega'$. In this case each solution of ω is feasible for $C^{\omega'}$ ($\omega \neq \omega'$). Since $z(\bullet)$ is the average of the values of the variables across scenarios (see line 6 of Algorithm 2), if its value is 1 (or 0) then it means all the scenarios met consensus that the variable should take a value of 1 (or 0), respectively. This realization is exploited in

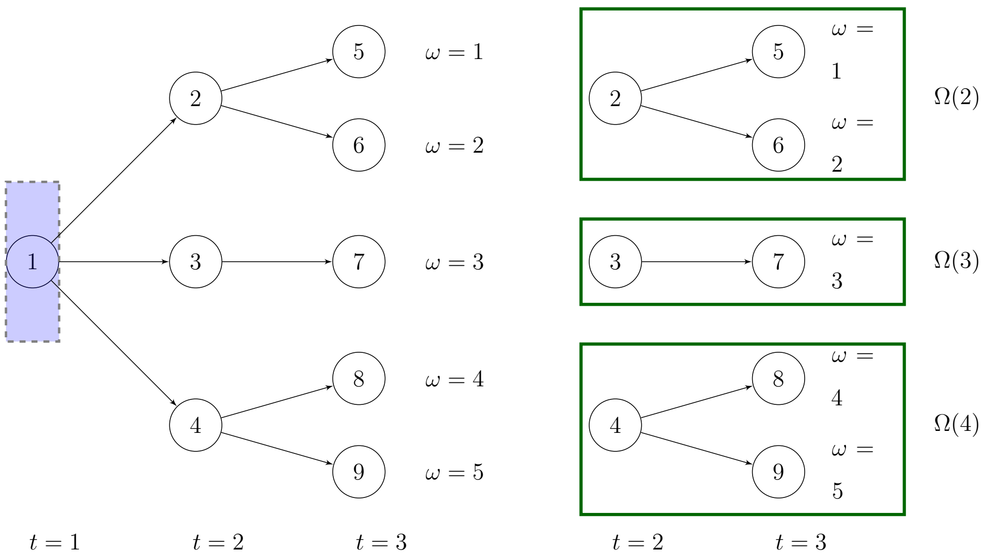

Figure 4.1: *Structure of stochastic problem after fixing the root-node (node 1). The three sub-extensive forms (SEF) denoted by* $\Omega(2)$, $\Omega(3)$ *and* $\Omega(4)$ *are independent.*

Algorithm 3 if it is supposed that the slamming factor $\theta_t = 1, \forall t$. The algorithm moves to the node at the next stage and performs variable fixation if that node belongs to the set of non-anticipativity nodes η and its predecessor is entirely fixed. The new feasible set created by constraints (4.2) and fixing some variables is denoted by C_*^ω. Note that this sub-problem is much smaller compared to the original sub-problem. In Algorithm 3, the inputs are θ, a function defining the value of the slamming factor depending on the stage t ($0 \leq \theta_t \leq 1$), see Section 4.3.3 for more information on this parameter; ω which is the scenario; and k which indicates the iteration.

Fixing variables impacts the optimality since some variables may be fixed to values that they may not have taken in the optimal solution. Hence, the algorithm has an impact on the optimality. The objective of fixing variables is not to completely solve the model through the procedure but to obtain a reduced extensive form (REF) that is tractable. Let τ denote the percentage of NAC variables that are fixed before switching to solving the REF. τ is a proxy to the number of nodes fixed. The question is what is the appropriate τ that will make the

REF tractable while not severely impacting the optimality? The answer to this question is investigated in Section 4.4.4.

Algorithm 3 Variables fixation module

---

function FIXVARIABLES(θ, ω, k)
stop = False;
for $t = 1$ to $|\mathcal{T}|$ **do**
n : $n \in \mathcal{N}^t \cap \eta \cap \mathcal{N}_\omega$
if α^n is fixed OR n is root-node **then**
for $i = 1$ to number of stands **do**
if $z_{n,i} \geq \theta_t$ **then**
Fix $X^{\omega}_{i,t}$ to 1
else if $z_{n,i} \leq 1 - \theta_t$ **then**
Fix $X^{\omega}_{i,t}$ to 0
else
stop = True
end if
end for
end if
if stop is True **then**
break
else if n not marked **then**
Mark n as fixed
end if
end for
$x^{k,\omega} = \arg\max_x \{g_\omega(x) = f_\omega(x) - \lambda^{k,\omega}(x - z^{k-1}) - \frac{\rho}{2}\|x - z^{k-1}\|_2^2 : x \in C_*^\omega\}$
return fixed nodes
end function

4.3.2 Parallel implementation

Algorithm 4 is designed for parallel implementation of PHVF. Hence, line 10 from Algorithm 2 has to be replaced by Algorithm 4. At each iteration of progressive hedging, the sub-problems can be solved in parallel because they are independent. However, fixing τ variables and switching to solve the reduced extensive form (the extensive form with some variables fixed, REF) is not parallelized. Nonetheless, since our algorithm (PHVF) fixes variables from the root-node to the leaf-nodes, after fixing each node, the problem can be separated into sub-extensive forms (SEF) that can be solved independently. For example, as illustrated in Figure 4.1, after fixing the root-node, we get three separate SEF models. Recursively, each sub-extensive form model can be solved through variable fixation leading to reduced sub-extensive form (RSEF). Each RSEF can then be solved directly if its size is deemed tractable. At the end, the solutions from all the REF can be combined to get the solution of the stochastic program.

Algorithm 4 PH variable fixing

function PHVF($\theta, \Omega(j), k$)
    fixed nodes = fixVaribles(θ, ω, k) $\quad \forall \omega \in \Omega(j)$
    if problem small enough **then**
        Solve reduced extensive form
    else
        for n in fixed nodes which successor are not fixed **do**
            for m $\in \mathcal{I}_n$ **do**
                PHVF($\theta, \Omega(m), k+1$)
            end for
        end for
    end if
    return x^{ω}
end function

4.3.3 Acceleration methods

Note from Algorithm 3 that if $\theta_t = 1$ then we fix a variable to 1 (or alternatively to 0) only if all scenarios of interest agree that the value of the variable should be 1 (or 0 alternatively), respectively. This requirement is hard to meet when dealing with hundreds of scenarios especially for the root-node variables which are replicated in all the scenarios. A variable may have the same value in all but one scenario for many iterations. Hence, that scenario slows the convergence. To avoid such a situation, "slamming" (Watson and Woodruff, 2011) forces variables to converge if the percentage of concordant scenarios for that variable reaches a threshold $\theta \leq 1$. However, instead of defining a scalar θ as in Watson and Woodruff (2011), we defined $\theta_t = f\big(\theta_0, Q(t)\big)$ as a function that depends on the stage because if a low value of θ is acceptable for the root-node, such a value is not acceptable when closer to the leaf-nodes (to avoid infeasibility). θ_0 is the initial value of θ, whereas $Q(t)$ can be a linear or exponential function term that increases θ value as a function of the t. Notice that if the uncertainty is in the objective function and we apply slamming, then the problem will always be feasible. In our case, preliminary tests allowed us to find the range of acceptable values of θ_0. Low values of θ_0 led to infeasibility.

In the same line of thought, even with slamming there is a chance that the algorithm is locked in a situation where there is no improvement of NAC convergence for many consecutive iterations. We define a "cascading" effect which lowers the value of θ to θ_{min} for one iteration if the algorithm does not improve (convergence of some non-anticipativity) for α consecutive iterations. This behavior allows to avoid getting stuck, since lowering θ allows to fix some variables for which almost all the scenario already reached consensus. For those variables, the percentage of variables that agree on the value the variable should take is close to θ_t and the consensus could eventually be reached after several iterations. We have noticed that the cascading effect may lead to infeasibility because it may be forcing some variables to a value they would not take otherwise. When infeasibility arises, we roll back and eliminate the cascading effect. In general, there is a trade-off between infeasibility and the value of θ. Low values of θ lead to a risk of infeasibility while raising that value may make the acceleration methods less efficient.

4.3.4 Stopping criteria

In the case of classic progressive hedging, the algorithm stops because we have reached an acceptable level of consensus for NAC or because all the NAC are satisfied. The algorithm terminates as well if the maximum number of iterations (k_{max}) is reached. In our algorithm, we keep these two stopping criteria, although we know that they may never be reached. We instead rely on the fact that at some points, many nodes will be fixed (NAC consensus is reached for some nodes) and the reduced sub-extensive forms can be solved directly. The number of NAC consensus reached is checked through the parameter τ which is the percentage of variables fixed. When the percentage of variables fixed is greater than or equal to τ, the algorithm switches to solve the REF or RSEF.

4.4 Numerical experiment

We describe here an empirical performance analysis of our proposed algorithm. For easiness to follow our experiment and replicate the results, we formulate the stochastic version of the so called 'Model I' of forest harvest scheduling.

4.4.1 Problem definition and formulation

$$\max \sum_{\omega \in \Omega} w^{\omega} \left[\sum_{t \in \mathcal{T}} \left(r_t H_t^{\omega} - \sum_{s \in \mathcal{S}} c_{st} x_{st}^{\omega} \right) \right] \tag{4.1}$$

subject to

$$n_s^{\omega} + \sum_{t \in \mathcal{T}} x_{st}^{\omega} = 1 \quad \forall s \in \mathcal{S},\ \forall \omega \in \Omega \tag{4.2}$$

Indices

ω, ω' scenario

s stand

t time period

Sets

$\mathcal{S}$ set of stands

Ω set of scenarios

$\Omega(n)$ set of scenarios passing by the node n

η set of nodes on which NAC should be reinforced

$\mathcal{N}^t$ set of nodes at stage t

$\mathcal{T}$ set of time in the planning horizon

Parameters

r_t profit from selling wood in period t (\$/mbf). It is the discounted profit that include selling cost

c_{st} cost of harvesting and hauling wood from stand s in period t (\$). It is the discounted cost

y_{st}^{ω} volume of wood harvestable per area from stand s in period t according to scenario ω (mbf/ac). This volume depends on the climate that materializes; therefore, it is a parameter that depends on the scenario ω

a_s area of stand s (acres)

age_{st} age of stand s at the end of the planning horizon if harvested in year t

$age_{s\cdot}$ current age of stand s

age_{s0} age of stand s if not harvested during the planning horizon

f_{min} allowable percentage of decrease of volume harvested from one period to another

f_{max} allowable percentage of increase of volume harvested from one period to another

w^{ω} probability or weight of scenario ω

Variables

x_{st}^{ω} binary variable taking a value of 1 if stand s should be harvested in period t according to scenario ω, and 0 otherwise

n_s^{ω} binary variable: 1 if management unit s should not be harvested during the planning horizon under scenario ω, and 0 otherwise

H_t^{ω} accounting variable storing the volume of wood harvested in period t according to scenario ω (mbf)

$$\sum_{s \in \mathcal{S}} a_s y_{st}^{\omega} x_{st}^{\omega} = H_t^{\omega} \quad \forall t \in \mathcal{T},\ \forall \omega \in \Omega \tag{4.3}$$

$$(1 - f_{min}) H_t^{\omega} \geq H_{t+1}^{\omega} \quad \forall \omega \in \Omega\ , \forall t = 1, ..., |\mathcal{T}| - 1 \tag{4.4}$$

$$(1 + f_{max}) H_t^{\omega} \leq H_{t+1}^{\omega} \quad \forall \omega \in \Omega\ , \forall t = 1, ..., |\mathcal{T}| - 1 \tag{4.5}$$

$$\sum_{s \in \mathcal{S}} a_s \left[\sum_{t \in \mathcal{T}} age_{st} x_{st}^{\omega} + age_{s0} n_s^{\omega} \right] \geq \sum_{s} a_s age_{s.} \quad \forall \omega \in \Omega \tag{4.6}$$

$$x_{st}^{\omega} = x_{st}^{\omega'} \quad \forall \omega \neq \omega';\ \omega, \omega' \in \Omega(n);\ n \in \eta;\ t = \{t \mid n \in \mathcal{N}^t\};\ \forall s \in \mathcal{S} \tag{4.7}$$

$$x_{st}^{\omega},\ n_s^{\omega} = \{0, 1\}, \quad H_t^{\omega} \in \mathcal{R}^{+} \tag{4.8}$$

The expression (4.1) maximizes the profit from timber harvest from all scenarios weighted by their respective probabilities. Constraints (4.2) require that a stand is at most harvested once during the planning horizon. We use the variable n_s to capture stands that are not prescribed to be harvested during the whole planning horizon. We need that variable to compute the average ending age of the forest as shown in constraints (4.6). Constraints (4.3) compute the volume harvested in each period during the planning horizon. It uses the parameter y_{st}^{ω} which values depend on the forest growth scenario ω of interest. Note that the set of constraints (4.3) is not necessary. We could have written the same model without using that set of constraints. However, doing so would require to rewrite the constraints (4.4) and (4.5) and finally it would negatively affect the readability of the model. Constraints (4.4) and (4.5) impose the even flow constraints so that the volume harvested from one period to another remain within an allowed fluctuation range. Constraints (4.6) require that on average, the forest at the end of the planning horizon is at least as old as the forest at the beginning of the planning horizon. Finally, constraints (4.7) impose the non-anticipativity constraints. It requires that for each stand s, at time t, if two scenarios are indistinguishable then the decision should be the same for the two scenarios at that time. If $\mathcal{N}_\omega \cap \mathcal{N}_{\omega'} \neq \emptyset$ then there exists t such that the two scenarios are indistinguishable at t. Constraints (4.8) enforce that the decision variables are binary, and the accounting variables are continuous. We remind the reader that variables H_t^ω are not required for this model.

4.4.2 Climate change data

The potential mean annual increment, which is an indicator of forest growth in a year might change in the Pacific North West because of climate change. The change depends on temperature, precipitation, and air moisture content, all driven by human activities and economic development (Latta et al., 2010). In addition, the change is not geographically uniform. Hence, the change tends to be negative in Oregon compared to Washington state. Similarly, the change tend to be negative in low altitudes in Oregon. We used the data from Latta et al. (2010) which forecast the potential mean annual increment change (pMAI) by the year 2100. The pMAI ($m^3/ha/year$) is the potential change in forest growth that will be observed in a given year, hence it is a volume given as a function of time and area. We assumed linear change of the growth from now until that year. For instance, the growth change for next two decades is the double of the growth change for the next decade. The climate paths defined in the Pacific Northwest are A2, A1B, B1 and Commit (or C). Tables 4.1 and 4.2 present the values of potential mean annual increment change for each one of the climate paths. In Table 4.2, climate paths D1 to D4 are artificial climate paths that suppose higher pMAI. We built forest growth scenarios by assuming it is possible to transit from one climate path to another because of mitigation or intensification of climate change due to human actions.

4.4.3 Experimental design

The experiments were conducted under a DELL Desktop computer running on Windows with Intel(R) Core(TM) 2 Quad CPU @ 3.70 GHz and 8 GB of memory. During PHVF iterations, each scenario is solved at optimality gap of 1%. This is a premature stop. Nevertheless, this criterion proved to accelerate solution time for each scenario. Furthermore, the last solutions of a mixed integer program are the most difficult ones with no to little improvement of the objective function value. All the models were solved using IBM ILOG CPLEX 12.6 (CPLEX, (CPLEX, 2019)). The memory allocated for storing the nodes was 3,000 MB and the nodes were set to be stored in a compressed format on the hard drive. All other parameters were left to their default values. The code was implemented in Java 10 using Concert Technology of CPLEX.

For parallel computation, we used the paradigm of master-workers. The master is in charge of coordinating the PHVF algorithm while distributing the task of solving individual sub-models or REF to the workers. Each worker sends back its solution upon completion. The workers compete for access to the memory. Therefore, the choice of the number of workers must be judicious to avoid the overhead which is the amount of time required to coordinate parallel tasks, as opposed to doing useful work. Preliminary experiments showed that two workers was the optimal number given the configurations of the computer. The general framework of the model is presented in Figure 4.1. The input data contains the information on the forest, the climate change (growth change), and the regulations that ought to be met by the harvest planning. The input is fed to PHVF module that is the master governing the optimization process. The workers are the ones interacting with the optimizer (CPLEX in this case). They send the model to the optimizer which returns the solution. The advantage of this framework is that we could change the optimizer without having to re-adapt our algorithm. At the end, the output module collects the harvest planning and informs the decision making.

Forest growth scenarios were generated using the information on the growth change reported in Latta et al. (2010) (see Table 4.1 and 4.2). We assumed that due to climate change and climate change mitigation efforts, it is possible to transition from one climate path to another in two consecutive periods. Hence, for instance, it is possible to transition from climate path A2 in year 2020 to climate path B1 in year 2030. We further assume that the probability of transiting from one climate path to the other is the same. As result, the

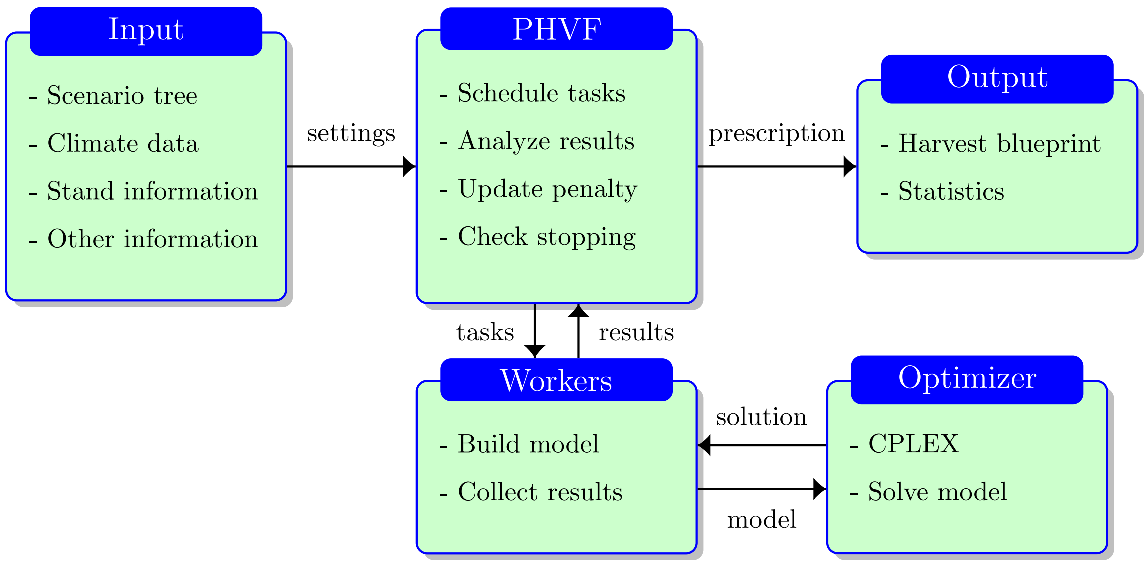

Figure 4.1: *Framework of PHVF algorithm for harvest scheduling under climate change*

scenarios are considered equally probable. Note that this assumption does not have much incidence on the performance of the algorithm. Based on the number of scenarios generated, we defined small, medium and big instances. The small instances have 64 scenarios (1 X 4 X 4 X 4 X 1) which is four branching for the first three periods. The medium instances have 256 scenarios which corresponds to four branching for the first four periods (1 X 4 X 4 X 4 X 4). For small and medium instances, pMAI corresponding to each climate path is reported in Table 4.1. The big instances have 512 scenarios made of eight branching for the first three periods (1 X 8 X 8 X 8 X 1). The in-depth description of the scenario tree generation methods and its quality are beyond the scope of this research. The interested reader could refer to Dupacová et al. (2000); Høyland and Wallace (2001); Høyland et al. (2003); Casey and Sen (2005); Pranevicius and Sutiene (2007); Heitsch and Römisch (2009); Löhndorf (2016) and more importantly Rios et al. (2016) who describe scenarios generation in forest management framework. We tested our algorithm on six different forests with three being real forests, the data of which are publicly available[1] (P1, P34, P36). The other three

[1] http://ifmlab.for.unb.ca/fmos/datasets/

were computer-generated forests (P75, P83, P100). The six forests are set to be located in three different altitude classes. The forests are supposed to be located in Oregon and in Washington state. The values of pMAI for the six forests for large instances is reported in Table 4.2. Table 4.3 shows the characteristics of the forests and the scenario instances. In the tables, values show the potential mean annual increment change by 2100. Hence, negative values mean there will be a decrease in forest growth whereas, positive values mean that there will be an increase in forest growth.

Table 4.1: *Value of pMAI ($m^3/ha/year$) for small and medium instances*

	Forests					
	P1	P34	P36	P75	P83	P100
A2	0.5	3.1	-0.3	1.8	0.4	2.1
A1B	0.4	2.5	-0.3	1.6	0.3	1.6
B1	0.4	1.3	0.0	1.0	0.3	1.0
C	0.2	0.2	0.1	0.2	0.1	0.3

Table 4.2: *Values of pMAI ($m^3/ha/year$) of all the six forests for large instances*

A2	A1B	B1	C	D1	D2	D3	D4
3.1	2.5	1.3	0.2	4.0	5.0	6.0	7.0

The medium instances were used as reference to investigate how many variables should be fixed in order to have a problem that is computationally tractable. For that purpose, we solved the stochastic models, using the serial version of our algorithm (Algorithm 2 and 3), setting τ to just 20%, 40%, 60% and 70% before switching to solving the reduced extensive form. $\tau = 20\%$ means some variables are fixed but the root-node is not completely fixed; and

$\tau = 40\%$ means that all the root-node variables are completely fixed and some variables from the second period nodes are fixed (As stated before τ is proxy to the number of nodes fixed. This scheme is possible because there are 25% of NAC variables at each stage, thus at the root-node as well).

We made the experiment by allocating 15, 30, 45 and 60 minutes for each problem. The time is chosen to allow the effect of τ to manifest itself. The tests were run with five repetitions and the average of the objective function value was reported. Notice that if the time is too long then eventually all problems can be solved even the extensive form. Conversely, if the time is too short then PHVF may not have enough time to finish fixing variables before the time limit and hence low values of τ will be favored. During the whole experiment, we defined $\theta_t = \min\{0.999, 1.05^{(t-1)}\theta_0\}$. As results, for the first stage ($t = 1$), $\theta_1 = \theta_0$. Similarly, we defined $\theta_{min} = \max\{0.75, \theta_t - 0.05t\}$. These values were defined from empirical experimentation.

For assessment of our algorithm performance, each problem was solved using our algorithm (PHVF) and comparing that solution to the one obtained by CPLEX solving directly the EF for the equivalent wall clock time. In addition, we report the optimality gap produced by CPLEX and the gain which is calculated according to $gain = \frac{PHVF-EF}{EF}$ where EF is the objective function value obtained by solving directly the extensive form model and $PHVF$ is the solution obtained by PHVF algorithm for the same runtime. For medium and large instances, we report as well the EF value after solving the EF problems for 86,000 seconds (24 hours).

Table 4.3: *Description of problems size*

Forest	$\|\Omega\|$	Binary Cols	Total Cols	Rows	Non-Zeros	Stands
	64	6,552,015	6,552,335	6,349,760	61,375,488	
P1	256	62,209,423	62,210,703	61,747,968	66,199,808	1,363
	512	64,286,635	64,289,195	62,798,592	614,320,640	
	64	612,960	613,280	69,024	633,472	
P34	256	651,872	653,152	644,288	6,150,272	32
	512	6,100,640	6,103,200	672,704	6,322,560	
	64	636,045	636,365	623,616	696,576	
P36	256	6,144,269	6,145,549	6,117,248	6,431,872	89
	512	6,279,905	6,282,465	6,189,440	6,920,576	
	64	6,121,500	6,121,820	677,632	6,311,808	
P75	256	6,486,300	6,487,580	6,387,328	61,400,832	300
	512	6,943,500	6,946,060	6,621,568	63,288,576	
	64	6,121,500	6,121,820	677,632	6,311,104	
P83	256	6,486,300	6,487,580	6,387,328	61,398,016	300
	512	6,943,500	6,946,060	6,621,568	63,277,312	
	64	6,121,500	6,121,820	677,632	6,310,400	
P100	256	6,486,300	6,487,580	6,387,328	61,395,200	300
	512	6,943,500	6,946,060	6,621,568	63,266,048	

4.4.4 Results of the experiment

In addition to the number of scenarios, SMIP size grows as well with the number of units (stands) because we need to define non-anticipativity constraint for each stand at the time periods on which constraints (4.7) should be imposed. The problem size increases almost by tenfold when going from small instances to the medium ones. The smallest problem in this experiment has 600k+ binary variables and over 69k constraints (Table 4.3).

Impact of τ on the optimality and solution time

Tables 4.4, 4.5, 4.6, 4.7, 4.8 and 4.9 report the effect of τ on the value of the objective function with respect to the runtime for forests P1, P34, P36, P75, P83 and P100, respectively. We report as well, *improvement*(%) which is the percentage of increase (if positive) or decrease (if negative) of the objective function value from the objective function value for $\tau = 20\%$ for the same runtime.

In summary, as expected, everything else being equal, longer runtimes allow a higher objective function. As we can see for $\tau > 40\%$ which corresponds to fixing entirely the root-node and fixing some variables from the second stage, we have numerical issues. The numerical issues have two sources. On one hand, the algorithm may run out of time while fixing the variables or finished fixing the variables but does not have enough time to find a feasible solution to the REF. On the other hand, the basis of the REF may be disturbed in a way that the number of constraints and variables is not balanced so it is hard for branch and cut algorithm used by CPLEX to find an integral solution for the REF in the allocated time. This is the case for forest P34 with no solution when $\tau = 60\%$ even when the time is 1 hour. However, for the same forest, there is an integral solution when τ is raised to 70%. This behavior occurred mainly for forest P34 and P100 and is not observed when $\tau = 40\%$.

The second aspect is the impact of τ on the optimality. The advantage that higher values of τ have over the small ones tend to vanish when the runtime is long. Similarly, the improvement in optimality from $\tau = 40\%$ to higher values of τ is low. In fact, for some forest such as P83, over $\tau = 40\%$, the objective function value diminishes as τ increases which can be interpreted as during PHVF, many variables are fixed to values that are sub-optimal. It clearly appears that fixing just the root-node is the best choice for these problems. It allows sufficient time for REF to find an integral solution while avoiding to impact the optimality, and limiting the disturbance on the structure of the basis matrix.

Table 4.4: *Effects of τ and allocated time for the forest P1*

Forest	ρ	Time (min)	τ	Iterations	α	θ_0	Value	Improvement (%)
P1	1000000	15	20	1	6	0.95	371,524,817	-
			40	9	6	0.95	386,068,433	3.9
			50	18	6	0.95	T	NA
			60	20	6	0.95	T	NA
			70	21	6	0.95	T	NA
		30	20	1	6	0.95	373,450,417	-
			40	9	6	0.95	386,156,779	3.4
			50	18	6	0.95	385,676,118	3.3
			60	20	6	0.95	385,394,686	3.2
			70	21	6	0.95	385,258,771	3.2
		45	20	1	6	0.95	375,427,413	-
			40	9	6	0.95	386,156,779	2.9
			50	18	6	0.95	385,676,118	2.7
			60	20	6	0.95	385,394,686	2.7
			70	21	6	0.95	385,258,771	2.6
		60	20	1	6	0.95	375,804,390	-
			40	9	6	0.95	386,156,779	2.8
			50	18	6	0.95	385,676,118	2.6
			60	20	6	0.95	385,394,686	2.6
			70	21	6	0.95	385,258,771	2.5

T: Termination because PHVF ran out of time while iterating; NA: Not applicable, ρ: Penalty factor; τ: Percentage of variables fixed; α: Cascading factor; θ_0: Initial slamming factor

Table 4.5: *Effects of τ and allocated time for the forest P34*

Forest	ρ	Time (min)	τ	Iterations	α	θ_0	Value	Improvement (%)
P34	10000	15	20	1	10	0.95	1,333,129	-
			40	1	10	0.95	1,332,692	-0.0
			50	6	10	0.95	N	NA
			60	9	10	0.95	N	NA
			70	18	10	0.95	1,347,152	1.1
		30	20	1	10	0.95	1,344,498	-
			40	1	10	0.95	1,344,260	-0.0
			50	6	10	0.95	N	NA
			60	9	10	0.95	N	NA
			70	18	10	0.95	1,347,491	0.2
		45	20	1	10	0.95	1,345,620	-
			40	1	10	0.95	1,345,761	0.0
			50	6	10	0.95	N	NA
			60	9	10	0.95	N	NA
			70	18	10	0.95	1,347,555	0.1
		60	20	1	10	0.95	1,346,799	-
			40	1	10	0.95	1,346,489	-0.0
			50	6	10	0.95	1,343,802	-0.2
			60	9	10	0.95	N	NA
			70	18	10	0.95	1,347,759	0.1

N: Terminated because could not find feasible solution; NA: Not applicable, ρ: Penalty factor; τ: Percentage of variables fixed; α: Cascading factor; θ_0: Initial slamming factor

Table 4.6: *Effects of τ and allocated time for the forest P36*

Forest	ρ	Time (min)	τ	Iterations	α	θ_0	Value	Improvement (%)
P36	5000	15	20	1	10	0.9	4,468,454	-
			40	22	10	0.9	4,513,717	1.0
			50	41	10	0.9	4,532,819	1.4
			60	51	10	0.9	4,522,013	1.2
			70	60	10	0.9	4,525,669	1.3
		30	20	1	10	0.9	4,570,040	-
			40	22	10	0.9	4,534,327	-0.8
			50	41	10	0.9	4,534,156	-0.8
			60	51	10	0.9	4,523,000	-1.0
			70	60	10	0.9	4,530,669	-0.9
		45	20	1	10	0.9	4,616,899	-
			40	22	10	0.9	4,534,470	-1.8
			50	41	10	0.9	4,534,161	-1.8
			60	51	10	0.9	4,532,251	-1.8
			70	60	10	0.9	4,530,669	-1.9
		60	20	1	10	0.9	4,662,056	-
			40	22	10	0.9	4,534,574	-2.7
			50	41	10	0.9	4,534,219	-2.7
			60	51	10	0.9	4,532,251	-2.8
			70	60	10	0.9	4,530,669	-2.8

ρ: Penalty factor; τ: Percentage of variables fixed; α: Cascading factor; θ_0: Initial slamming factor

Table 4.7: *Effects of τ and allocated time for the forest P75*

Forest	ρ	Time (min)	τ	Iterations	α	θ_0	Value	Improvement (%)
P75	2000	15	20	1	10	0.9	58,202,734	-
			40	19	10	0.9	59,007,403	1.4
			50	55	10	0.9	T	NA
			60	57	10	0.9	T	NA
			70	70	10	0.9	T	NA
		30	20	1	10	0.9	58,272,824	-
			40	19	10	0.9	59,106,277	1.4
			50	55	10	0.9	59,387,884	1.9
			60	57	10	0.9	59,324,544	1.8
			70	70	10	0.9	59,337,782	1.8
		45	20	1	10	0.9	58,297,317	-
			40	19	10	0.9	59,131,601	1.4
			50	55	10	0.9	59,394,942	1.9
			60	57	10	0.9	59,336,592	1.8
			70	70	10	0.9	59,354,249	1.8
		60	20	1	10	0.9	58,310,384	-
			40	19	10	0.9	59,248,444	1.6
			50	55	10	0.9	59,395,816	1.9
			60	57	10	0.9	59,339,145	1.8
			70	70	10	0.9	59,354,525	1.8

T: Termination because run out of time iterating; NA: Not applicable, ρ: Penalty factor; τ: Percentage of variables fixed; α: Cascading factor; θ_0: Initial slamming factor

Table 4.8: *Effects of τ and allocated time for the forest P83*

Forest	ρ	Time (min)	τ	Iterations	α	θ_0	Value	Improvement (%)
P83	2000	15	20	1	10	0.9	57,970,162	-
			40	14	10	0.9	58,558,170	1.0
			50	30	10	0.9	58,516,976	0.9
			60	32	10	0.9	58,559,069	1.0
			70	34	10	0.9	58,592,562	1.1
		30	20	1	10	0.9	58,305,853	-
			40	14	10	0.9	58,891,381	1.0
			50	30	10	0.9	58,833,317	0.9
			60	32	10	0.9	58,733,563	0.7
			70	34	10	0.9	58,661,347	0.6
		45	20	1	10	0.9	59,052,205	-
			40	14	10	0.9	58,898,935	-0.3
			50	30	10	0.9	58,834,898	-0.4
			60	32	10	0.9	58,733,746	-0.5
			70	34	10	0.9	58,661,964	-0.7
		60	20	1	10	0.9	59,052,215	-
			40	14	10	0.9	58,904,481	-0.3
			50	30	10	0.9	58,835,134	-0.4
			60	32	10	0.9	58,733,734	-0.5
			70	34	10	0.9	58,661,851	-0.7

ρ: Penalty factor; τ: Percentage of variables fixed; α: Cascading factor; θ_0: Initial slamming factor

Table 4.9: *Effects of τ and allocated time for the forest P100*

Forest	ρ	Time (min)	τ	Iterations	α	θ_0	Value	Improvement (%)
P100	50000	15	20	1	10	0.95	42,331,212	-
			40	27	10	0.95	T	NA
			50	63	10	0.95	T	NA
			60	69	10	0.95	T	NA
			70	79	10	0.95	T	NA
		30	20	1	10	0.95	42,494,130	-
			40	27	10	0.95	43,307,744	1.9
			50	63	10	0.95	43,298,439	1.9
			60	69	10	0.95	N	NA
			70	79	10	0.95	43,288,841	1.9
		45	20	1	10	0.95	42,819,969	-
			40	27	10	0.95	43,309,455	1.1
			50	63	10	0.95	43,299,189	1.1
			60	69	10	0.95	N	NA
			70	79	10	0.95	43,290,127	1.1
		60	20	1	10	0.95	42,931,057	-
			40	27	10	0.95	43,309,402	0.9
			50	63	10	0.95	43,299,759	0.9
			60	69	10	0.95	N	NA
			70	79	10	0.95	43,290,127	0.8

T: Termination because run out of time iterating; N: Terminated because could not find feasible solution; NA: Not applicable, ρ: Penalty factor; τ: Percentage of variables fixed; α: Cascading factor; θ_0: Initial slamming factor

PHVF versus EF solved directly

Table 4.10 presents the results from PHVF using $\tau = 40\%$ which is equivalent to fixing the root-node and then solving in parallel the SEF. As we can see for the small instances (64 scenarios), solving directly the extensive form outperformed using PHVF. This means the overhead of decomposing the problem into scenarios and solving each one overweighs the benefit. For the medium instances, the results are mixed. Out of the six forests, PHVF outperformed the EF in two cases. Even when PHVF under performed, it had results that were less than 1% away from the optimal solution. The benefit of using PHVF over the state of art commercial solver such as CPLEX is highlighted when dealing with big instances (512 scenarios). PHVF outperformed the EF for the six forests. In the case of P1 which is the biggest model with 1,363 units (Table 4.3), EF completely failed to solve the model because it could not fit it in the memory. For other cases for the same runtime, PHVF reached gains ranging from 0.84 % to over 767% corresponding to forests P34 and P100, respectively. Even after leaving EF for 24h, PHVF run for 15 min still outperformed in some cases. Comparing the gain to the gap from EF suggests that PHVF almost reached the optimal solution or its solution has a relative optimal gap less than 1%.

4.5 Conclusions

In this paper, we have developed a method for solving multistage stochastic mixed integer programs that arise in natural resources management such as forest harvest planning. Although tested for growth uncertainty due to climate change, the method is valid as well for other sources of uncertainty such as errors in the model predicting forest growth, and uncertainty in the price of wood. This algorithm is also applicable to other disciplines where the decision variables are binary.

In the forest industry, managers solve multiple instances of the same forest model. It is therefore necessary to have an algorithm that allows one to quickly solve the SMIP. Furthermore, having an algorithm that is faster allows the practitioners to explore different

Table 4.10: *Comparison of solutions from PHVF and the extensive form*

				same duration with PHVF			24 h		
$\|\Omega\|$	Time(s)	Forest	PHVF	EF	Gap(%)	Gain(%)	EF	Gap(%)	Gain(%)
64	120	P1	2.99E+08	3.08E+08	0.14	-2.69	-	-	-
64	120	P34	1.04E+06	1.05E+06	0.14	-1.64	-	-	-
64	120	P36	3.48E+06	3.73E+06	0.32	-6.77	-	-	-
64	120	P75	4.71E+07	4.75E+07	1.59	-0.81	-	-	-
64	120	P83	4.70E+07	4.72E+07	0.43	-0.46	-	-	-
64	120	P100	6.53E+07	6.54E+07	0.51	-0.05	-	-	-
256	600	P1	3.86E+08	3.87E+08	0.05	-0.17	3.87E+08	0.02	-0.28
256	600	P34	1.35E+06	1.33E+06	2.38	**1.56**	1.35E+06	0.73	-0.05
256	600	P36	4.73E+06	4.64E+06	2.05	**1.75**	4.70E+06	0.82	**0.52**
256	600	P75	5.94E+07	5.94E+07	0.69	-0.06	5.97E+07	0.19	-0.55
256	600	P83	5.90E+07	5.93E+07	0.28	-0.47	5.93E+07	0.22	-0.50
256	600	P100	4.34E+07	4.34E+07	0.34	-0.06	4.35E+07	0.14	-0.22
512	900	P1	2.91E+08	NA	NA	∞	NA	NA	∞
512	900	P34	2.07E+06	2.05E+06	1.2	**0.84**	2.07E+06	0.27	-0.08
512	900	P36	6.85E+06	6.78E+06	1.876	**1.13**	6.79E+06	1.64	**0.89**
512	900	P75	8.48E+07	4.50E+07	89.57	**88.63**	8.50E+07	0.22	-0.28
512	900	P83	8.47E+07	4.49E+07	89.44	**88.76**	8.45E+07	0.63	**0.27**
512	900	P100	4.74E+07	5.49E+06	767.9	**763.3**	5.49E+06	767.9	**763.3**

NA: No results because of memory limitation.

management options. However, problems tested in this experiment are quite small compared to the models in the industrial standard. Nevertheless, this requirement may be compensated by the availability of more powerful computation resources in the industry.

The PHVF presented here overcomes some limitations listed in the literature regarding the choice of the penalty term ρ. It is documented that large values of ρ lead to the phenomenon of cycles (Boland et al., 2018). However, because PHVF fixes variables, such a problem is avoided. Notwithstanding all these benefits, PHVF has more parameters that need to be set compared to the classic PH. Fortunately, most of those parameters are easy to set and the limitation remains on the choice of the penalty term ρ. In the preliminary explorations, too low values of ρ led to some numerical issues while too high ones, although accelerated the convergence, negatively impacted the objective function value.

The future extension of this work is to investigate the impact of different parameters on the solution quality. Similarly, having an algorithm that can dynamically determine the value of the penalty term would be an improvement for practitioners. On practical aspects, the question of the optimal number of scenarios necessary to approximate the growth change under climate change remains open. This can be done by computing the value of the stochastic solution, the expected value of perfect information for different scenario trees (Gupta et al., 2014; Di Domenica et al., 2007; Apap and Grossmann, 2017; Pantuso and Boomsma, 2019).

Appendix

4.A Proof of infeasibility of classic progressive hedging coupled with variables fixation

Let consider a hypothetical problem under studies for a structure with four scenarios and three stages as shown on the figure below (Figure 4.A.1). Let's suppose the forest has four stands. The decision variable for each scenario is therefore:

$$x = \begin{bmatrix} x_{11} & x_{12} & x_{13} \\ x_{21} & x_{22} & x_{23} \\ x_{31} & x_{32} & x_{33} \\ x_{41} & x_{42} & x_{43} \end{bmatrix} \tag{4.A.1}$$

The variables x_{ij} in the matrix x are all binary. $x_{ij} = 1$ means that the stand i should be harvested in period j. Since a stand cannot be harvested more than once, $\sum_j x_{ij} \leq 1 \; \forall i$.

During progressive hedging, at iteration k, we can have this solution. We use the superscript x^ω to refer to the solution from scenario $\omega \in \{1, 2, 3, 4\}$, whenever necessary.

$$x^1 = \begin{bmatrix} 0 & 0 & 1 \\ 1 & 0 & 0 \\ 1 & 0 & 0 \\ 0 & 1 & 0 \end{bmatrix} \quad x^2 = \begin{bmatrix} 0 & 0 & 1 \\ 1 & 0 & 0 \\ 1 & 0 & 0 \\ 0 & 1 & 0 \end{bmatrix} \quad x^3 = \begin{bmatrix} 0 & 1 & 0 \\ 1 & 0 & 0 \\ 0 & 0 & 1 \\ 0 & 1 & 0 \end{bmatrix} \quad x^4 = \begin{bmatrix} 0 & 1 & 0 \\ 1 & 0 & 0 \\ 0 & 0 & 1 \\ 0 & 1 & 0 \end{bmatrix} \tag{4.A.2}$$

Since solutions of the second stage are identical for scenarios 1 and 2, we can fix entirely the variables of the second stage for the two scenarios. Similarly, we can fix entirely the second stage variables for scenarios 3 and 4.

$$x_{i2}^{1} = x_{i2}^{2} = \begin{bmatrix} 0 \\ 0 \\ 0 \\ 1 \end{bmatrix} \quad \text{and} \quad x_{i2}^{3} = x_{i2}^{4} = \begin{bmatrix} 1 \\ 0 \\ 0 \\ 1 \end{bmatrix} \tag{4.A.3}$$

$$x_{i1}^{\omega} = \begin{bmatrix} 0 \\ 1 \\ 0 \end{bmatrix} \quad \forall \omega,\ i = 1, 2, 4 \tag{4.A.4}$$

Comparing variables of the first stage across the four scenarios we can see that we can fix all variable except the stand 3 which is scheduled for harvest in period 1 for scenario 1 and 2 but is scheduled for harvest in period 3 for the two other scenarios (equation 4.A.4). Therefore, the reduced problem will have all variables fixed except the third period variables as well as x_{31} for all scenarios. For this problem to be feasible, either $x_{31} = 0$ or $x_{31} = 1$ for all scenario. However, there is a constraint that links the volume harvested in one period to another (Constraints 4.4 and 4.5). Hence, setting $x_{31} = 0$ means there will be less than acceptable volume in period 1 for scenario 1 and 2. Similarly, setting $x_{31} = 1$ leads to volume of zero in period 3 for scenarios 3 and 4 which may not be acceptable as well. This situation occur because the productivity of each stand is different with respect to the scenarios.

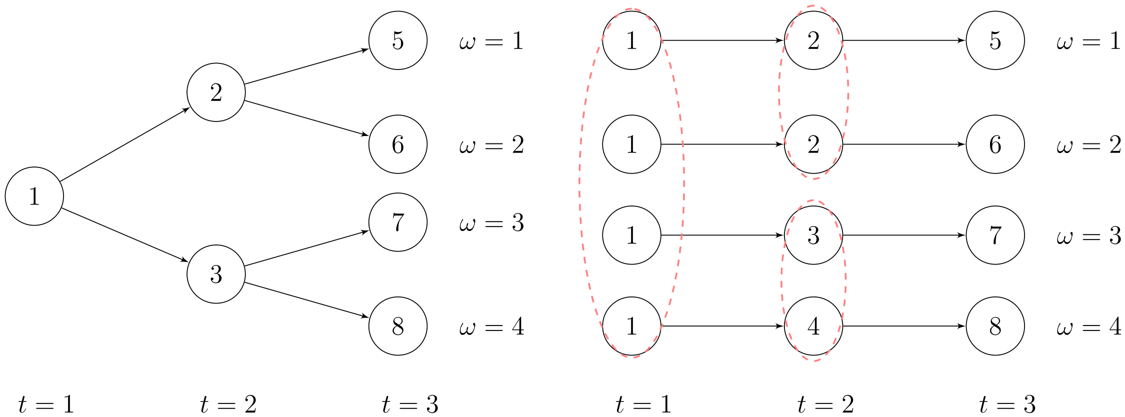

Figure 4.A.1: *Scenario tree of the problem for proof of the PH with direct variable fixation failure when there is uncertainty in the volumes. Standard representation (left) and detached form representation (right)*

References

Alonso-Ayuso, A., Escudero, L. F., Guignard, M., and Weintraub, A. (2018). Risk management for forestry planning under uncertainty in demand and prices. *European Journal of Operational Research*, 267(3):1051–1074.

Álvarez-Miranda, E., Garcia-Gonzalo, J., Ulloa-Fierro, F., Weintraub, A., and Barreiro, S. (2018). A multicriteria optimization model for sustainable forest management under climate change uncertainty: An application in Portugal. *European Journal of Operational Research*, 269(1):79–98.

Apap, R. M. and Grossmann, I. E. (2017). Models and computational strategies for multistage stochastic programming under endogenous and exogenous uncertainties. *Computers and Chemical Engineering*, 103:233–274.

Atakan, S. and Sen, S. (2018). A Progressive Hedging based branch-and-bound algorithm for mixed-integer stochastic programs. *Computational Management Science*, 15(3-4):501–540.

Barnett, J., Watson, J. P., and Woodruff, D. L. (2017). BBPH: Using progressive hedging within branch and bound to solve multi-stage stochastic mixed integer programs. *Operations Research Letters*, 45(1):34–39.

Benders, J. F. (1962). Partitioning procedures for solving mixed-variables programming problems. *Numerische Mathematik*, 4(1):238–252.

Beraldi, P. and Bruni, M. E. (2013). A clustering approach for scenario tree reduction: An application to a stochastic programming portfolio optimization problem. *Top*, 22(3):1–16.

Boland, N., Christiansen, J., Dandurand, B., Eberhard, A., Linderoth, J., Luedtke, J., and Oliveira, F. (2018). Combining Progressive Hedging with a Frank–Wolfe Method to Compute Lagrangian Dual Bounds in Stochastic Mixed-Integer Programming. *SIAM Journal on Optimization*, 28(2):1312–1336.

Boland, N., Dumitrescu, I., Froyland, G., and Kalinowski, T. (2016). Minimum cardinality non-anticipativity constraint sets for multistage stochastic programming. *Mathematical Programming*, 157(1):69–93.

Casey, M. S. and Sen, S. (2005). The Scenario Generation Algorithm for Multistage Stochastic Linear Programming. *Mathematics of Operations Research*, 30(3):615–631.

CPLEX, I. I. (2019). ibm.

Di Domenica, N., Mitra, G., Valente, P., and Birbilis, G. (2007). Stochastic programming and scenario generation within a simulation framework: An information systems perspective. *Decision Support Systems*, 42(4):2197–2218.

Dupacová, J., Consigli, G., and Wallace, S. W. (2000). Scenarios for Multistage Stochastic Programs. *Annals of Operations Research*, 100:25–53.

Egging, R. (2013). Benders Decomposition for multi-stage stochastic mixed complementarity problems-Applied to a global natural gas market model. *European Journal of Operational Research*, 226(2):341–353.

Escudero, L. F., Garín, M. A., Monge, J. F., and Unzueta, A. (2018). On preparedness resource allocation planning for natural disaster relief under endogenous uncertainty with time-consistent risk-averse management. *Computers and Operations Research*, 98:84–102.

Fattahi, M., Govindan, K., and Keyvanshokooh, E. (2018). A multi-stage stochastic program for supply chain network redesign problem with price-dependent uncertain demands. *Computers and Operations Research*, 100:314–332.

Feizollahi, M. J., Ahmed, S., and Sun, A. (2017). Exact augmented Lagrangian duality for mixed integer linear programming. *Mathematical Programming*, 161(1-2):365–387.

Gade, D., Hackebeil, G., Ryan, S. M., Watson, J.-P., Wets, R. J.-B., and Woodruff, D. L. (2016). Obtaining lower bounds from the progressive hedging algorithm for stochastic mixed-integer programs. *Mathematical Programming*, 157(1):47–67.

Gupta, N., Dutta, G., and Fourer, R. (2014). An expanded database structure for a class of multi-period, stochastic mathematical programming models for process industries. *Decision Support Systems*, 64:43–56.

Heitsch, H. and Römisch, W. (2009). Scenario tree reduction for multistage stochastic programs. *Computational Management Science*, 6(2):117–133.

Hestenes, M. R. (1969). Multiplier and gradient methods. *Journal of Optimization Theory and Applications*, 4(5):303–320.

Higle, J. L., Rayco, B., and Sen, S. (2010). Stochastic scenario decomposition for multistage stochastic programs. *IMA Journal of Management Mathematics*, 21(1):39–66.

Høyland, K., Kaut, M., and Wallace, S. W. (2003). A Heuristic for Moment-Matching. *Computational Optimization and Applications*, 24:169–185.

Høyland, K. and Wallace, S. W. (2001). Generating Scenario Trees for Multistage Decision Problems. *Management Science*, 47(2):295–307.

Kaut, M. and Wallace, S. W. (2007). Evaluation of scenario-generation methods for stochastic programming. *Pacific Journal of Optimization*, 3(2):257–271.

Küçükyavuz, S. and Sen, S. (2017). An Introduction to Two-Stage Stochastic Mixed-Integer Programming. In *The Operations Research Revolution*, number October, pages 1–27. INFORMS.

Latta, G., Temesgen, H., Adams, D., and Barrett, T. (2010). Analysis of potential impacts of climate change on forests of the United States Pacific Northwest. *Forest Ecology and Management*, 259(4):720–729.

Löhndorf, N. (2016). An empirical analysis of scenario generation methods for stochastic optimization. *European Journal of Operational Research*, 255(1):121–132.

Manerba, D. and Perboli, G. (2019). New solution approaches for the capacitated supplier selection problem with total quantity discount and activation costs under demand uncertainty. *Computers and Operations Research*, 101:29–42.

Moss, R. H., Edmonds, J. A., Hibbard, K. A., Manning, M. R., Rose, S. K., van Vuuren, D. P., Carter, T. R., Emori, S., Kainuma, M., Kram, T., Meehl, G. A., Mitchell, J. F. B., Nakicenovic, N., Riahi, K., Smith, S. J., Stouffer, R. J., Thomson, A. M., Weyant, J. P., and Wilbanks, T. J. (2010). The next generation of scenarios for climate change research and assessment. *Nature*, 463(7282):747–756.

Pantuso, G. and Boomsma, T. K. (2019). On the number of stages in multistage stochastic programs. *Annals of Operations Research*, 1(1985):1–8.

Pranevicius, H. and Sutiene, K. (2007). Scenario tree generation by clustering the simulated data paths. *Proceedings of 21st European Conference on Modeling and Simulation*, page 203208.

Rios, I., Weintraub, A., and Wets, R. J. (2016). Building a stochastic programming model from scratch: a harvesting management example. *Quantitative Finance*, 16(2):189–199.

Rockafellar, R. (1977). Measures as Lagrange multipliers in multistage stochastic programming. *Journal of Mathematical Analysis and Applications*, 60(2):301–313.

Rockafellar, R. and Wets, R. J.-B. (1991). Scenarios and policy aggregation in optimization under uncertainty. *Mathematics of Operations Research*, 16(1):119–147.

Sanei Bajgiran, O., Kazemi Zanjani, M., and Nourelfath, M. (2017). Forest harvesting planning under uncertainty: a cardinality-constrained approach. *International Journal of Production Research*, 55(7):1914–1929.

Sen, S. (2005). Algorithms for Stochastic Mixed-Integer Programming Models. *Handbooks in Operations Research and Management Science*, 12(C):515–558.

St. John, R. and Tóth, S. F. (2015). Spatially explicit forest harvest scheduling with difference equations. *Annals of Operations Research*, 232:235257.

Thénié, J. and Vial, J. P. (2008). Step decision rules for multistage stochastic programming: A heuristic approach. *Automatica*, 44(6):1569–1584.

Veliz, F. B., Watson, J.-P., Weintraub, A., Wets, R. J.-B., and Woodruff, D. L. (2014). Stochastic optimization models in forest planning: a progressive hedging solution approach. *Annals of Operations Research*, pages 259–274.

Watson, J. P. and Woodruff, D. L. (2011). Progressive hedging innovations for a class of stochastic mixed-integer resource allocation problems. *Computational Management Science*, 8(4):355–370.

Yossiri, A., Cordeau, J. F., and Jans, R. (2015). Benders decomposition for production routing under demand uncertainty. *Operations Research*, 63(4):851–867.

Zhou, H., Zheng, J. H., Li, Z., Wu, Q. H., and Zhou, X. X. (2019). Multi-stage contingency-constrained co-planning for electricity-gas systems interconnected with gas-fired units and power-to-gas plants using iterative Benders decomposition. *Energy*, 180:689–701.

Zou, J., Ahmed, S., and Sun, X. A. (2019). Stochastic dual dynamic integer programming. *Mathematical Programming*, 175(1-2):461–502.

Chapter 5. Conclusions and outlook

Climate change affects forests in many ways including uncertainty in growth and yield of merchantable timber. Therefore, it is important to explicitly consider climate change uncertainty in forest management planning. In this dissertation, I have proposed several methods for incorporating climate uncertainty in forest harvest scheduling. I proposed to model harvest scheduling as a stochastic optimization problem where the uncertainty is the forest growth.

First, I proposed a method that allows to incorporate climate uncertainty in harvest scheduling by offering the set of optimal actions that a decision maker can make here and now with limited knowledge on what the actual climate will be. This approach allows to quickly solve the stochastic optimization problem; however, it does not offer long term policies that may be necessary for some forest companies which need a long-term planning (long term set of actions) and are bounded by contracts based on the anticipated revenues. To address such a shortcoming, I proposed in the second chapter (Chapter 3) a method that incorporates climate change in harvest scheduling by considering the set of climate paths. A climate path is a forecast of possible future climate. Nonetheless, the planning focuses mainly on one climate path instead of harvest planning that intends at hedging against all climate paths simultaneously.

Finally, I developed a heuristic to solve multistage stochastic optimization problems with binary decision variables. The heuristic allows to handle large scale optimization problems with little to no loss of optimality. For forests with large number of management units, the heuristic allowed to solve the harvest scheduling problem, whereas the extensive form which is the total optimization problem solved directly with a commercial solver was intractable. Therefore, this heuristic increases the space of solutions and management possibilities that a decision maker can take. Indeed, the capability to solve large problems and the decrease in solution time allow managers to consider different management alternatives and make sound decisions that would not be possible otherwise.

In this dissertation, I focused on one aspect of climate change which is the change in forest growth and yield. However, there are other aspects of climate change that may affect forests and thus the management. For instance, climate change may affect the occurrence of wildfire and thus forest management needs to be adapted to hedge against that uncertainty. Similarly, climate change may entirely displace forest on the landscape. Some sites that are suitable today to a forest may not be suitable in the future for the same forest species. This aspect needs to be explicitly considered once we have more information on climate change and its impact on forests.

In this dissertation, I considered that the price of forest products is independent of climate change. However, this simplification may need to be revisited if in the future we have more information on how the price of forest products will change depending on forest yield. This aspect is a bit difficult to comprehend since there does not seem to be straightforward relationship between climate change and the price of wood products. For instance, the reduction of forest yield due to climate change may lead to advancement in technology and development of forest products alternatives and consequently, the price of wood may not be affected.

To sum, there is still a need to develop more accurate models that convert climate change data into forest growth. One of the limitations of most of the currently available models is their validation and their generalization to different tree species and landscapes. Although, this dissertation advocates for consideration of climate change in forest management plans, I acknowledge that there are many other uncertainties in forestry and the decision to focus on climate uncertainty or not depends on the decision makers since it is almost impossible to incorporate all those uncertainties in the management planning.